Modal Analysis of the First Production Design Heliostat Used at the Solar Thermal Test Facility (STTF)

John R. Janczy

Sandia Laboratories

MODAL ANALYSIS OF THE FIRST PRODUCTION DESIGN

HELIOSTAT USED AT THE SOLAR THERMAL TEST FACILITY (STTF)

John R. Janczy
Vibration & Shock Testing Division 9342
Sandia Laboratories
Albuquerque, NM 87115

ABSTRACT

The experimental study sought to characterize the dynamic modal
characteristics of a heliostat to be used at the Sandia operated
Solar Thermal Test Facility. Three modal studies were performed.
Two studies were conducted of the yoke and one on the facet
assembly. During the course of the test, Power Spectral Density
studies were performed using wind-loading and transport environ-
mental data. The modal (frequency, damping and stiffness) data
is presented. The data obtained through the various studies
compares favorably. The data indicates a possible structural
modification, and this modification is discussed.

TABLE OF CONTENTS

MODAL ANALYSIS OF THE FIRST PRODUCTION DESIGN
HELIOSTAT USED AT THE SOLAR THERMAL TEST FACILITY (STTF)

Introduction

Last summer Division 9342 was asked to study the feasibility of experimentally
determining the dynamic structural properties of a Martin-Marietta designed and built
heliostat. The heliostat is a solar tracking array of 25 flat plate mirrors. These
mirrors focus solar energy onto a point on a central receiver tower for the purpose of
generating steam. The steam could then be used to generate electricity. Several
hundred of these structures will be used at STTF. A photograph of a heliostat in its
"stowed" (non-duty) position is given in Appendix D and a diagram of the structure is
given as Figure 1. The heliostat is composed of two major assemblies--the yoke and the
facet-arm. Both of these assemblies are depicted in Figure 1. The yoke is mounted on
a vertical support containing a motor which allows rotation of the structure in azimuth.
The facet-arm assembly is mounted at two points on the yoke. One support point holds a
motor and the other contains a set of bearings to allow rotation of the substructure in
elevation.

After some consideration, it was decided to proceed with a series of tests to
empirically characterize the modal properties of a complete heliostat. The results
would be used to verify and update analytic models of the structure. Due to the size
and complexity of the test item, response measurements were taken by considering it to
be comprised of two assemblies, the yoke and the facet (see Figure 1). Each of these
sections was studied separately, but with total test item in its assembled state. The
point of input excitation was the same for both studies, enabling comparison of results
for both assemblies.

Preliminary work was started in early fall of this past year on a test heliostat
located in Area III. As this work involved obtaining field data for full-scale struc-
tures, special requirements arose such as the need for an instrumentation trailer,

special test fixturing and new test techniques.

Dynamic testing on a structure of this size had not been performed by Division 9342. The bulk of the work done by this organization has been in the lab on component type test items. Field testing of such a large structure required a slightly different perspective and some progression along the learning curve.

Explanation of Theory Used

Modal analysis is a method of experimentation and analysis which allows the engineer to characterize the dynamics of a test structure in terms of its natural frequencies, damping, and mode shapes. The mode shape can be thought of in two ways (for our purposes). The first is that a "mode shape" can be considered as a set of generalized coordinates which, when used in an operator form, transforms the mass, stiffness and damping matrices of a multi-degree-of-freedom second-order system equation to diagonal form. The second way of considering the mode shape (and the way it is represented here) is as a "map" of residue (or dynamic compliance) values for each measurement point along the structure at each natural frequency.

Modal analysis is valuable, in that it permits verification and adjustment of analytic structural models. This means that effects of varying the elastic properties (mass, stiffness and damping) can be studied. This technique also allows for the identification of structural weaknesses and provides information which can be used to eliminate unwanted noise and vibration.

Division 9342 performs modal analysis using the Hewlett-Packard 5451B Fourier Analysis system. Most structural modeling techniques (i.e., analytic models) represent the test article as a system of lumped masses, springs and dampers (see Figure 2). The modal analysis system makes use of this fact.

Before proceeding, it is prudent to state the basic assumptions involved in this type of modeling. Briefly, we must assume that the structure may be modeled using a finite number of masses, springs and dampers. Secondly, we assume that the test article

obeys Maxwell's Reciprocity Theorem. This last assumption is basic to the experimental technique used. In terms of frequency response measurements, reciprocity means that if a structure is excited at point A and its response is measured at point B, then the frequency response function formed, by the division of the Fourier Transform of the output by the Fourier Transform of the input, is identical to the frequency response function that would be obtained by exciting the structure at point B and measuring the response at A. This assumption allows simplification of the transfer matrix in that only one row or column need be measured, as the other rows or columns would contain the mode shape vector multiplied by a component of itself. This leads to a requirement for making inertial measurements (i.e., force input and acceleration, velocity or displacement response measurements). This requirement is imposed when it is desired to go from the uncoupled response (normal mode concept) to the coupled (see Figure 2) mass, stiffness and damping matrices for modeling.

The modal analysis method used by Division 9342 uses frequency response techniques. Frequency response measurements are obtained so that the structure's dynamic properties (modal stiffness, frequency and damping) can be identified.

If we express Figure 2 in analytic form, we get

$$[M]\{\ddot{x}(t)\} + [C]\{\dot{x}(t)\} + [K]\{x(t)\} = \{f(t)\} \tag{1}$$

where

1) The quantities enclosed by brackets denote matrices.

2) The quantities enclosed by parentheses denote components of vector quantities.

3) The dots denote differentation with respect to time.

4) $[M] \equiv$ mass matrix

       $[C] \equiv$ damping matrix

       $[K] \equiv$ stiffness matrix

    $\{x(t)\} \equiv$ components of position vector

    $\{f(t)\} \equiv$ components of force vector

We can now take the Laplace transform of equation (1) and assuming all initial

conditions to be zero, we get

$$\left[[M]s^2 + [C]s + [K]\right]\{x(s)\} = \{F(s)\} \tag{2}$$

or,

$$[B(s)]\{x(s)\} = \{F(s)\} \tag{3}$$

where

$$[B(s)] = [M]s^2 + [C]s + [K] \tag{4}$$

$[B(s)]$ is called the System Matrix. Let,

$$[B(s)]^{-1} = [H(s)] \tag{5}$$

$[H(s)]$ is the inverse of $[B(s)]$ and is called the Transfer Matrix.

$$H(s) = \frac{\text{cofactor } [B(s)]}{\det [B(s)]} = \frac{\begin{bmatrix} \beta_n & \beta_{12} & \cdots & \beta_{1n} \\ \vdots & & & \vdots \\ \beta_{n1} & & & \beta_{nn} \end{bmatrix}}{\det [B(s)]} \tag{6}$$

where, $\det [B(s)]$ is the determinant of the matrix within the brackets.

$$[H(s)] = \begin{bmatrix} h_{11}(s) & h_{12}(s) & \cdots & h_{1n}(s) \\ h_{21}(s) & \cdots & & \vdots \\ \vdots & & & \vdots \\ h_{n1}(s) & \cdots & & h_{nn}(s) \end{bmatrix} \tag{7}$$

Consider, as an example, the element $h_{11}(s)$.

$$h_{11}(s) = \frac{X_1(s)}{F_1(s)} \tag{8}$$

or, in partial fraction form,

8

$$h_{11}(s) = \frac{X_1(s)}{F_1(s)} = \sum_{k=1}^{a_n} \frac{a_k}{(s - p_k)} \qquad (9)$$

a_k is obtained for at each pole by solving

$$\frac{B_{11}}{\det [B(s)]} = \sum_{k=1}^{a_n} \frac{a_k}{(s - p_k)} \qquad (10)$$

where $p_k \equiv$ pole, or the value of s, such that $(s - p_k) = 0$. Further,

$$s_k = p_k = d_k + i f_k \qquad (11)$$

and
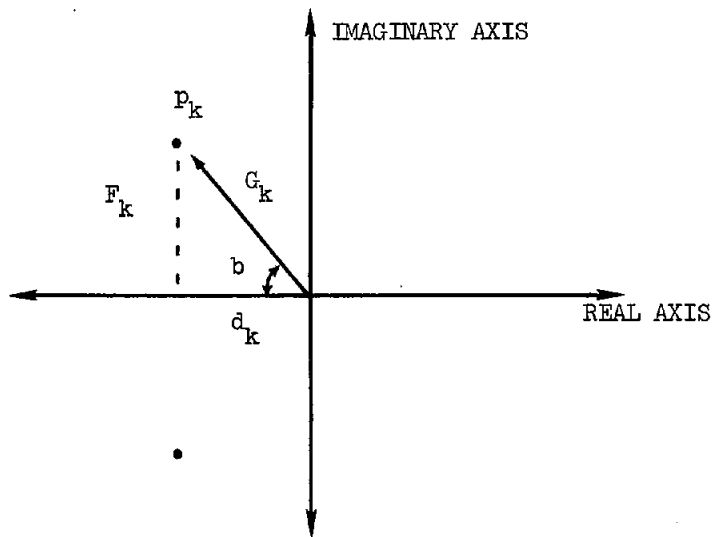
where,

$\qquad d_k \equiv$ damping

$\qquad f_k \equiv$ natural frequency

$\qquad a_k \equiv$ residue

$\qquad i \equiv \sqrt{-1}$

$\qquad G_k \equiv$ resonant frequency

$\qquad F_k \equiv$ damping factor

An equation of the form (10) can be written for each element h_{nj}. As $[H(s)]$ is made of up elements h_{nj} and the adjoint of the System Matrix (adj $[H(s)]^{-1}$) is proportional to the mode shape (so that the residue matrix is proportional to the mode shape), then the Transfer Matrix contains all the modal information we are interested in.

To perform this analysis using experimental data, we must have (as previously stated) a linear structure that obeys reciprocity. This being the case, we can place motion transducers (either acceleration, velocity or displacement) on the structure, at specified locations, and input a known force at a specified point. We can record these time domain signals and Fourier transform them using a Fast Fourier Transform (FFT) algorithm. A division (output by input) is performed and the frequency response function obtained. (9) can be rewritten as

$$h_{nj}(s) = \frac{X_n(s)}{F_j(s)} = \sum_{k=1}^{R} \left[\frac{r_{njk}}{2i(s - p_k)} - \frac{r^*_{njk}}{2i(s - p_k)} \right] \tag{12}$$

where,

$$a_{njk} = \frac{r_{njk}}{2i} \tag{13}$$

and the asterisk denotes complex conjugation.

Since the experimental data is in the Fourier domain, we want to transform it to the Laplace domain (without loss of information), so that the foregoing analysis can be used. Realizing that the frequency response function is just the transfer function evaluated at $s = i\omega$ (where, ω = frequency), we can fit the frequency response measurements to an equation of the form (12) and extract the modal parameters. The fit is accomplished with a least-squares-fit curve-fitting algorithm. The effect of this process is to decouple the frequency response measurement into a sum of single degree of freedom systems.

10

Experimentation/Analysis

The data used in this study was obtained and analyzed in essentially three phases. The first phase was a modal study of the test heliostat installed in Area III. A report was written and submitted to Division 5713 concerning the results of that test. That report is included here as Appendix A so that it can be used for comparison between the various phases of the present study. Appendix A presents data taken on the yoke assembly (Figure 1) while it was loaded by the facet assembly, as this is its service environment. The data was taken and analyzed as stated previously.

The second phase of the study started after heliostat installation at the STTF. A modal study was made for the yoke loaded by the facet assembly, as in the first test. The major difference in the test procedure between these two studies was that a much longer record length was taken on tape for each excitation/response signal. The longer record length allowed finer frequency resolution for the frequency response functions of the second test, enabling the whole response signal to be sampled.

Included as Appendix B is a report concerning the road environment seen by the facet assembly as it is transported by truck to and from the assembly hangar (located at Kirtland AFB-West) and the STTF. The facet assembly is transported such that the plane of the mirrors is perpendicular to the truck bed. The facets had suffered breakage due to excessive lateral motion. It was desired to characterize this motion, thereby finding a method of reducing facet damage during transport. To obtain data for this study, a facet assembly (and the truck bed) was instrumented and transported along the typical route. Acceleration versus time signals were obtained at various positions on the structure as it was transported. These signals were recorded and used to obtain Power Spectral Density (PSD) estimates for the test structure due to the transport environment. Resonant frequencies and energy levels can be viewed on the PSD plots (given in Appendix B). These frequencies can be compared against those obtained for the modal study performed for the facet assembly.

A flow chart for the instrumentation used to perform the modal study of the yoke is shown in Figure 3. The figure pictorially describes how the data for the frequency

response measurements was obtained. Various methods for providing the input excitation were considered. Possible means included: a load-cell instrumented sledge-hammer, step relaxation, electro-dynamic shaker, and an electro-hydraulic ram. After considering the various procedures, it was decided that an electro-hydraulic ram (such as the one depicted in Figure 3) would best combine the advantages of long pulse duration and ease of set up and fixturing. Pulse duration on the order of 0.2 to 0.3 second was necessary since the test structure is relatively "soft." The natural frequencies found were as low as approximately 1.8 Hz. The electro-hydraulic exciter that was constructed consists of a hydraulic ram, a support structure, and a pump/motor/supply. The force was delivered to the structure through a 5000 lb strain gage load cell, which was flexibly coupled to the shaft of the ram. The ram/transducer combination was supported by an aluminum truss-work (see Figure 4). The truss-work was bolted to an aluminum base plate. Reaction force was provided to the exciter assembly by means of approximately 2000 pounds of lead, loaded on top of the base plate.

The acceleration response signals were measured using three Kistler model 303T servo-accelerometers. These accelerometers were used because of their extreme sensitivity (approximately 2.6 volts per g). Power supplies were used for both transducers. An external amplifier was only required for the strain gage load cell, as the servo-accelerometer had an internal amplifier. Both time waveforms (input and response signals) were monitored on a Tektronix dual-beam oscilloscope, so that any overloads could be detected during the course of data acquisition. Finally, the signals were simultaneously fed to an Ampex FR1300 analog FM tape recorder for analysis in Area I on the Division 9342 modal analysis system. A diagram of the location of the measurement points referenced to the structure is presented in Figure 5 for the yoke assembly.

The technique used to analyze the data requires multiple samples to be taken at each measurement point. This is a requirement of the software used. But it also is necessary for reducing noise on the data. If the noise source is incoherent with the input, then taking multiple measurements at the data point will average out the effects of the noise.

The theory behind the analysis system was briefly described in the beginning of this report. The theory was implemented by using a Hewlett-Packard 5451B Fourier analysis system. The modal analysis capability is software based. The analog input and response signals are low-pass filtered at a cut-off frequency, f_c, which is one half of some desired sampling frequency. The signal is then converted to a digital form (by the A/D converter). The digital conversion takes place at the sampling frequency (twice the maximum frequency). Analyzing only to f_c eliminates the problem of aliasing the data, or "folding-back" of the higher frequencies above the desired range to some lower value, on the frequency axis within the analysis bandwidth. These digitized time signals are now Fourier transformed using a "hard-wired" Fourier analyzer. The frequency response function is then formed. Next, the software based curve-fitting algorithm is implemented, so that the modal parameters can be identified from the Laplace domain signal. See Figure 6 for an analysis flow chart.

Figure 7 lists the modal frequencies and damping for the yoke assembly. Figures 8 and 9 tabulate the dynamic compliance values and residues, respectively, for the five modes identified at the ten measurement points.

Figures 10, 11 and 12 give Power Spectral Density (PSD) plots for three accelerometer locations on the yoke (positions 1, 4 and 6--see Figure 5 for locations). These PSD plots were obtained by measuring accelerations at the specified positions on the structure when the heliostat was in its duty position (i.e., facet assembly perpendicular to ground--as in all tests presented here) and the structure loaded by wind gusts reaching speeds of approximately 25 mph. Comparison of these plots (Figures 10, 11 and 12) with Figure 7 shows very good agreement concerning frequency content. The only exception is the fourth mode at 3.99 Hz. This mode is only hinted at on the PSD plots.

Figure 13A shows photographs of the animated mode shapes displayed by the modal analysis system. Appendix C lists the tabulated modal characteristics at each measurement point on the yoke.

Agreement is less pronounced when Figures 10, 11 and 12 are compared with

Figure C1 of Appendix C. The values of frequency and damping vary somewhat, with respect to the plots of power spectral density and from measurement point to measurement point. This behavior seems to be more pronounced when considering the first mode. The discrepancies can be due to slight variations in frequency resolution of the analysis routines used by the PSD and modal packages, and by the fact that a low-pass filter was not used in the data acquisition system loop (see Figure 3). Dynamic range of the tape recorded time domain signals was a problem since accelerometers were chosen as the response transducers, and the frequency range of interest was discovered to be below 40 Hz. It was worthwhile to cut down the testing time, so multiple channels were recorded simultaneously. A low-pass filter was not used because the problem was not judged to be severe and a multi-channel filter was not available (a multi-channel filter is necessary so that any phase changes due to the filter are introduced on all channels). This consideration arose since an accelerometer responds to small displacement, high acceleration, high frequency (above 20 to 30 Hz) structural motion with a greater output signal than it does for the large displacement, low acceleration, low frequency (1 to 20 Hz) output motions. This raises the possibility of saturating the recording with the high acceleration, low structural displacement signals, which are not of great interest. The difficulty was partially overcome by recording whatever signal the transducer delivered. The signal was filtered after recording by means of the modal system's anti-aliasing filters, at some f_c. This method was not completely satisfactory for two reasons:

1. The lower the cutoff frequency, f_c, the longer the data record that is required for sampling by the A/D converter. Since the following sampling relations hold:

$$f_{max} = 2 f_c = 2 \text{ (sample frequency)} \qquad (14)$$

$$\frac{f_{max}}{N/2} = \Delta f = \frac{1}{T} \qquad (15)$$

where $\quad f_c \equiv$ cutoff frequency

$\Delta f \equiv$ frequency resolution

$$T \equiv \text{time of total record length}$$

$$N \equiv \text{data block size}$$

2. Because of the possibility of saturating the dynamic range of the tape
   with signals that are not of interest, it is possible the low frequency
   information could be partially buried in tape noise.

Due to these considerations, when data was obtained and analyzed, the largest possible
transducer signal amplification and the lowest possible cutoff frequency were used.

Comparison of the data of Figures 7, 8, 9 with Appendix A is not straightforward.
The major procedural difference between these two studies is that the frequency resolu-
tion is at least twice as fine for the data of Figures 7 thru 9 due to a much longer
data record for each impulse/response measurement. The only mode from the first study
that can be used for comparison is the first, at 2.38 Hz. The 2.38 Hz mode falls
between the first and second modes listed in Figure 7. Comparison of Figure 13A for
the first and second modes with the first mode of Appendix A also indicates that it is
some combination of the 1.8 and 2.8 Hz modes of Figure 7. This is explained by the
improved frequency resolution of the second study. Viewing the dynamic compliance
values for modes which can be compared indicates a decrease in magnitude by approxi-
mately a factor of ten in the final yoke study. The new values are most probably more
correct than those of the previous analysis (and report). But they do have possible
errors due to the lack of sufficient low frequency dynamic range. It is also possible
that the input excitation system calibration could have small errors, due to back-
slippage of the exciter when exerting force on the ground-fixed heliostat, as the
exciter was not so attached. There is confidence in the latest data due to the suffi-
cient agreement between the redundant information of the two modal studies and the
PSD studies.

The third phase of the experimentation began immediately following the comple-
tion of data acquisition on the yoke (at STTF).

The instrumentation diagram for this part of the experiment is given in Figure
14. The only difference between Figures 3 and 14 (other than the test assemblies

studied) is that the two tests used different response transducers and signal conditioners. The response transducers used for the facet assembly modal study were Endevco model 2262-25 piezo-resistive accelerometers. Eight of these transducers were available for use, whereas only three of the Kistler 303T accelerometers were available. The model 2262-25 still gave high sensitivity and it was possible to tune each transducer to a common value for sensitivity. Thirty-three response points were used for the facet study. Use of eight accelerometers allowed simultaneous measurement of eight response points each time the structure was excited, thereby expediting the test. Data was recorded and analyzed in the same manner as in the previous tests.

Response data due to wind loading was not taken on the facet assembly. PSD plots were made for the heliostat transport test. In the transport test, the facet assembly was subjected to rough road input, which can be approximated as random. The assembly was secured to the transport trailer in a manner similar to its service state. The acceleration response was measured using the model 2265-25 accelerometers. The PSD plots (Figures 2 thru 16) of Appendix B can be roughly compared with the modal frequencies of the facet as the behavior of the arm should be approximately the same in both transverse directions, far from the point of attachment to the center shaft, due to the shape of the facet arm.

Figure 15 tabulates the average modal frequencies and damping for the heliostat facet assembly. Figures 16 and 17 give the dynamic compliance and residue values, respectively. Figure C2 of Appendix C gives the modal fit data for the individual (33) measurement points used for the assembly. Figure 18 illustrates the location of the response points with respect to the structure. Figure 13B shows pictures of the animated mode shapes obtained through the modal system. The undeformed position is shown along with the deformations about the neutral plane.

For the purpose of this analysis, a mode is considered a "global" property of the structure. This means that the properties for a particular mode of vibration can be measured at any point along the structure, with the exception of one that coincides with a node. This assumption has physical limitations. For example, one could not detect the modal contribution of a flagpole atop a large building by measuring response

16

on the floor of that building. The example illustrates what is called a "local" mode (one that can be measured only on a substructure of the test item). This poses no major problem with the test structure at hand. For the present study, the concept of "global" modes means that modal content should be the same for the yoke and facet assemblies (amplitude from point to point, of course, varies) except at nodal lines. This can be verified by considering Figures 7 and 15. Five modes were identified for the yoke and six for the facet assembly. Comparison shows good agreement for the first three modes of each structure. The first mode for each agrees very well for both frequency and damping. The next two modes show good agreement for frequency, but not damping. The remaining modes do not compare as well. Considering the possible error sources (i.e., the lack of low-pass filter before recording, etc.), the agreement is quite encouraging. The limited dynamic range on the recording for the low frequency content and the attendant problems with frequency resolution mean that some modes may get "smeared together" or be partially buried in noise. This can account for possible errors. Another error source is inherent structural non-linearities. These non-linear effects arise due to slippage at points of rotation when loading the heliostat yoke. Two such points are at the ground support of the yoke and at the facet assembly support points on the yoke.

Figures 19 thru 28 are Power Spectral Density plots for the response signals from various positions on the facet assembly. Comparison of these plots with the modal frequencies of Figure 15 show relatively good agreement. These PSD plots also illustrate the noise problem due to the lack of a low-pass filter in the data acquisition system before the data is recorded.

Comparison of Figure 15 with Appendix B (Figures 3, 5 and 7) show reasonable agreement. The pertinent graphs of Appendix B show sufficient energy at the modes found in the final modal study (especially the first three) to warrant confidence in the results.

Conclusions

The good agreement with respect to modal frequencies for the various types of analysis performed (i.e., PSD, transport environment, wind excitation, modal) lend confidence to the data obtained for the latest yoke and facet assembly modal analyses. Errors apparent in the data are most probably due to a need for improved dynamic range for the low frequency response signals on the FM tape recording, and due to inherent structural non-linearities. The dynamic range for the low frequencies can be improved by passing the input and response signals through low-pass filters before recording the time domain signals. The effect of the non-linearities can be further studied by making two or three sets of frequency response measurements at a few points on the structure using a different input force level for each set of measurements.

Based on the modal data obtained, it can be concluded that the mode shapes (particularly the first three) show pronounced out-of-phase motion of the facet arms. If this motion could be forced in-phase and made to approximate a rigid body mode, then it is probable that image resolution could be improved and structural integrity enhanced. One possible method for doing this is to use lateral restraints between all vertical arms above the yoke support shaft (as the structure stows in one direction only) and lateral restraints for the three inner arms below the support shafts (see Figure 29).

Most equipment necessary for field environment frequency response measurement is available to Division 9342, and additional personnel have been added to the Modal Testing project group. This means that the time required to perform further modal analyses of the heliostat (e.g., a study of the final design heliostat) would be considerably less than the previous studies. If additional work is performed, it would be instructive to install temporary lateral supports (as previously suggested) and perform a modal analysis of the structure so that the degree to which the dynamic properties have been altered can be discerned.

18

REFERENCES

1. Formenti, D., "Analytic and Experimental Modal Analysis," Hewlett-Packard Co.

2. Richardson, M., "Modal Analysis Using Digital Test Systems," Hewlett-Packard Co.

3. Doeblin, E. O., Measurement Systems: Application & Design, McGraw-Hill.

4. Fertis, D. G., Dynamics and Vibration of Structures, Wiley-Interscience.
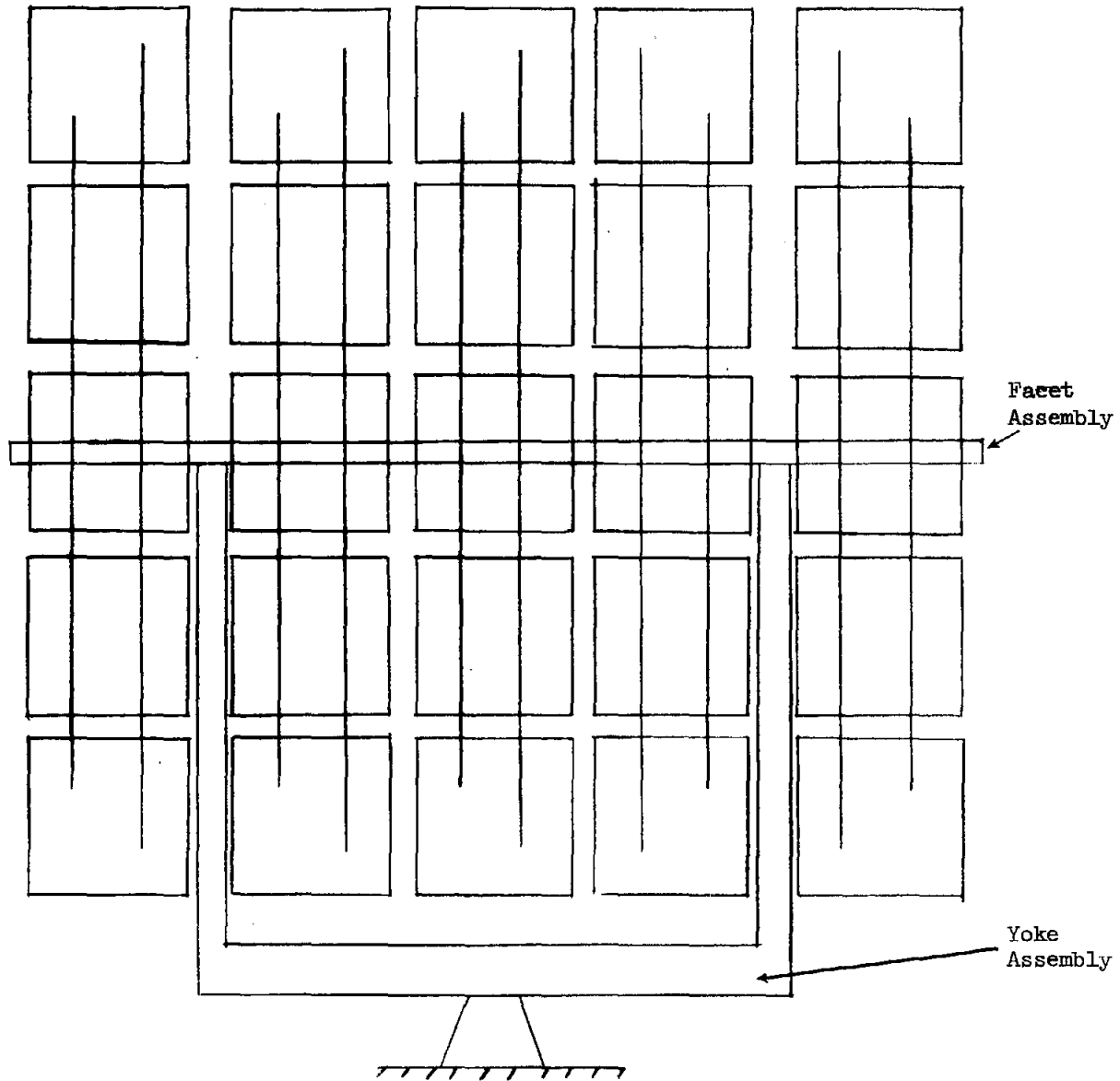
Figure 1. Heliostat
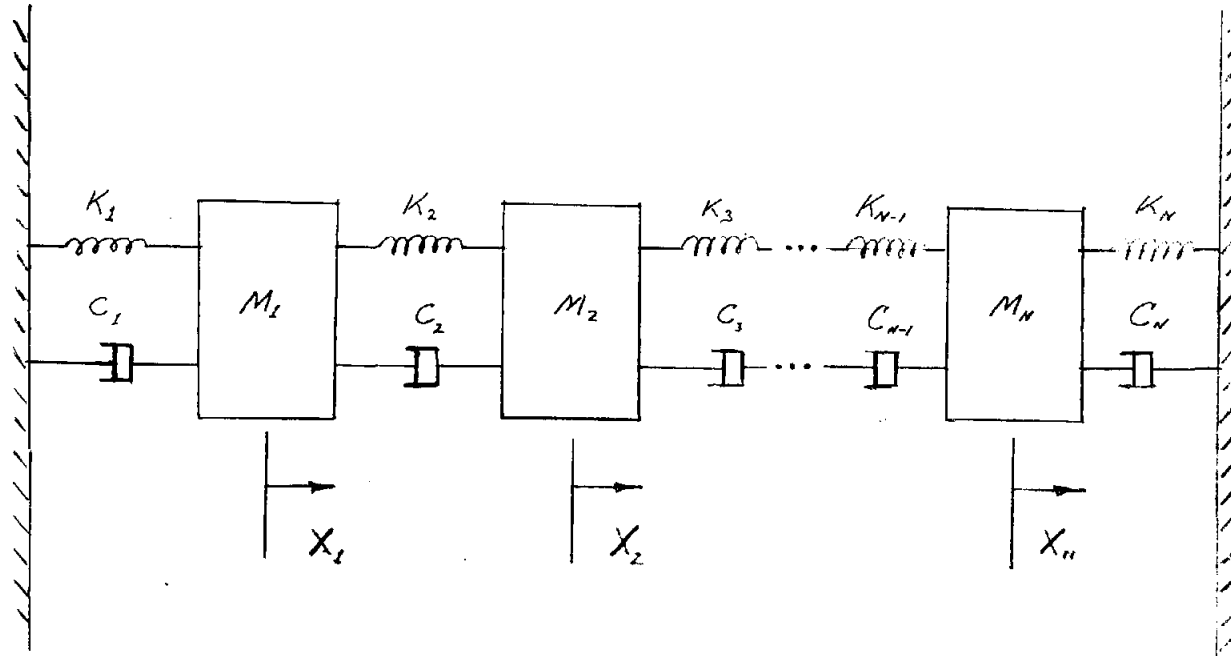
Figure 2.   Generalized Multi-Degree of Freedom System

Heliostat Yoke Assembly
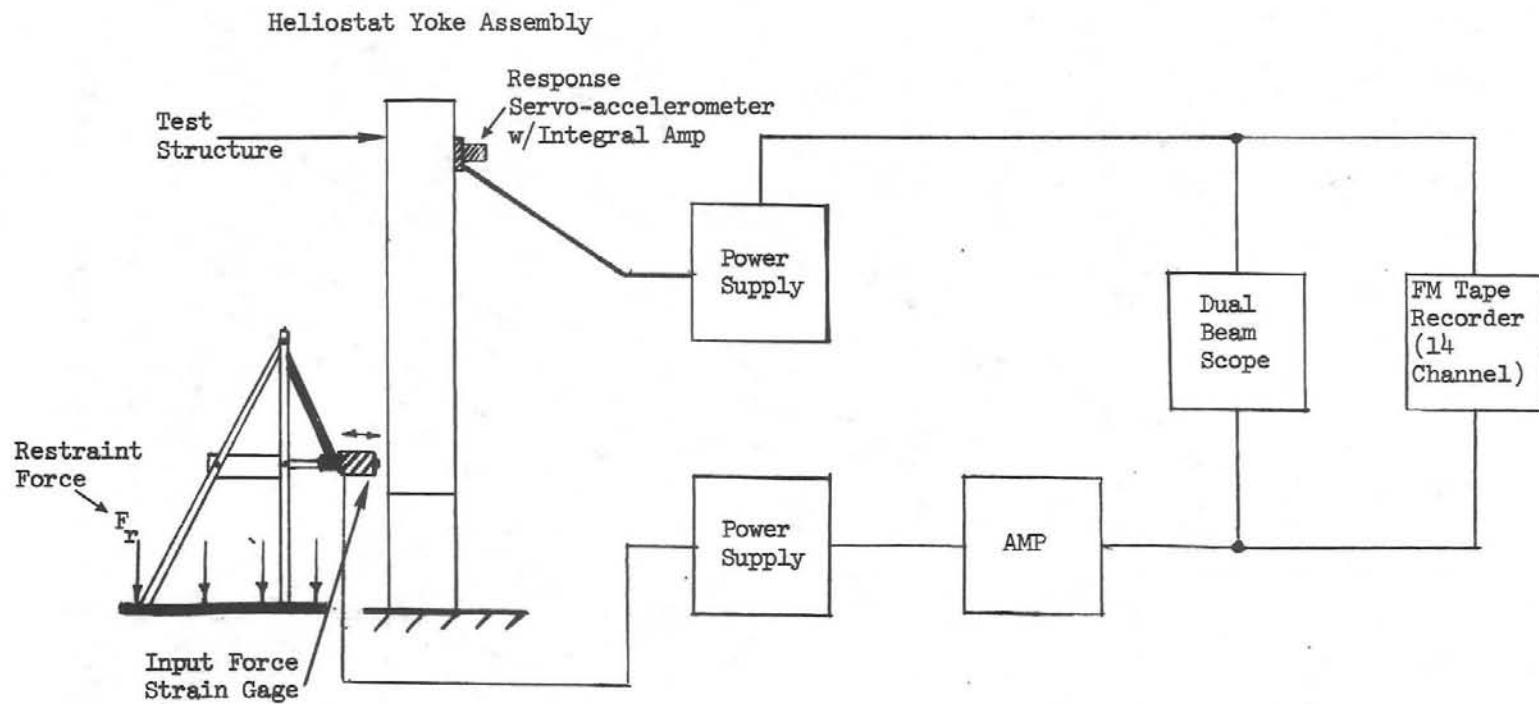
Figure 3. Instrumentation Diagram for Phase 1 & 2
Modal Studies of Heliostat Yoke Assembly
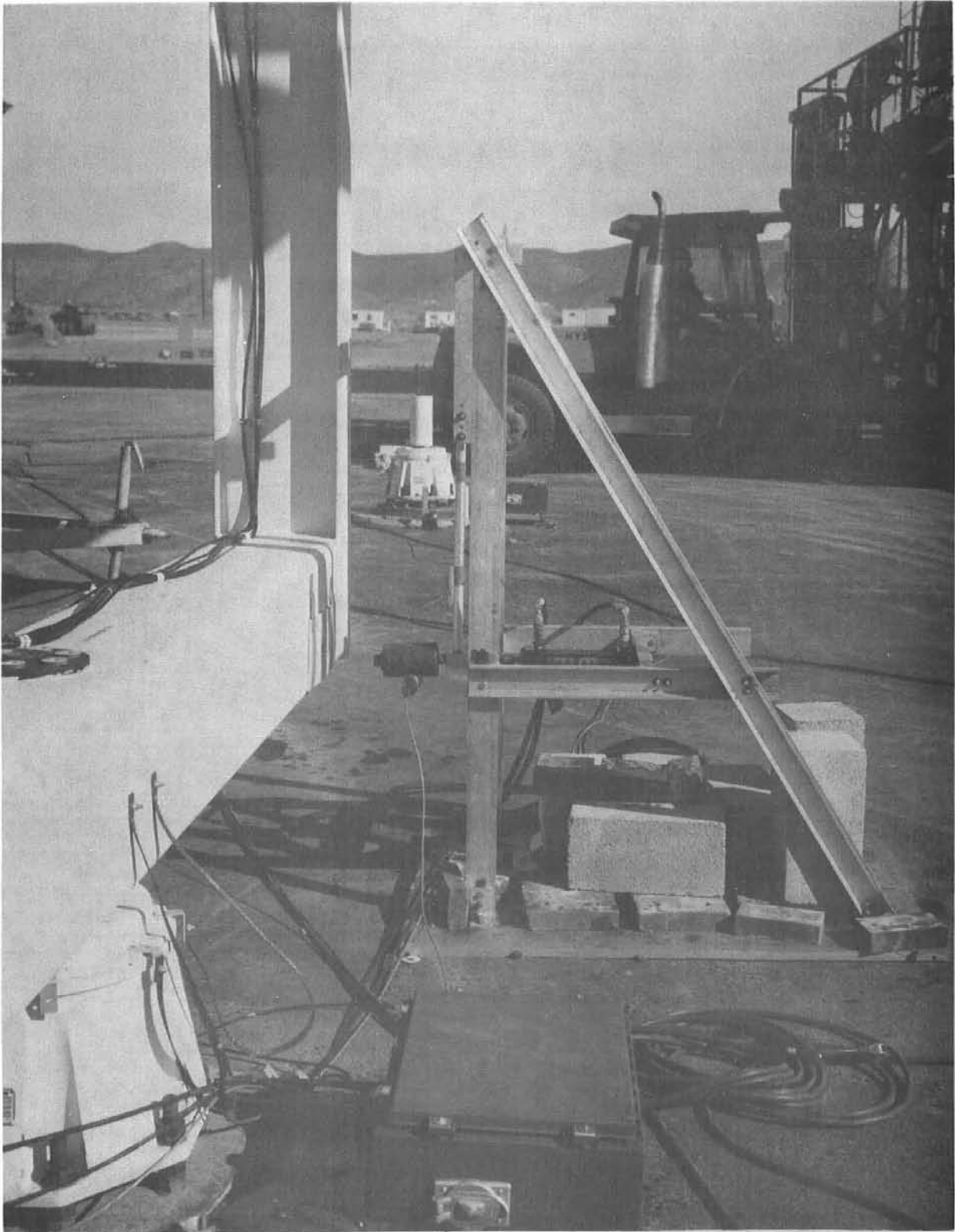
Figure 4. Picture of Electro-Hydraulic Exciter System
Developed for this Study
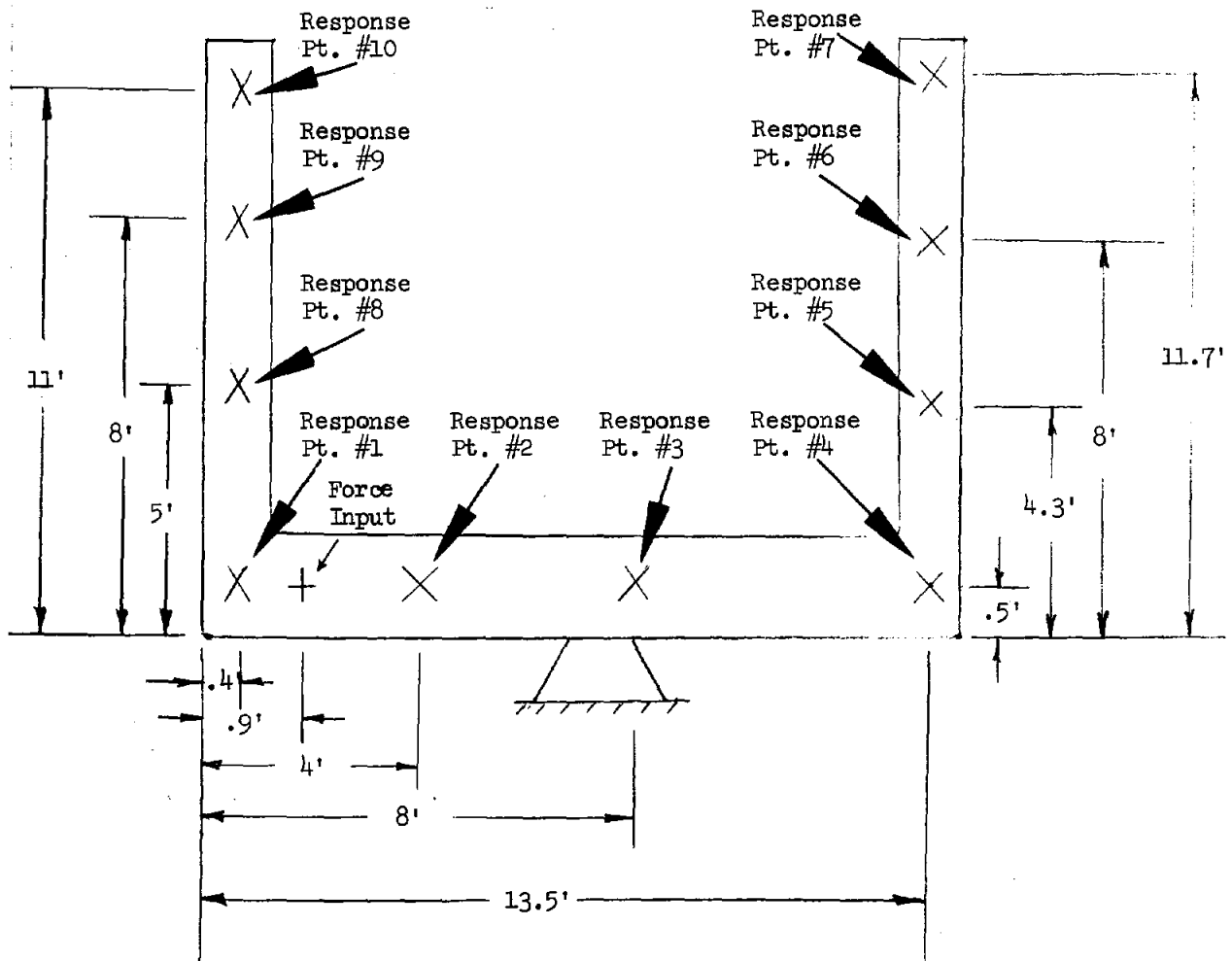
Figure 5. Measurement Point Diagram
Used on the Heliostat Yoke

Impulsive
Force
Input Signal

Yoke
Acceleration
Response Signal

Low-Pass
Filter

A/D
Converter

Fourier
Transform

Frequency
Response

Frequency
Response
Function

Output & Display
of Modal Parameter

Curve Fitting
Algorithm
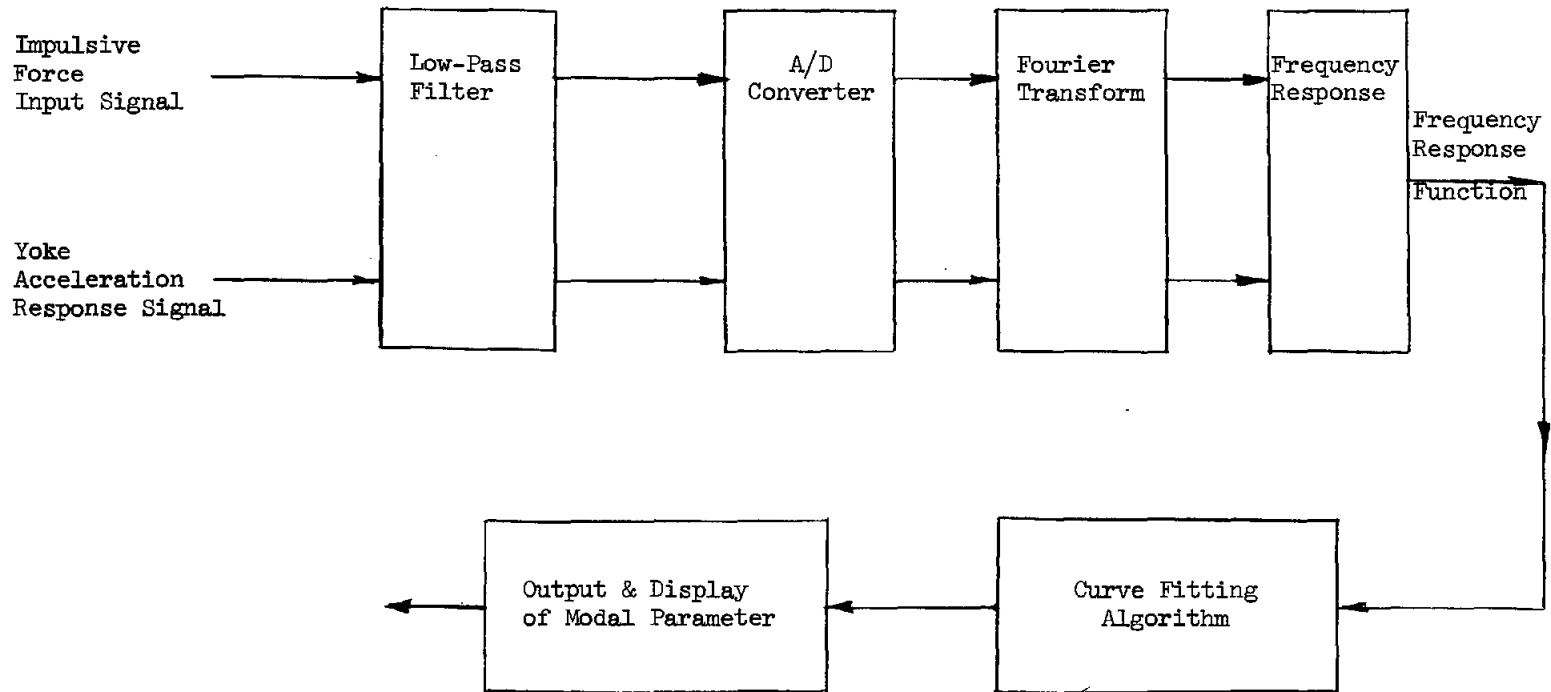
Figure 6. Flow Diagram of Analysis Steps

```
        AVERAGE MODAL FREQUENCIES AND DAMPING
     *      *      *      *      *      *      *      *      *


           NAT.FREQ.      DAMP.FACT.      DAMP.COEFF.
    MODE     (HZ)            (%)           (RAD/SEC)
      1      1.8179        28.3445          3.3780
      2      2.8075         2.3434           .4135
      3      3.4418          .3669           .0793
      4      3.9967          .0880           .0221
      5      4.5623          .2191           .0628
```

Figure 7.   Average Modal Frequencies and
            Damping for the Heliostat Yoke

AMPLITUDE UNITS: IN/LB

MEAS   *   *   *   *   *   MODES   *   *   *   *   *   *   *   *

	1		2		3		4		5	
	AMPL	PHS	AMPL	PHS	AMPL	PHS	AMPL	PHS	AMPL	PHS
1	.5290E-04	155.5	.5863E-03	195.4	.1538E-02	32.9	.4859E-02	283.1	.3209E-02	205.9
2	.8822E-04	160.8	.6772E-03	206.4	.8464E-02	32.7	.7716E-02	274.3	.4006E-02	245.6
3	.3836E-03	60.5	.7304E-04	311.1	.1804E-02	13.8	.3885E-02	322.6	.1875E-03	257.9
4	.7117E-03	11.9	.7265E-05	342.4	.1343E-02	20.9	.5423E-03	3.2	.2870E-03	115.6
5	.3624E-03	333.9	.2418E-04	295.4	.5715E-03	17.1	.9123E-03	298.6	.2360E-03	255.3
6	.2395E-03	157.8	.1284E-04	282.3	.3819E-03	202.7	.3575E-03	103.4	.9503E-04	142.8
7	.1022E-02	143.3	.1635E-04	257.5	.9767E-03	195.6	.7957E-03	93.4	.1942E-03	134.5
8	.2287E-02	139.1	.3882E-03	175.5	.1985E-02	198.4	.1625E-02	90.6	.3469E-03	146.2
9	.1430E-02	151.8	.4931E-03	167.0	.1195E-02	197.5	.1067E-02	85.5	.1346E-03	152.1
10	.4008E-04	113.7	.4863E-03	172.2	.1433E-02	217.1	.4599E-02	143.2	.4791E-03	237.4

Figure 8. Dynamic Compliance Values for the Heliostat Yoke

AMPLITUDE UNITS: G'S/ LB-SEC

MEAS   *   *   *   *   *   MODES   *   *   *   *   *   *   *   *

	1		2		3		4		5	
	AMPL	PHS	AMPL	PHS	AMPL	PHS	AMPL	PHS	AMPL	PHS
1	.1207E-03	155.5	.3908E-03	195.4	.2060E-03	32.9	.3509E-03	283.1	.8581E-03	205.9
2	.2013E-03	160.8	.4514E-03	206.4	.4730E-03	32.7	.5572E-03	274.3	.1071E-02	245.6
3	.8753E-03	60.5	.4860E-04	311.1	.3002E-03	13.2	.2006E-03	322.6	.5013E-04	257.9
4	.1624E-02	11.9	.4843E-05	342.4	.2581E-03	20.9	.3916E-04	3.2	.7676E-04	115.6
5	.8269E-03	333.9	.1612E-04	295.4	.1099E-03	17.1	.6588E-04	298.6	.6310E-04	255.3
6	.5465E-03	157.8	.8562E-06	282.3	.7341E-04	282.7	.2582E-04	103.4	.2541E-04	142.8
7	.2331E-02	143.3	.1090E-04	257.5	.1877E-03	195.6	.5746E-04	93.4	.5194E-04	134.5
8	.5217E-02	139.1	.2588E-03	175.5	.3815E-03	198.4	.1173E-03	90.6	.9275E-04	146.2
9	.3262E-02	151.8	.3287E-03	167.0	.2297E-03	197.5	.7705E-04	85.5	.3598E-04	152.1
10	.9145E-04	113.7	.3241E-03	172.2	.2754E-03	217.1	.3381E-03	143.2	.1281E-03	237.4

Figure 9. Residue Values for the Heliostat Yoke Assembly

HELIOSTAT   WIND TEST   ACCELEROMETER LOCATION 1
POWER SPECTRAL DENSITY
RMS LEVEL = .0169
10^N G**2/HZ

100   5000
10^{-2} HZ LOG   PSD HELIOSTAT YOKE ASSEMBLY
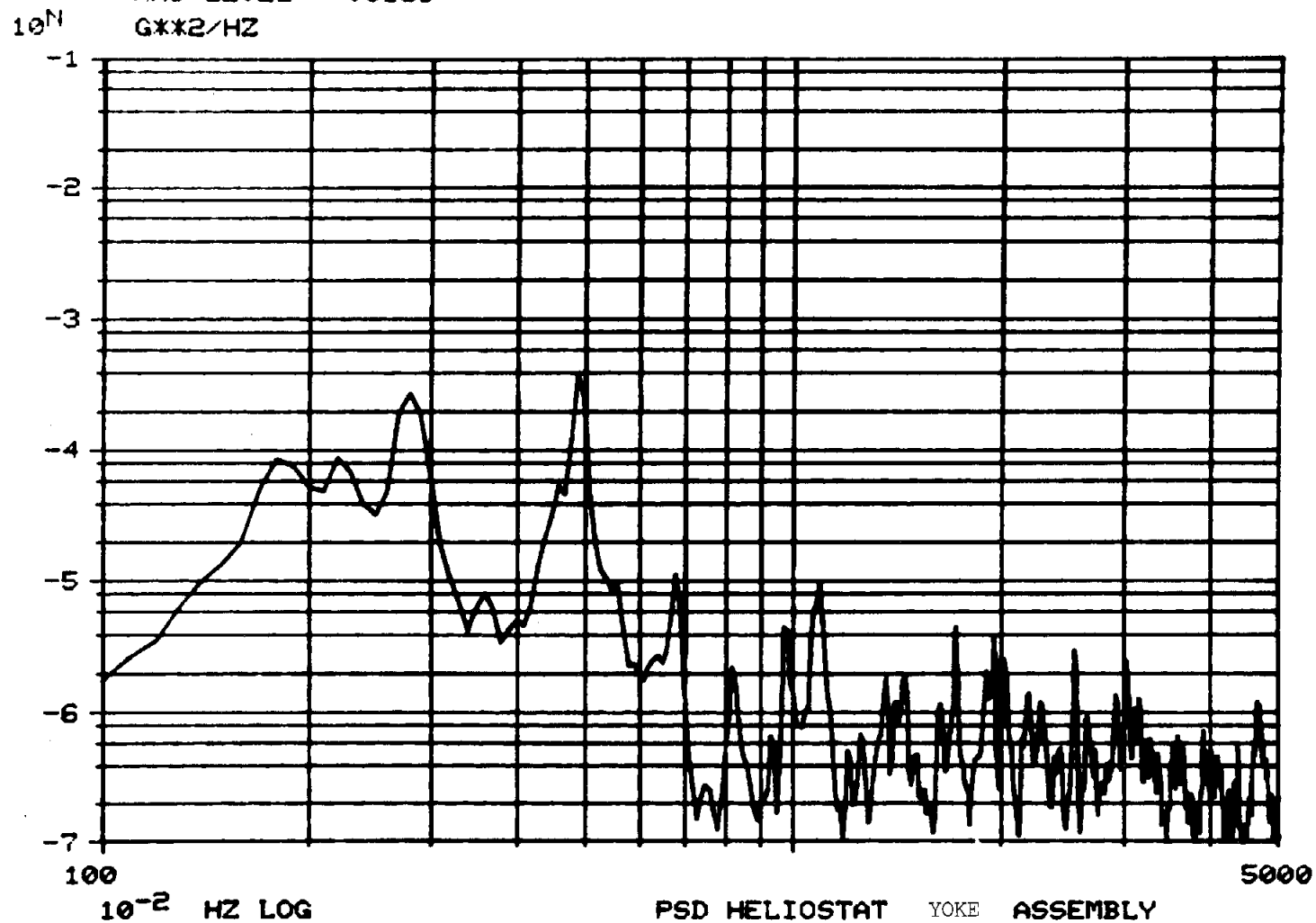
Figure 10. PSD Plot - Heliostat Yoke Assembly

HELIOSTAT   WIND TEST   ACCELEROMETER LOCATION 4
POWER SPECTRAL DENSITY
RMS LEVEL = .0210

10^N G**2/HZ
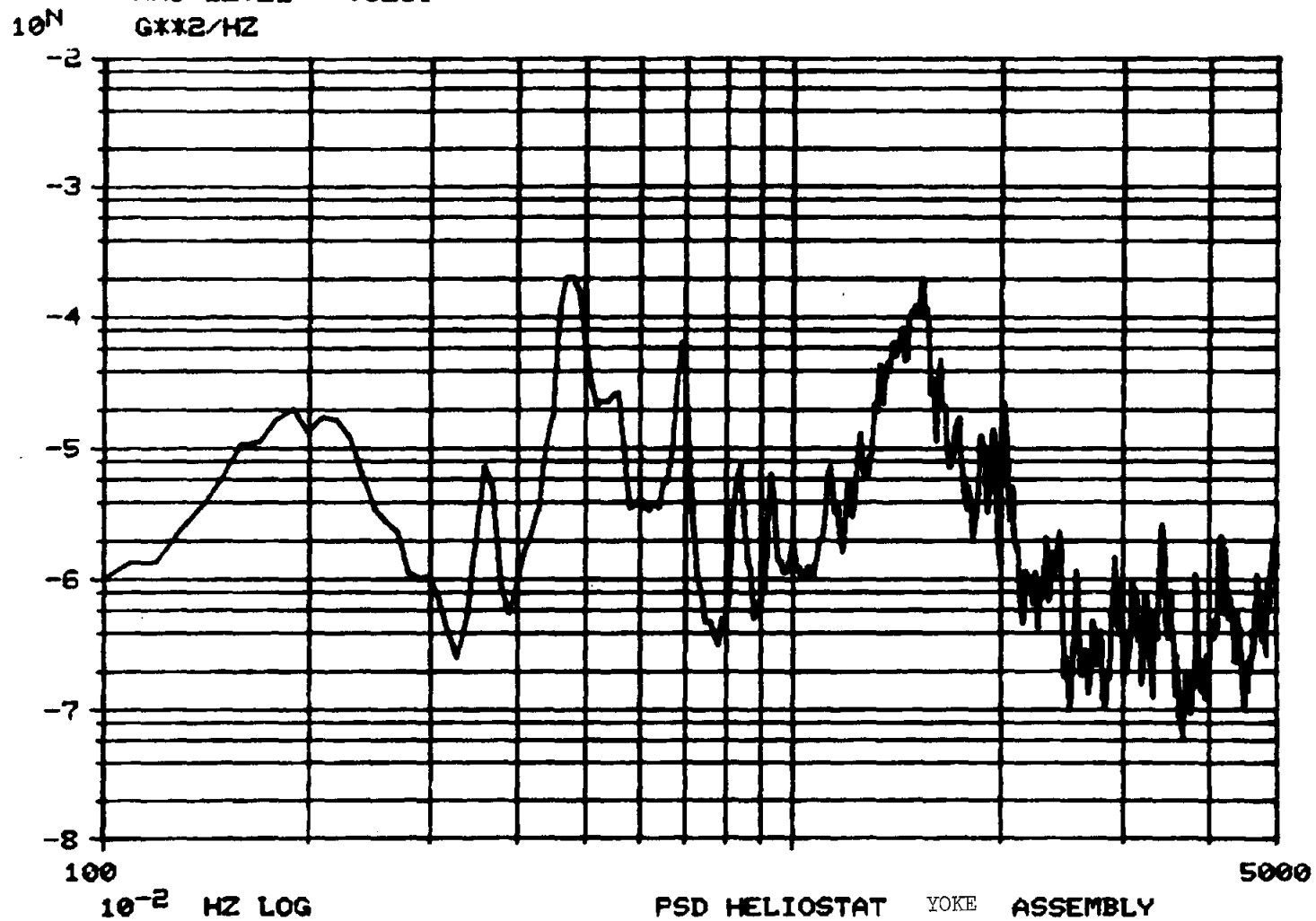
Figure 11. PSD Plot - Heliostat Yoke Assembly

32

HELIOSTST   WIND TEST   ACCELEROMETER LOCATION 6
POWER SPECTRAL DENSITY
RMS LEVEL = .0041

10^N G**2/HZ

100   5000
10^{-2} HZ LOG   PSD HELIOSTAT YOKE   ASSEMBLY
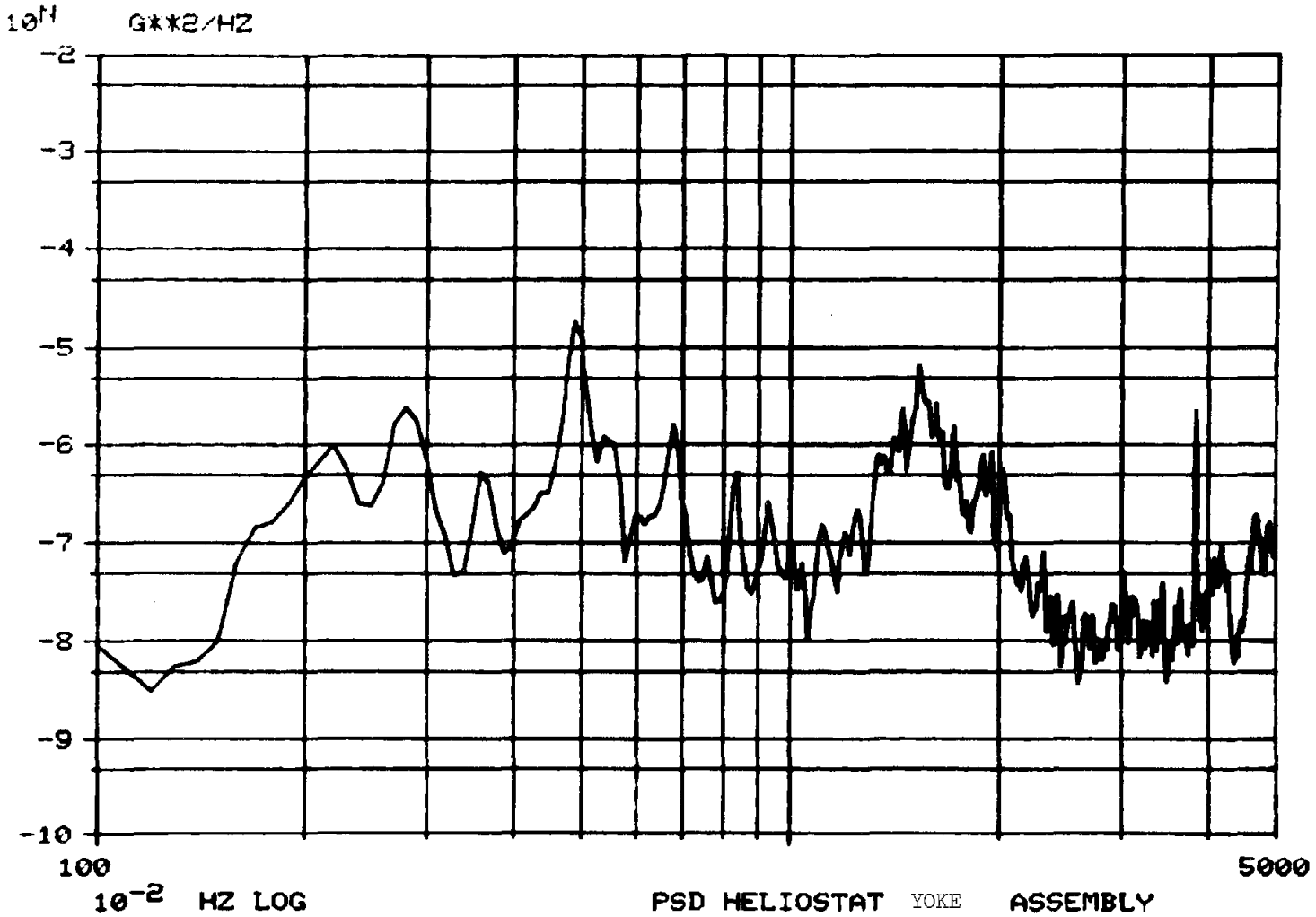
Figure 12.   PSD Plot - Heliostat Yoke Assembly
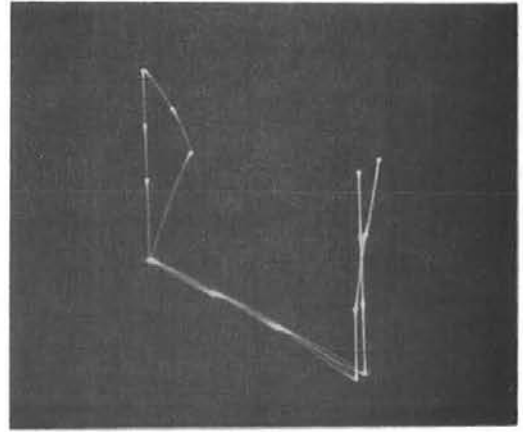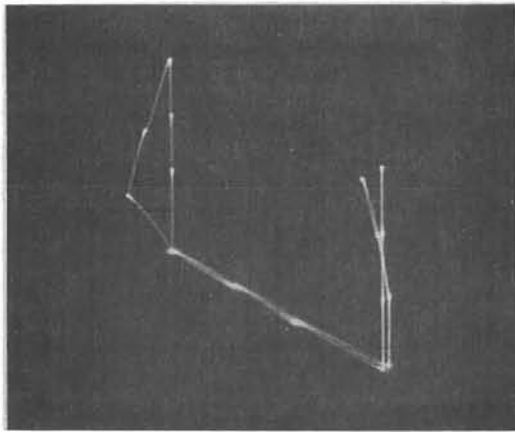
Yoke Assembly - Mode 1 - 1.81 Hz
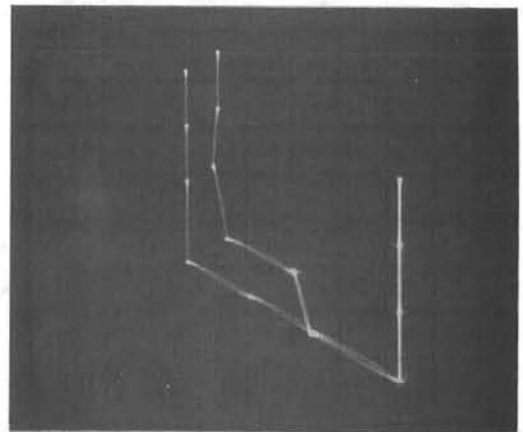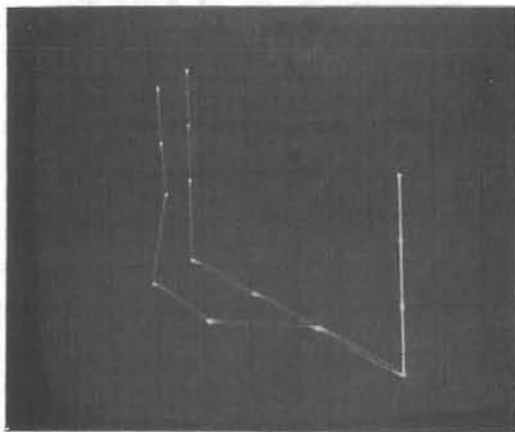
Yoke Assembly - Mode 2 - 2.80 Hz

Figure 13. Yoke and Facet Assembly Mode Shapes
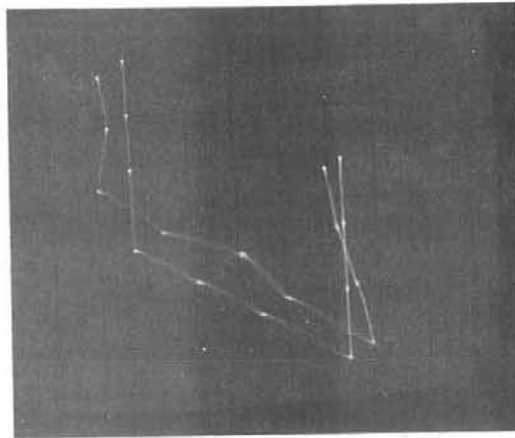
Yoke Assembly - Mode 3 - 3.44 Hz
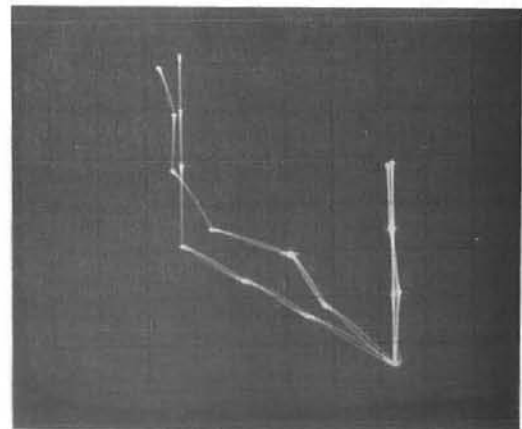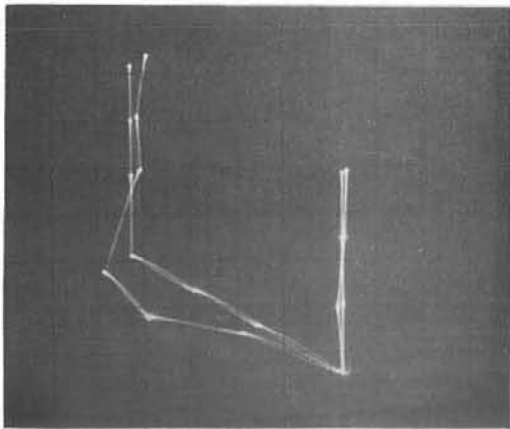
Yoke Assembly - Mode 4 - 3.99 Hz
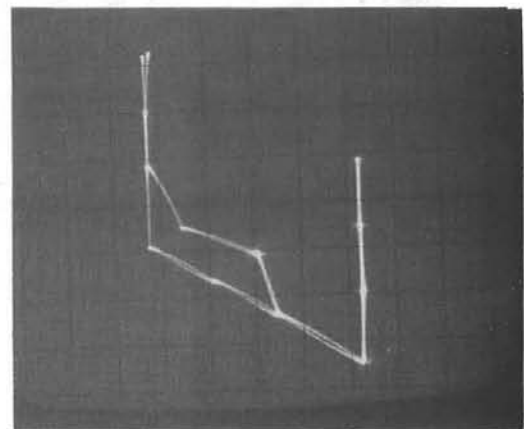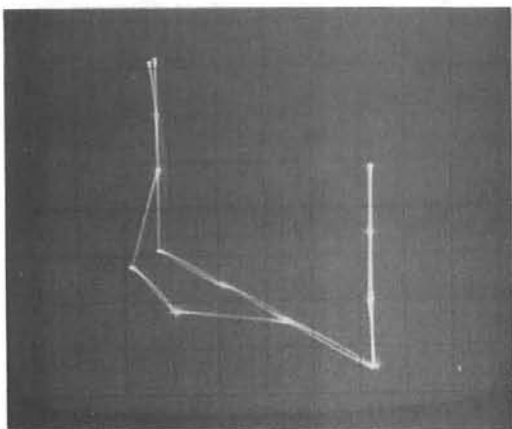
Yoke Assembly - Mode 5 - 4.56 Hz

Figure 13.   Cont'd
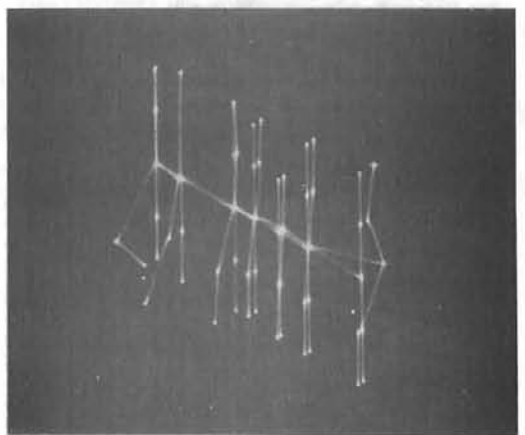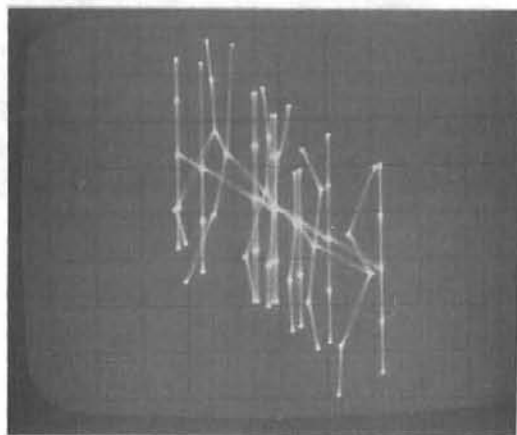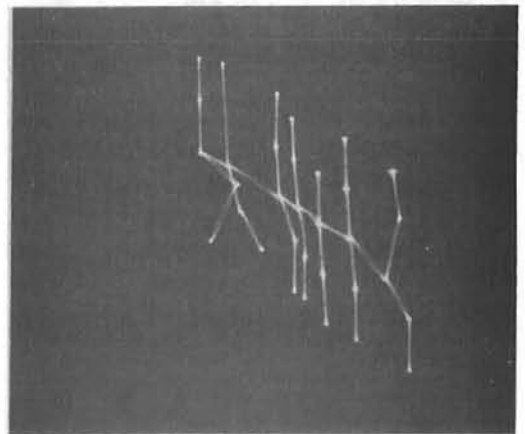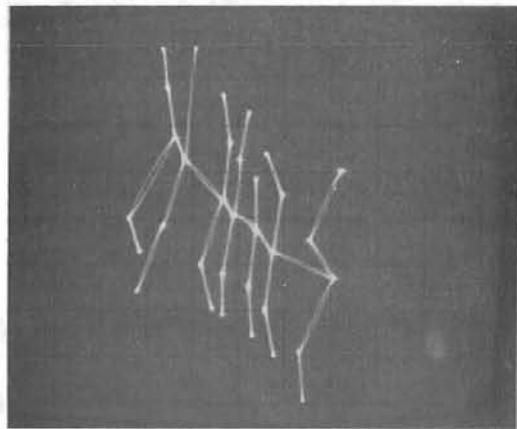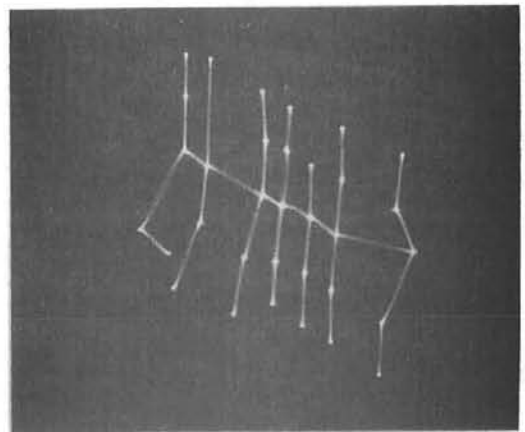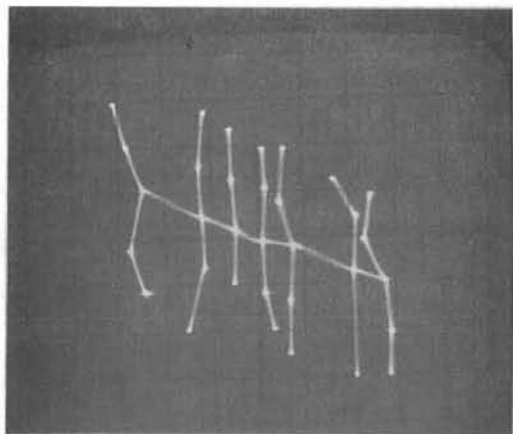
Facet Assembly - Mode 1 - 1.85 Hz   Facet Assembly - Mode 2 - 2.2 Hz

Figure 13. Cont'd
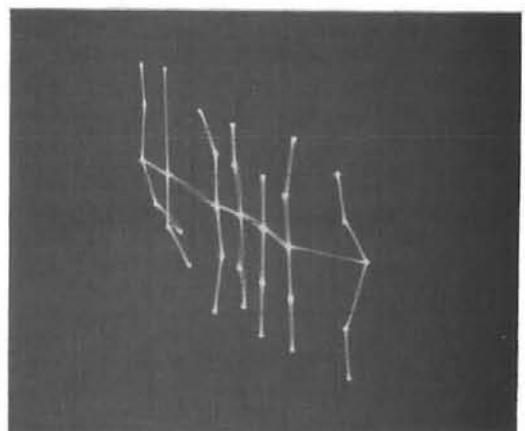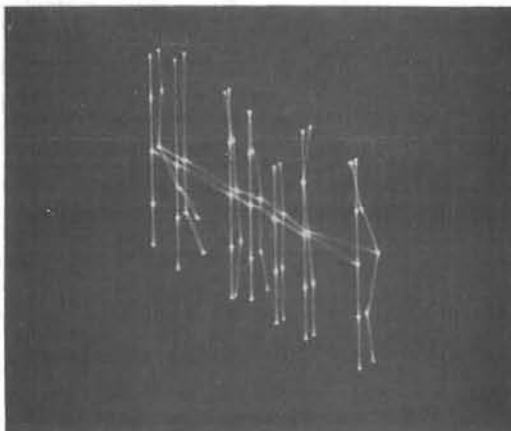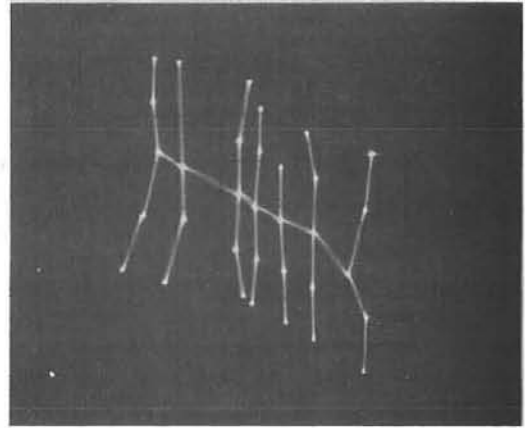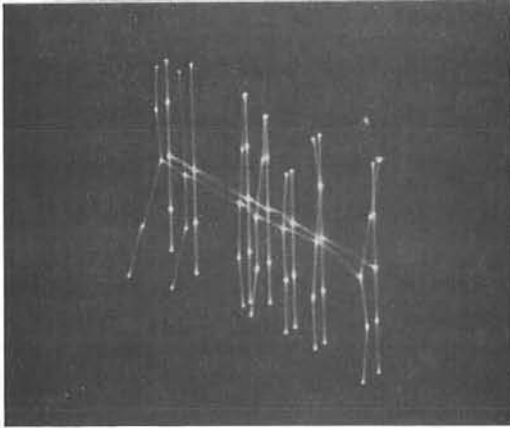
Facet Assembly - Mode 3 - 3.34 Hz

Figure 13. Cont'd
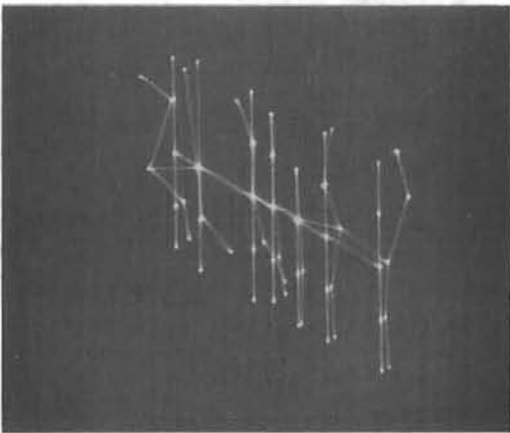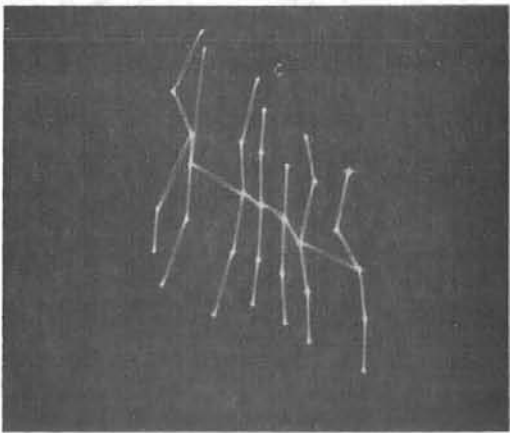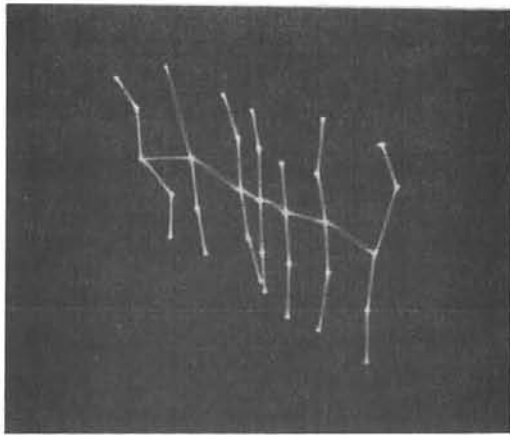
Facet Assembly - Mode 4 - 5.42 Hz   Facet Assembly - Mode 5 - 5.69 Hz
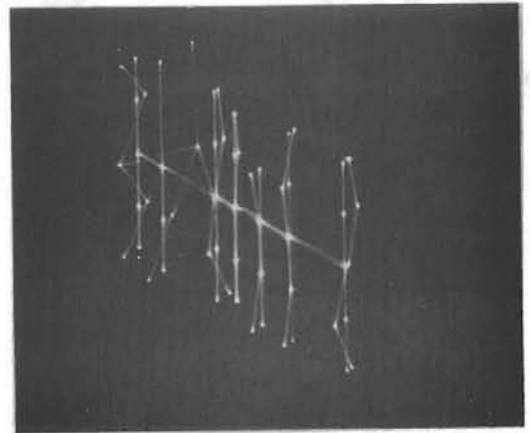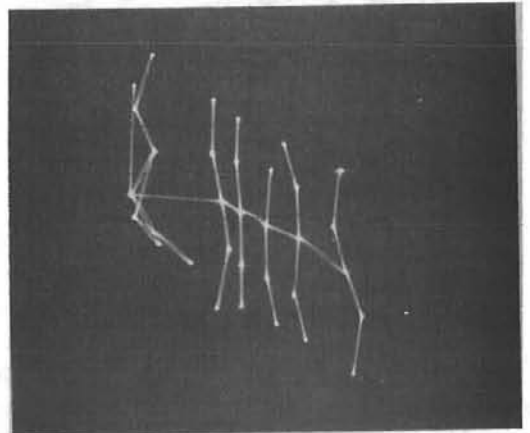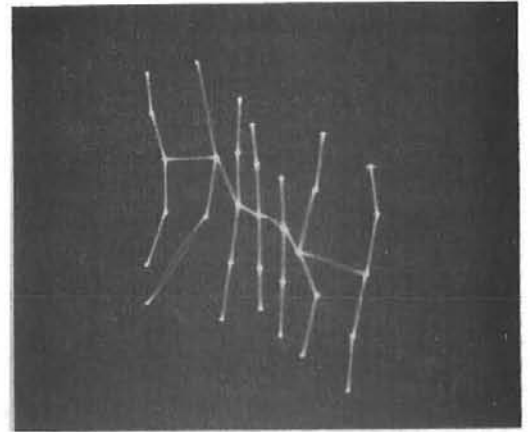
Figure 13.   Cont'd
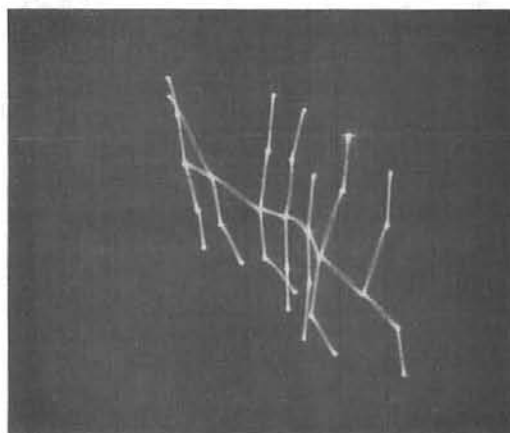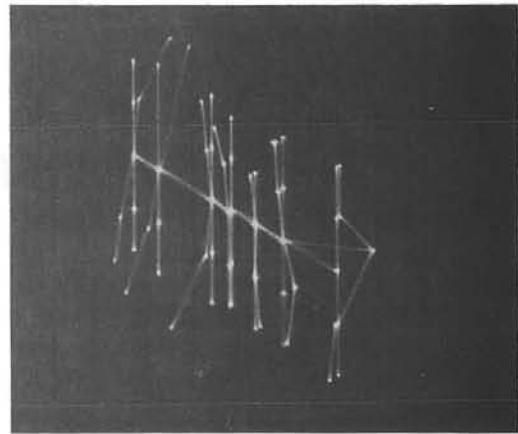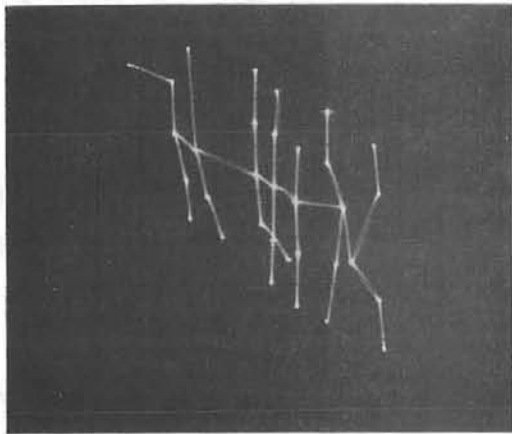
Facet Assembly - Mode 6 - 6.48 Hz

Figure 13. Cont'd
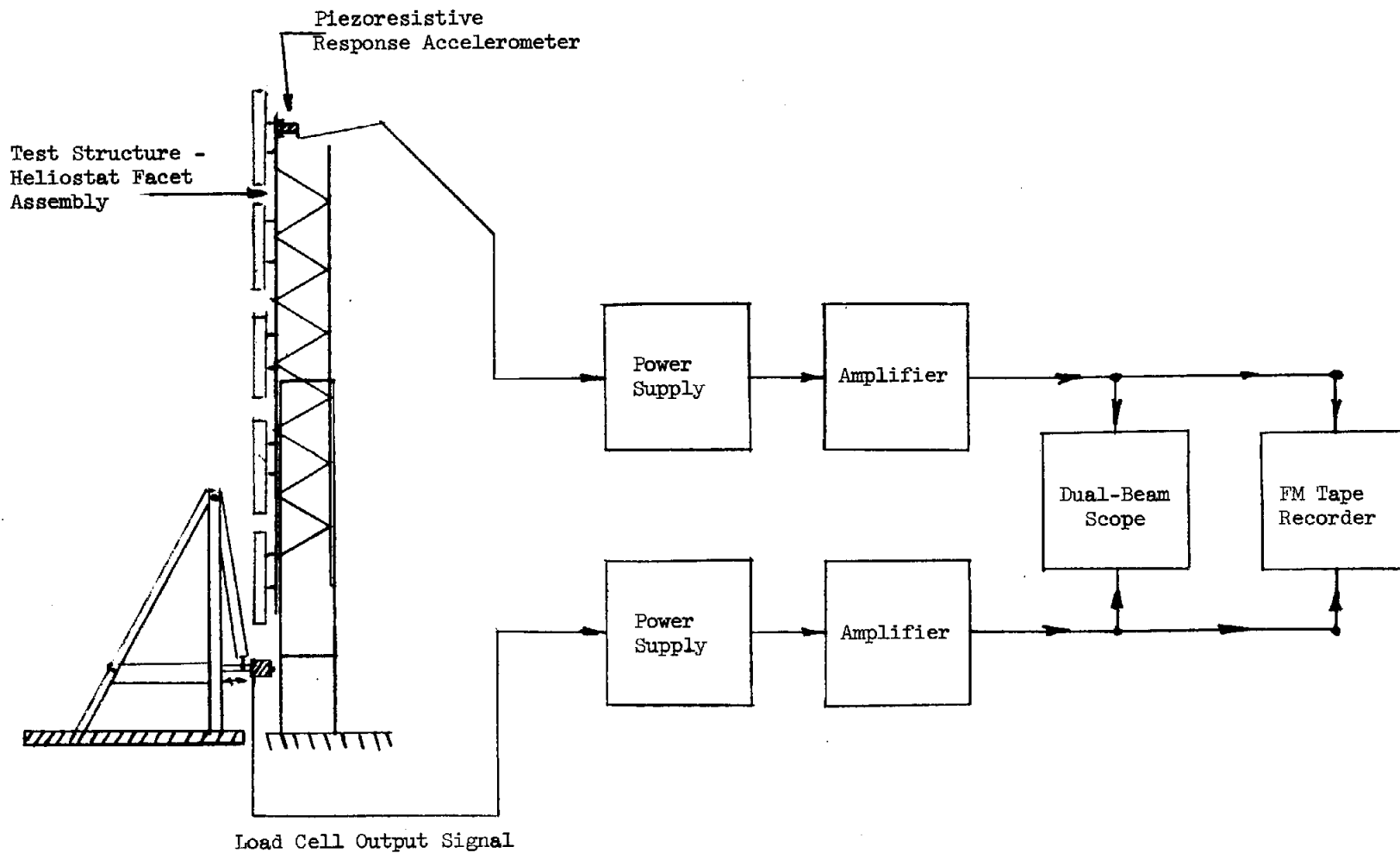
Figure 14. Instrumentation Diagram for Phase 3
Study of Heliostat Facet Assembly

AVERAGE MODAL FREQUENCIES AND DAMPING

*   *   *   *   *   *   *   *   *

MODE	NAT.FREQ. (HZ)	DAMP.FACT. (%)	DAMP.COEFF. (RAD/SEC)
1	1.3526	22.9623	2.7462
2	2.2032	12.7859	1.7846
3	3.3425	5.0983	1.0721
4	5.4214	3.5774	1.2194
5	5.6938	1.4484	.5182
6	6.4891	1.9695	.8032

Figure 15. Modal Frequencies and Damping
for Heliostat Facet Assembly

AMPLITUDE UNITS: IN/LB

	MODES							
	1		**2**		**3**		**4**	
	AMPL	PHS	AMPL	PHS	AMPL	PHS	AMPL	PHS
1	.1295E-02	319.0	.1687E-02	28.6	.2906E-03	1.5	.7293E-03	160.2
2	.3251E-02	31.9	.8872E-03	14.8	.1593E-03	143.3	.1292E-02	168.5
3	.1228E-02	347.7	.3089E-02	13.9	.1017E-02	99.3	.3600E-03	173.5
4	.4096E-02	38.9	.7678E-03	176.5	.5794E-03	195.7	.1990E-03	98.7
5	.4486E-02	16.5	.1201E-02	163.5	.8958E-03	191.4	.3845E-03	90.0
6	.2548E-02	18.5	.9019E-03	38.9	.3100E-03	120.1	.4570E-03	189.9
7	.6191E-03	2.5	.8442E-03	13.1	.1349E-03	235.4	.3743E-03	243.5
8	.1334E-02	45.1	.1955E-03	32.3	.3184E-03	199.7	.5909E-03	152.5
9	.2125E-02	53.8	.4428E-03	209.3	.6101E-03	196.6	.6475E-03	212.7
10	.1213E-02	60.4	.5026E-03	212.4	.5546E-03	194.6	.2747E-03	127.1
11	.5135E-03	354.1	.6339E-03	44.4	.2249E-03	146.1	.9611E-04	32.0
12	.2372E-03	13.3	.5053E-03	37.3	.4685E-03	180.6	.9225E-04	137.2
13	.9310E-03	41.7	.4180E-03	136.9	.4431E-03	191.6	.1933E-03	146.7
14	.7870E-03	11.0	.4328E-03	192.3	.6158E-03	201.7	.9694E-04	113.7
15	.1475E-02	217.3	.9721E-03	24.6	.1537E-03	218.0	.3309E-03	44.7
16	.4795E-03	241.9	.6363E-03	43.1	.2337E-03	197.1	.1005E-03	84.5
17	.1106E-03	86.6	.1088E-03	98.8	.5751E-03	182.6	.6383E-04	100.1
18	.1521E-02	95.0	.7899E-03	212.8	.6168E-03	187.9	.2624E-03	103.5
19	.1353E-02	88.0	.1024E-02	185.0	.9576E-03	184.4	.5381E-03	102.9
20	.7381E-03	211.0	.6274E-03	118.2	.1048E-02	236.5	.6443E-03	349.2
21	.1453E-02	231.8	.4178E-03	43.2	.2276E-03	183.8	.1966E-03	80.1
22	.1197E-02	185.1	.3222E-04	180.0	.4796E-03	196.2	.2264E-04	55.7
23	.1565E-02	75.2	.2182E-02	207.6	.4732E-03	171.3	.4329E-03	187.4
24	.5204E-03	113.5	.3697E-02	174.0	.5460E-03	211.3	.1220E-02	193.7
25	.1259E-02	227.9	.5162E-03	96.2	.5738E-03	181.9	.7715E-03	9.3
26	.2398E-02	212.9	.3211E-03	184.2	.3841E-03	165.7	.2565E-03	209.8
27	.2570E-02	144.2	.1766E-02	248.5	.4126E-03	171.1	.3852E-03	214.1
28	.2814E-02	82.2	.4534E-02	215.8	.1100E-02	124.7	.1252E-02	187.6
29	.3054E-02	198.2	.2297E-03	69.7	.4197E-03	165.7	.1760E-02	2.7
30	.3430E-02	202.5	.1928E-03	88.9	.4776E-03	151.8	.1278E-02	47.0
31	.3730E-02	221.0	.2747E-03	120.6	.3237E-03	160.7	.1040E-02	329.5
32	.1463E-02	104.7	.5458E-02	197.8	.1208E-02	164.4	.3549E-03	162.2
33	.1286E-02	155.8	.2039E-02	177.6	.1837E-02	131.9	.5665E-03	120.2

Figure 16. Dynamic Compliance Values for Heliostat Facet Assembly

AMPLITUDE UNITS: IN/LB

MEAS   *   *   MODES   *   *

	5		6	
	AMPL	PHS	AMPL	PHS
1	.1877E-03	353.9	.5272E-04	98.8
2	.4692E-03	358.6	.5610E-04	340.8
3	.2217E-03	294.3	.4726E-03	40.0
4	.5455E-03	220.2	.6330E-04	166.2
5	.1195E-02	272.7	.1371E-03	190.2
6	.3486E-03	46.0	.1675E-03	181.8
7	.3728E-03	121.8	.8749E-04	189.7
8	.6521E-03	257.1	.4044E-03	311.0
9	.9954E-04	79.8	.4526E-03	330.2
10	.4868E-03	229.2	.5832E-04	346.2
11	.3468E-03	152.2	.9274E-04	183.5
12	.6325E-04	177.2	.1344E-04	95.4
13	.1169E-03	251.6	.1156E-04	251.1
14	.3583E-03	168.6	.8090E-04	357.8
15	.3657E-03	267.7	.3055E-03	181.4
16	.2873E-03	237.8	.1254E-03	184.2
17	.6473E-04	137.8	.3695E-04	218.4
18	.5282E-04	219.9	.4321E-04	179.3
19	.5236E-04	253.0	.6616E-04	147.7
20	.1610E-03	313.3	.1642E-03	186.7
21	.4936E-03	299.7	.7468E-04	192.6
22	.9759E-04	214.8	.7850E-04	313.0
23	.3799E-03	218.1	.1163E-03	268.3
24	.1390E-02	282.0	.5523E-03	227.6
25	.1189E-02	330.6	.5346E-03	3.7
26	.1234E-02	5.3	.7450E-04	115.6
27	.5880E-03	52.1	.1423E-03	204.3
28	.1562E-02	243.8	.4558E-03	209.4
29	.5396E-03	195.4	.6093E-03	75.9
30	.8287E-03	286.8	.9468E-04	6.5
31	.9813E-03	127.1	.5179E-05	16.0
32	.3834E-03	322.1	.1857E-03	218.3
33	.6301E-03	206.5	.2639E-03	213.7

Figure 16.   Cont'd

AMPLITUDE UNITS: G/S/ LB-SEC

MEAS * * * * * MODES * * * * *

	1		2		3		4	
	AMPL	PHS	AMPL	PHS	AMPL	PHS	AMPL	PHS
1	.2495E-02	319.0	.2989E-02	28.6	.7119E-03	1.5	.5345E-02	160.2
2	.6265E-02	31.9	.1572E-02	14.8	.3903E-03	143.3	.9467E-02	168.5
3	.2366E-02	347.7	.5471E-02	13.9	.2490E-02	99.3	.2639E-02	170.5
4	.7395E-02	38.9	.1360E-02	176.5	.1419E-02	195.7	.1459E-02	93.7
5	.8647E-02	16.5	.2128E-02	163.5	.2194E-02	191.4	.2818E-02	90.0
6	.4912E-02	18.5	.1598E-02	38.9	.7593E-03	120.1	.3350E-02	189.0
7	.1193E-02	2.5	.1496E-02	13.1	.3304E-03	235.4	.2743E-02	243.5
8	.2572E-02	45.1	.3462E-03	32.3	.7799E-03	199.7	.4331E-02	152.5
9	.4095E-02	53.8	.7844E-03	209.3	.1494E-02	196.6	.4746E-02	212.7
10	.2339E-02	60.4	.8904E-03	212.4	.1359E-02	194.6	.2014E-02	127.1
11	.9897E-03	354.1	.1123E-02	44.4	.5509E-03	146.1	.7044E-03	32.0
12	.5535E-03	13.3	.8951E-03	37.3	.1148E-02	180.6	.6761E-03	137.3
13	.1891E-02	41.7	.7406E-03	136.9	.1085E-02	191.6	.1417E-02	146.7
14	.1517E-02	11.0	.7666E-03	192.3	.1508E-02	201.7	.7105E-03	113.7
15	.2842E-02	217.3	.1722E-02	24.6	.3766E-03	218.0	.2425E-02	44.7
16	.9243E-03	241.9	.1127E-02	43.1	.5724E-03	197.1	.7366E-03	24.5
17	.2131E-03	86.6	.1927E-03	98.8	.1409E-02	182.6	.4678E-03	100.1
18	.2932E-02	95.0	.1399E-02	212.8	.1511E-02	187.9	.1923E-02	103.5
19	.2508E-02	83.0	.1814E-02	185.0	.2346E-02	184.4	.3944E-02	102.9
20	.1519E-02	211.0	.1111E-02	118.2	.2567E-02	236.5	.4723E-02	349.3
21	.2300E-02	231.8	.7402E-03	43.2	.5576E-03	188.8	.1441E-02	89.1
22	.2308E-02	135.1	.5708E-04	130.0	.1175E-02	196.2	.1659E-03	55.7
23	.3916E-02	75.2	.3365E-02	207.6	.1159E-02	171.3	.3217E-02	120.4
24	.1003E-02	113.5	.6550E-02	174.0	.1337E-02	211.3	.3945E-02	123.7
25	.6281E-02	227.9	.9144E-03	96.2	.1406E-02	181.9	.5655E-02	3.2
26	.4603E-02	212.9	.5688E-03	184.2	.9409E-03	165.7	.1880E-02	359.0
27	.4955E-02	144.2	.3129E-02	248.5	.1011E-02	171.1	.2323E-02	214.1
28	.5423E-02	82.2	.8031E-02	215.8	.2695E-02	124.7	.9175E-03	127.6
29	.5887E-02	198.2	.4069E-03	69.7	.1028E-02	165.7	.1290E-01	2.7
30	.6011E-02	202.5	.3415E-03	88.9	.1170E-02	151.8	.9364E-02	47.0
31	.7226E-02	221.0	.4866E-03	120.6	.7930E-03	160.7	.7626E-02	329.5
32	.2219E-02	104.7	.9668E-02	197.8	.2959E-02	164.4	.2601E-02	162.1
33	.2479E-02	155.8	.3611E-02	177.6	.4500E-02	131.9	.4152E-02	180.2

Figure 17. Residue Values for Heliostat Facet Assembly

AMPLITUDE UNITS: G'S/ LB-SEC

MODE		MODES		
	5		**6**	
	AMPL	PHS	AMPL	PHS
1	.6448E-03	353.9	.3647E-03	98.8
2	.1612E-02	358.6	.3880E-03	340.8
3	.7617E-03	294.3	.3268E-02	40.0
4	.1574E-02	220.2	.4378E-03	166.2
5	.4107E-02	272.7	.9486E-03	190.2
6	.1198E-02	46.0	.1159E-02	181.8
7	.1291E-02	121.8	.6051E-03	189.7
8	.2240E-02	257.1	.2797E-02	311.0
9	.3420E-03	79.8	.3130E-02	330.2
10	.1604E-02	229.2	.4034E-03	346.2
11	.1192E-02	152.2	.6414E-03	183.5
12	.2173E-03	177.2	.9295E-04	95.4
13	.4017E-03	251.6	.7995E-04	251.1
14	.1231E-02	168.6	.5595E-03	357.8
15	.1256E-02	267.7	.2113E-02	181.4
16	.9289E-03	237.3	.8674E-03	184.2
17	.2204E-03	187.8	.2556E-03	218.4
18	.1315E-03	219.9	.2938E-03	179.3
19	.1799E-03	253.0	.4576E-03	147.7
20	.9501E-03	313.3	.1136E-02	186.7
21	.1713E-02	299.7	.5165E-03	192.6
22	.3253E-03	214.8	.5429E-03	313.0
23	.1305E-02	218.1	.8047E-03	268.3
24	.4775E-02	282.0	.3820E-02	227.6
25	.4086E-02	330.6	.3698E-02	3.7
26	.4239E-02	5.3	.5153E-03	115.6
27	.2020E-02	52.1	.9841E-03	204.3
28	.5366E-02	243.8	.3152E-02	209.4
29	.1854E-02	195.4	.4214E-02	75.9
30	.2847E-02	286.8	.6549E-03	6.5
31	.3372E-02	127.1	.3582E-04	16.0
32	.1317E-02	322.1	.1284E-02	218.3
33	.2165E-02	206.5	.1825E-02	213.7

Figure 17. Cont'd
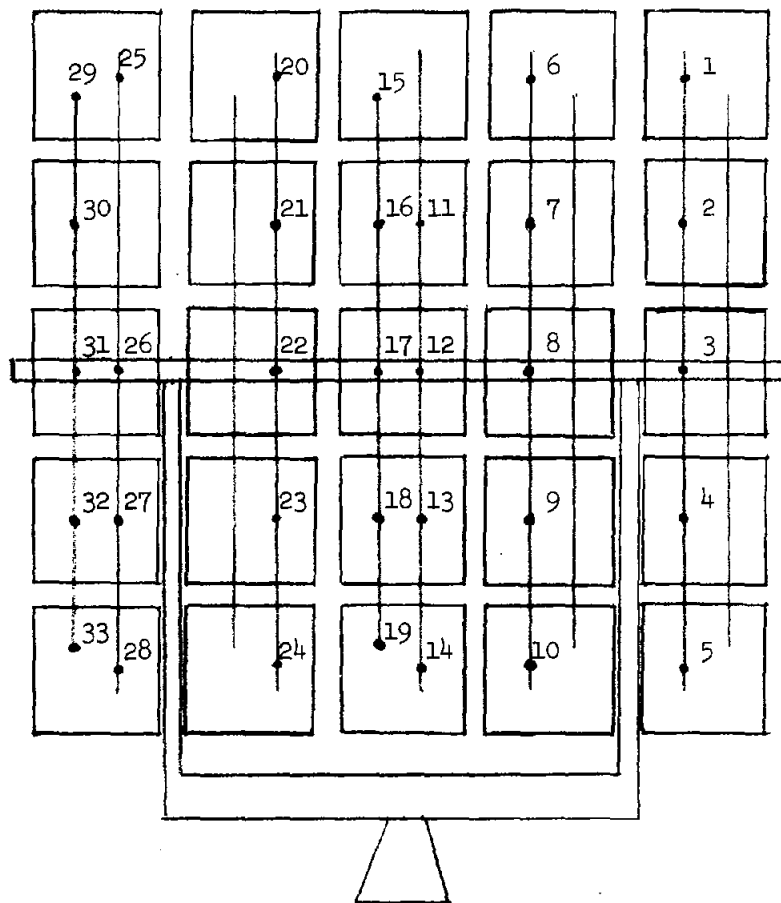
Figure 18. Response Transducer Locations
with Respect to Test Structure
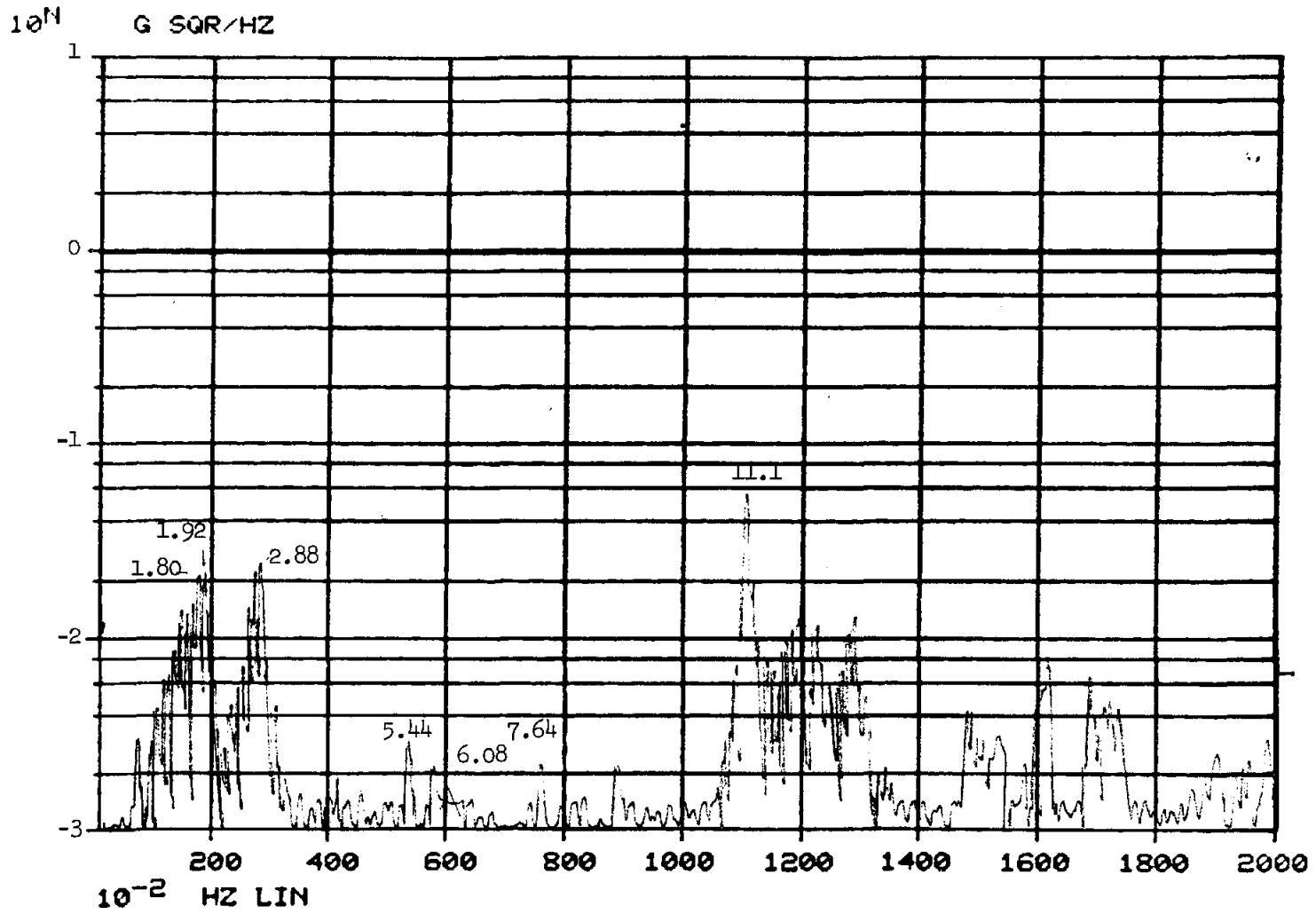
Figure 19.   PSD Plot - Accelerometer Position 14, Facet Assembly
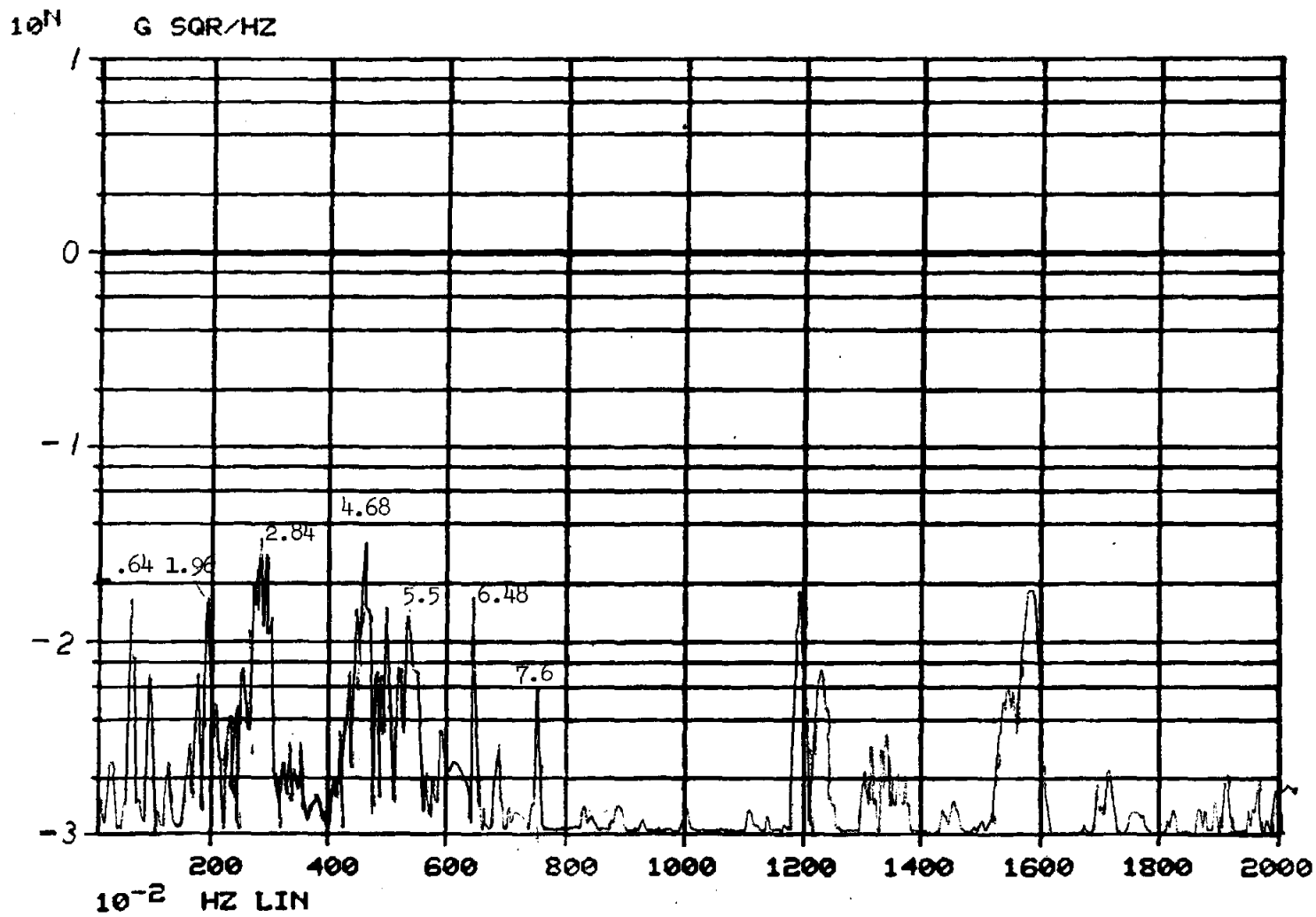
Figure 20.   PSD Plot - Accelerometer Position 19, Facet Assembly

47
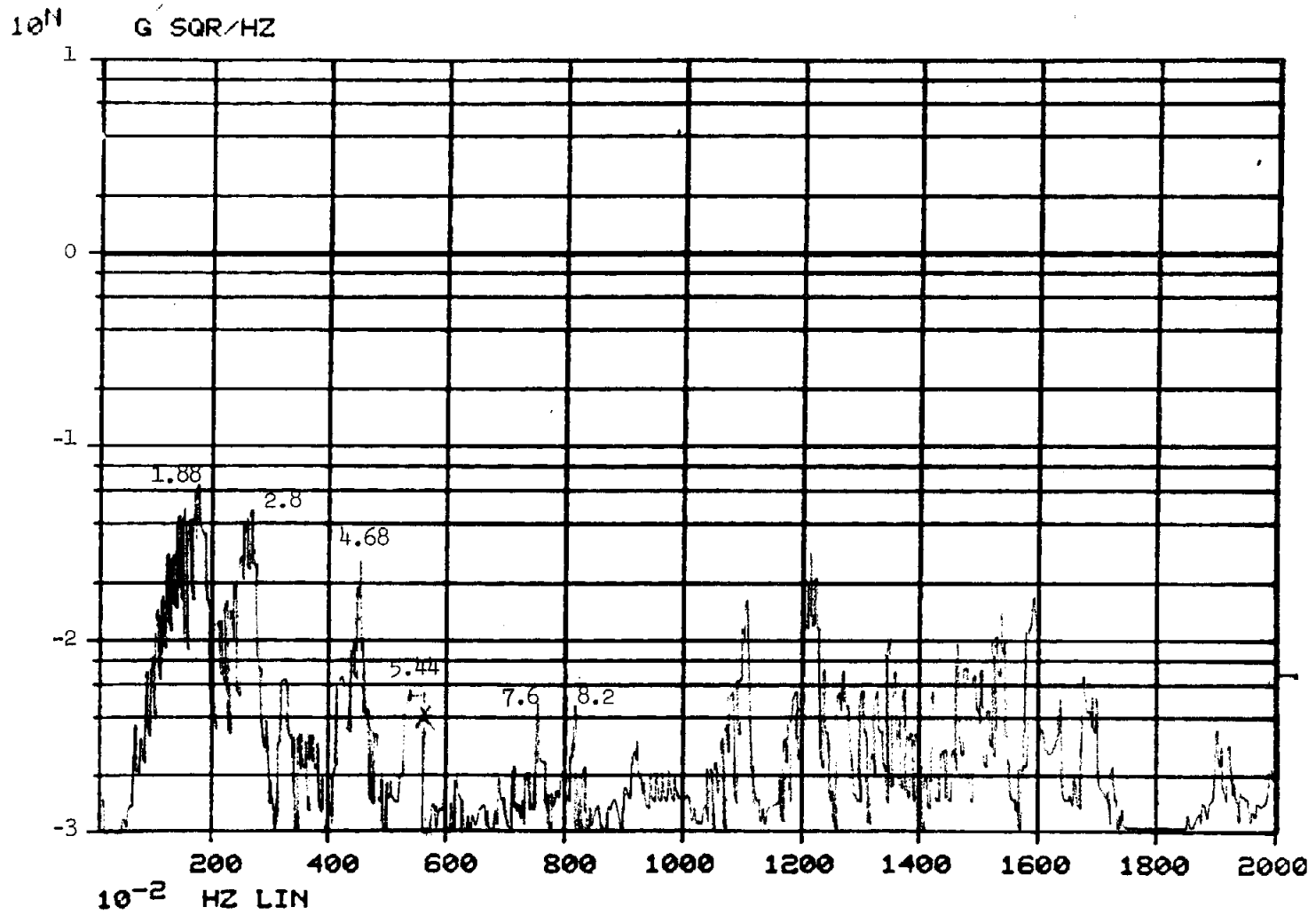
Figure 21. PSD Plot - Accelerometer Position 5, Facet Assembly
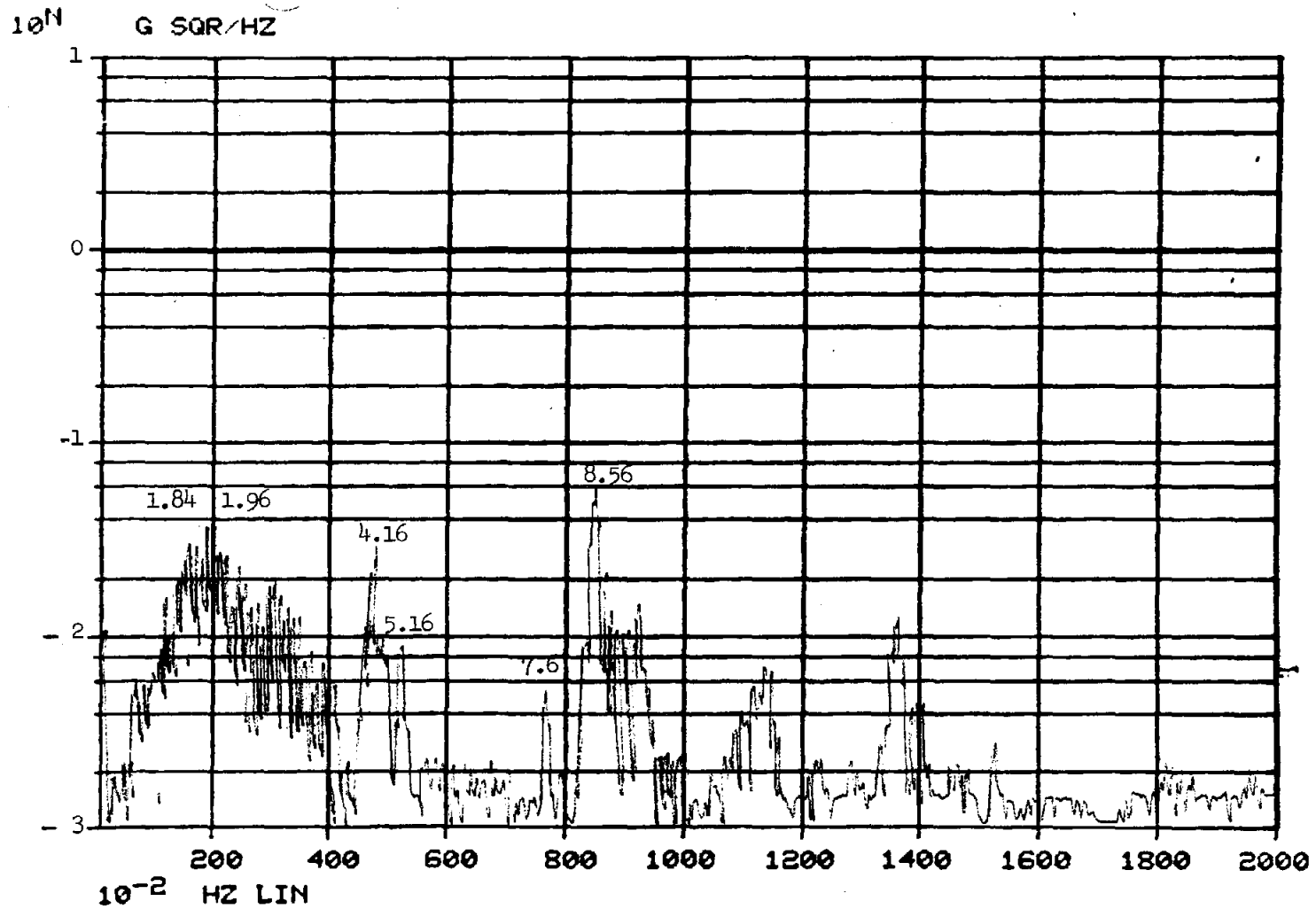
Figure 22. PSD Plot - Accelerometer Position 33, Facet Assembly
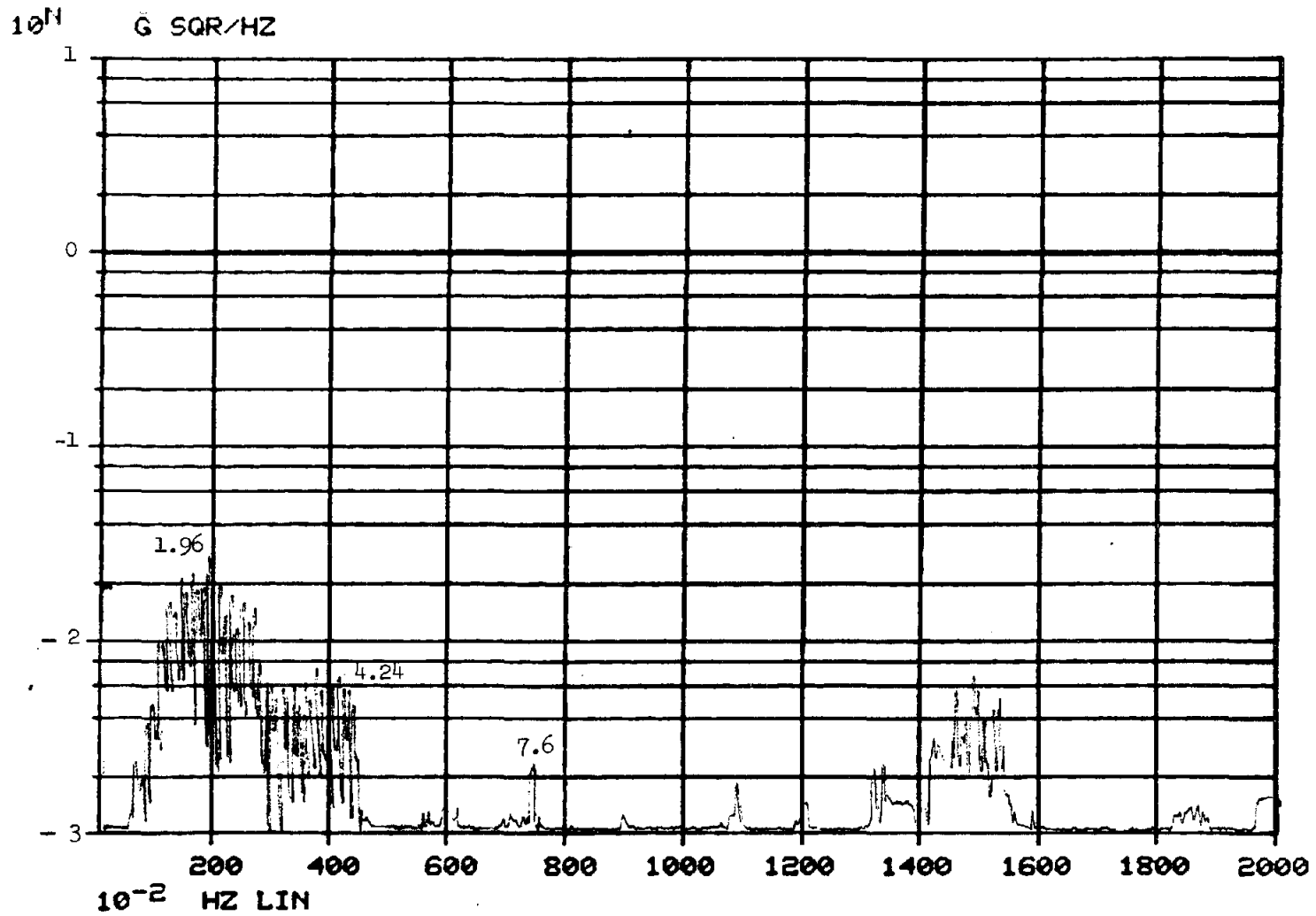
Figure 23. PSD Plot - Accelerometer Position 3, Facet Assembly

10^N   G SQR/HZ
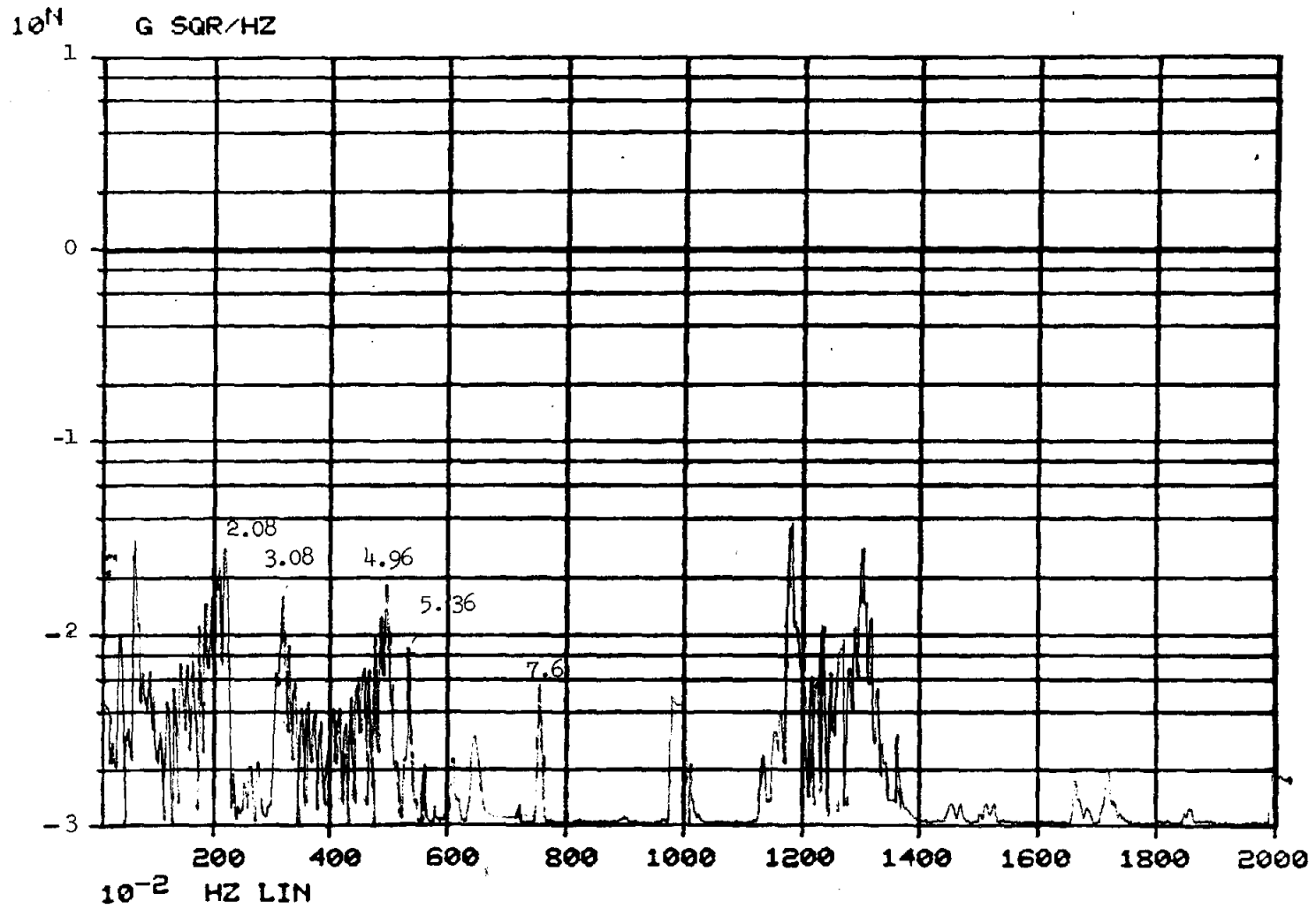
Figure 24.   PSD Plot - Accelerometer Position 21, Facet Assembly
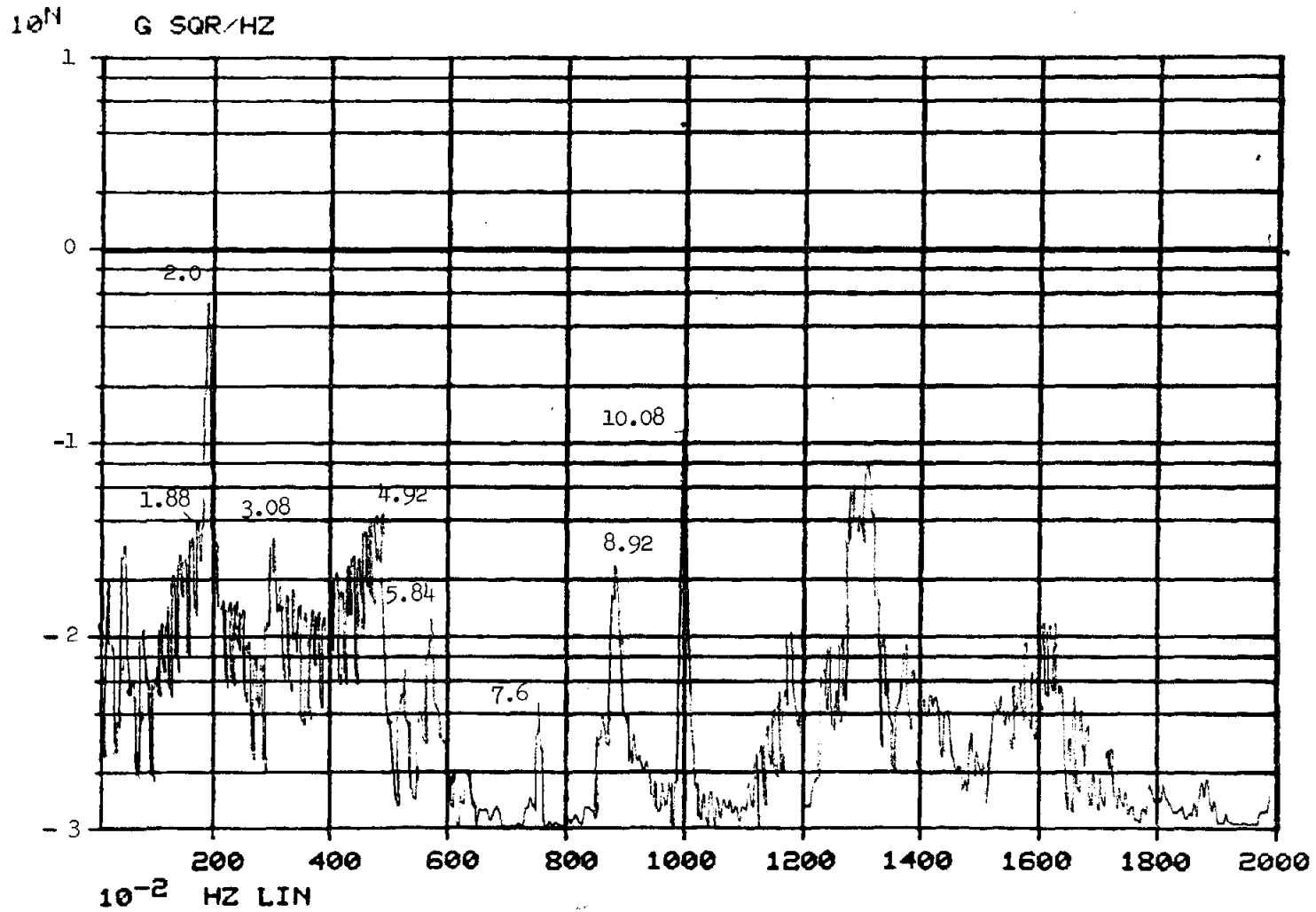
Figure 25. PSD Plot - Accelerometer Position 25, Facet Assembly
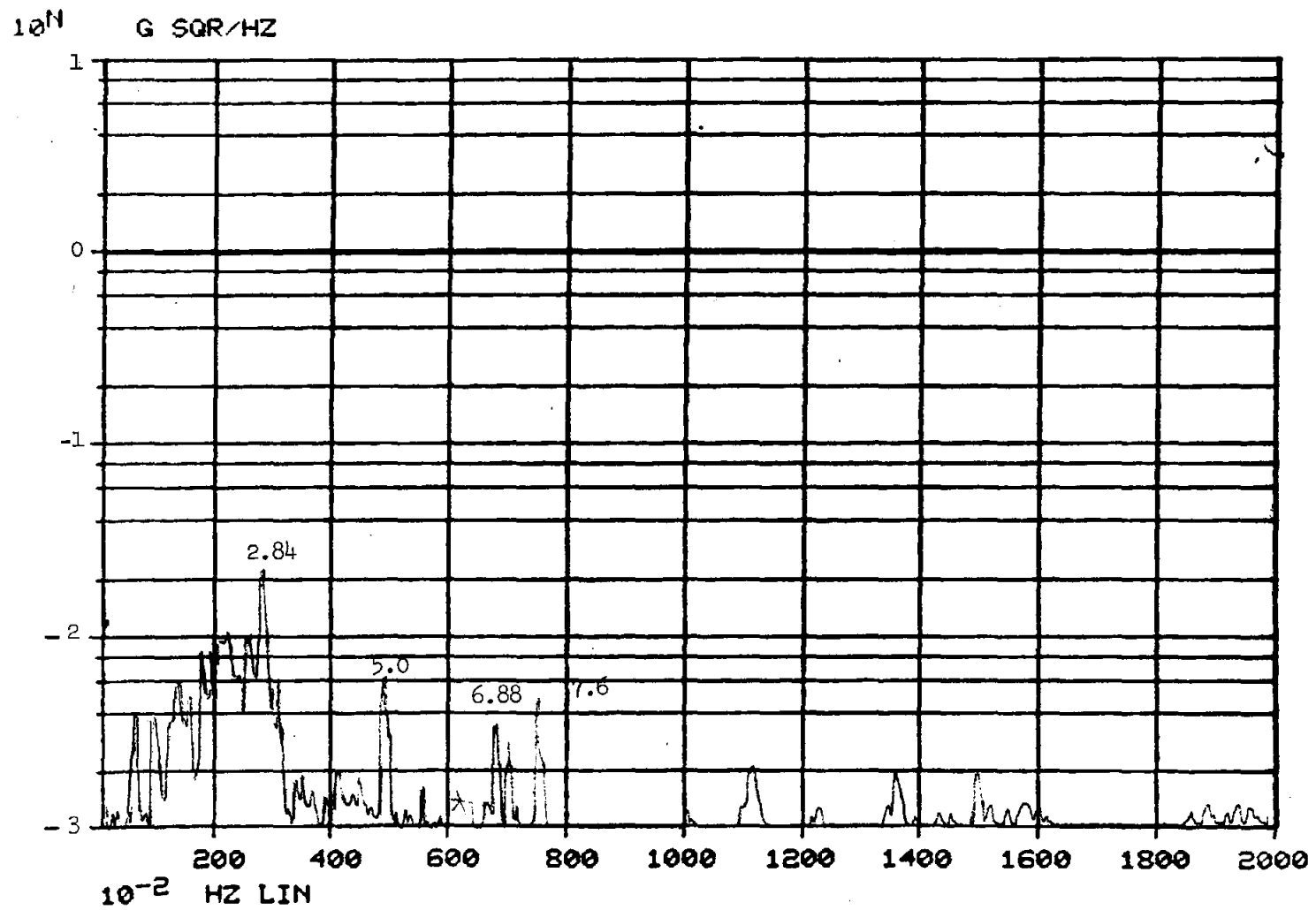
Figure 26. PSD Plot - Accelerometer Position 12, Facet Assembly

10^N G SQR/HZ
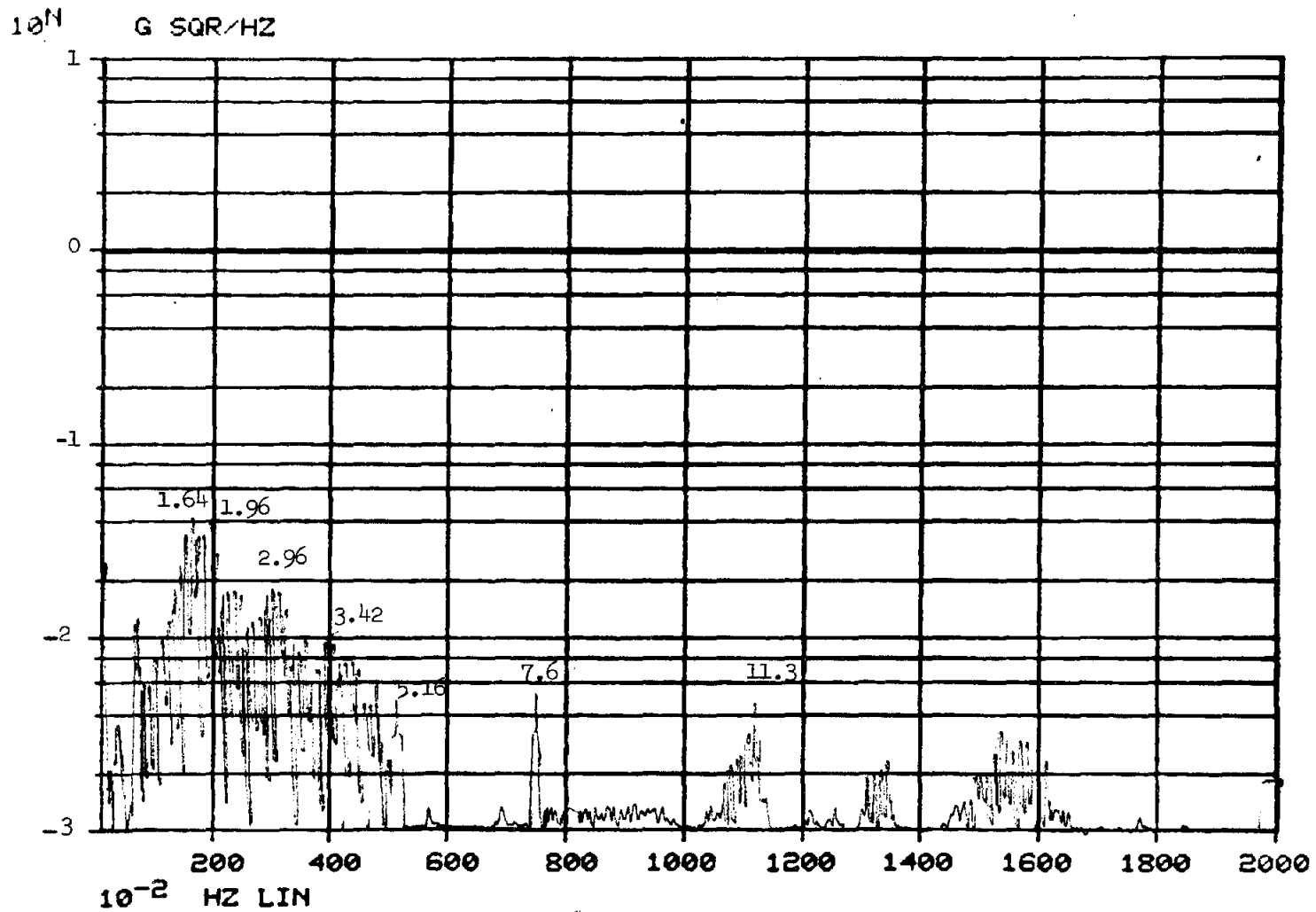
Figure 27.   PSD Plot - Accelerometer Position 31, Facet Assembly
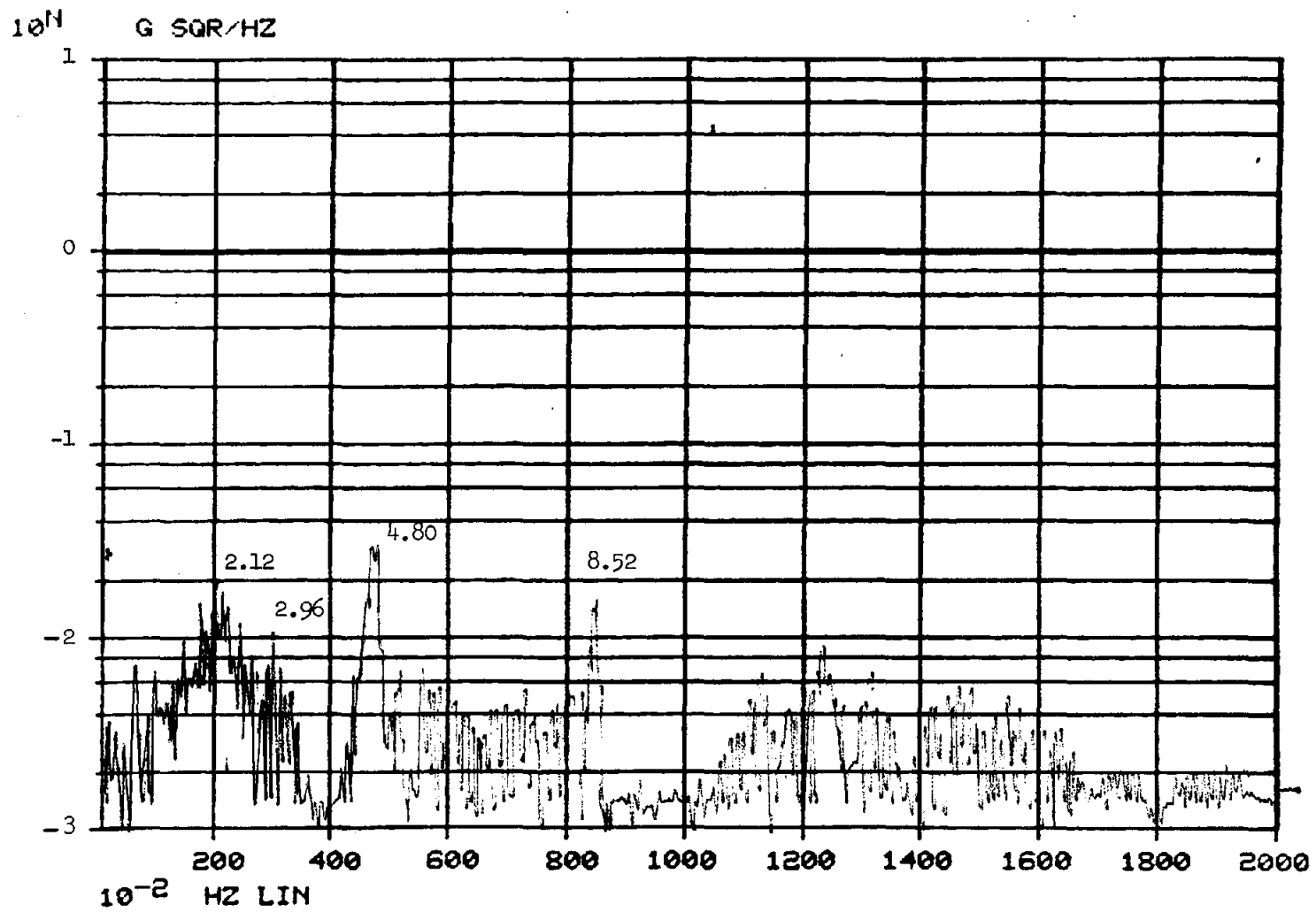
Figure 28. PSD Plot - Accelerometer Position 28, Facet Assembly

55

Lateral
Restraints
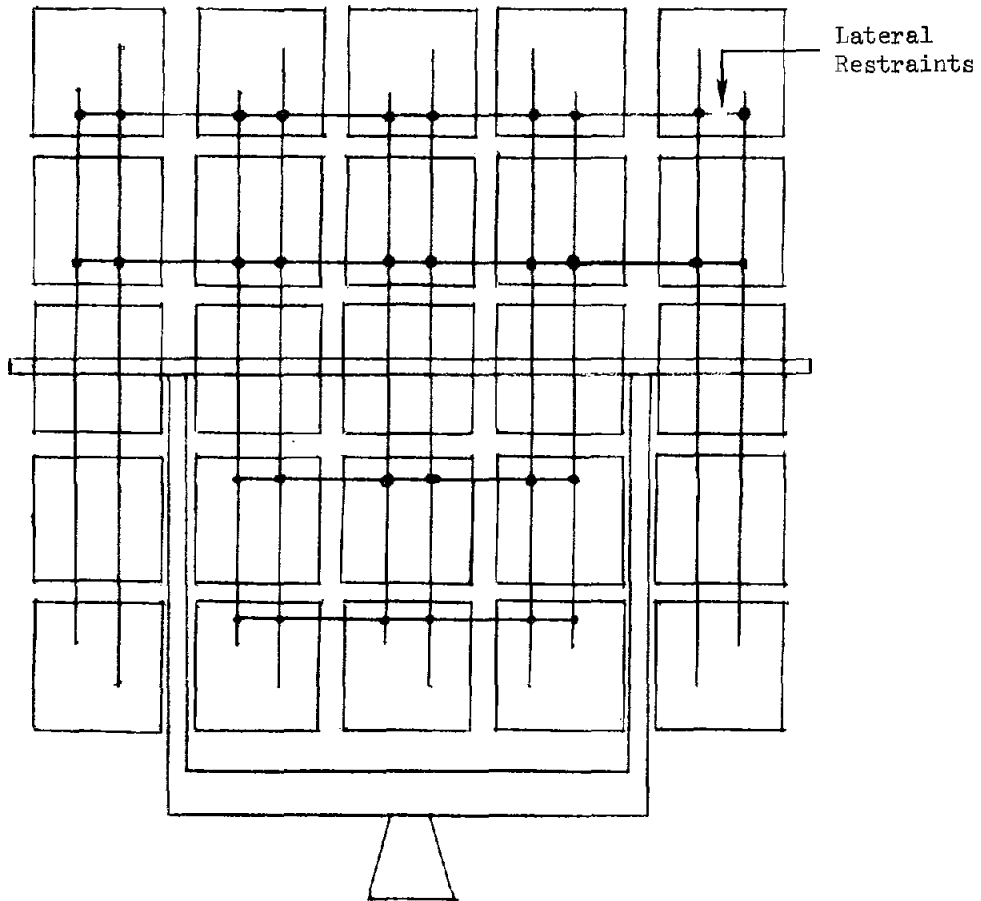
Figure 29. Possible Structural Modification
to Heliostat Facet Assembly

APPENDIX A

APPENDIX A

Preliminary (Phase 1) Yoke Assembly Modal Study

Introduction

This brief report contains a summary of data and some conclusions which can be drawn from this first, albeit rough, data acquisition/analysis session.

A short overview of the HP-2100 Modal Analysis data system is presented as an insert to this report.

To obtain the data presented herein, an impulsive input was used for excitation to obtain the system transfer functions. The structure was excited (at one location) by means of a hydraulic ram. The input excitation was measured by a strain gage load cell. The response was obtained at ten locations along the structure, and was measured by means of a Kistler 303B servo-accelerometer.

Since this was intended as a preliminary study, data was taken only on the heliostat yoke.

Discussion of Figures/Tables

The average modal frequencies and damping are presented in Figure 1. Figures 2 thru 5 show plots (made by the computer) of the 1st thru 4th mode shapes, along with the undeformed yoke shape. Figure 6 lists the amplitude and phase for the four modes, at the ten measurement points.

I believe that it is quite likely that there are additional modes between the 1st and 2nd listed in Figure 1. But due to limitations encountered with the present data, they weren't identified. (This point will be clarified shortly.)

Due to the remoteness of the structure from Area I, the input and response

signals were recorded on magnetic tape for playback and analysis on the Division 9342 computer in Area I. Data-taking was further constrained to be completed within a few days, as the heliostat was being shipped out. When using the transient test technique, multiple samples of input/response must be taken to obtain the transfer function. With the above considerations, and upon viewing the resultant transfer functions, it appears that:

1. More samples should have been obtained per measurement point, as this would have improved the value of the coherence function (i.e., a measure of causality between response signal and input). Hence a better fit for the transfer functions would have been arrived at; and

2. Longer record lengths (i.e., 1 sample of input and response) are necessary, as resolution would be possible.

Data Conversion to the Time Domain

The steady-state impulse-response of a second order system is given by

$$X(t) = |A| \sin (Ft + p)$$

where,

$|A|$ = mode shape amplitude (or compliance as given by Figure 6)

p = phase angle

F = modal frequency

t = time

As an example, we will find the displacements at points 7 and 10 (the tips of the yoke vertical sections), at times such that, for the 1st mode:

$$(Ft) = 180°, 90°$$

For measurement point 7,

$$|A| = .11 \times 10^{-1} \text{ in/lb}$$

$$F_1 = 2.39 \text{ Hz} = 14.70 \text{ rad/sec}$$

$$P = 8.8° = .15 \text{ rad}$$

for

$$Ft = 90° = 1.57 \text{ rad}$$

$$\Rightarrow t = .11 \text{ sec}$$

$$X(.11) = (.011) \cdot \sin\left[(1.57 \text{ rad}) + .15 \text{ rad}\right]$$

$$= (.011)(.99)$$

$$= \underline{.0109 \text{ in/lb}}$$

at

$$(Ft) = 180° = 3.14 \text{ rad}$$

$$t = .22 \text{ sec}$$

$$X(.22) = (.011) \sin\left[\left((\pi) + .15 \text{ rad}\right)\right]$$

$$= (.011)(-.148) = \underline{-.0016 \text{ in/lb}}$$

For measurement point 10,

$$|A| = .69 \times 10^{-2} \text{ in/lb}$$

$$P = 193.3° = 3.37 \text{ rad}$$

$$F_1 = 2.39 \text{ Hz} = 14.7 \text{ rad/sec}$$

for

$$(Ft) = 90° \Rightarrow t = .11 \text{ sec}$$

$$X(.11) = (.011) \sin\left[\left((\pi/2) + 3.37\right)\right]$$

$$= .011(-.97) = \underline{-.0107 \text{ in/lb}}$$

for

$$(Ft) = 180° \Rightarrow t = .22 \text{ sec}$$

$$X(.22) = .011\left[\sin(\pi + 3.37)\right]$$

$$= (.011)(.225) = \underline{.0025 \text{ in/lb}}$$

Therefore, considering the points 7 and 10 at

$$(Wt) = 90°$$

then there is a net displacement about zero equal to

$$= (.0109 + .0107) = \underline{.0216 \text{ in/lb}}$$

The "true" value of displacement depends on the magnitude of the input force at the particular modal frequency. This would be determined through a shock spectra or

Fourier analysis of the input signal.

By a Fourier analysis of a typical input signal (see Figures 7, 8 and 9), it was found that approximately 163 lb_f existed at a frequency of 2.38 Hz. This means that the maximum relative displacement of the two yoke vertical sections was

$$(.0216 \ in/lb)(163 \ lb_f) = \underline{\underline{3.5 \ inches}}$$

Conclusions

From the data that has been obtained, it is felt that this is a promising technique for determining the modal displacements of the structure. With the determination of the modal displacement field for the structure, it should prove possible through the geometry to determine pointing errors which would be caused by some input.

Further work definitely needs to be done. In particular, it is necessary to determine whether the input force spectrum used in this experiment closely approximates the shock spectrum due to a wind gust. If not, then this needs to be corrected.

More data needs to be taken with more samples (of input/response) per measurement point to improve the coherence between the input and response, thereby improving the transfer functions obtained. It is also necessary to lengthen (in time) the records taken, so that frequency resolution can be increased, and all significant modes can be identified.

As has been pointed out, the numbers obtained thus far have to be viewed very cautiously until it can be determined whether or not the force levels used are reasonably close to the actual in-service levels.

```
AVERAGE MODAL FREQUENCIES AND DAMPING
 *    *   ·  *     *     *     *     *     *     *


        NAT.FREQ.    DAMP.FACT.    DAMP.COEFF.
MODE     (HZ)          (%)          (RAD/SEC)
  1      2.3869        .0885          .0133
  2     12.7746      10.8544         8.7641
  3     13.6752       6.6456         5.7228
  4     18.2966       3.8071         4.3798
```

Figure A-1

1ST MODE —

2.38HZ

HELIOSTAT YOKE   11/12
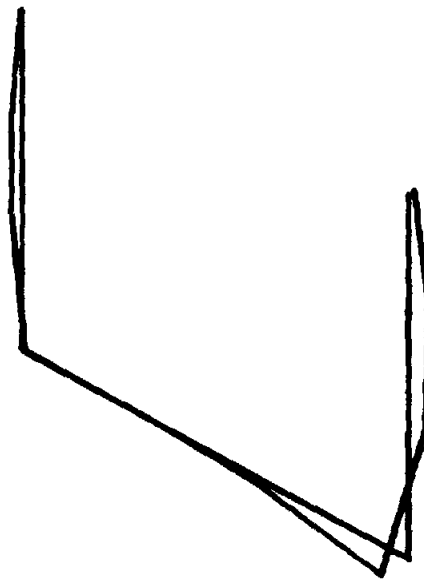
Figure A-2

2ND MODE —

12.8HZ

HELIO. YOKE
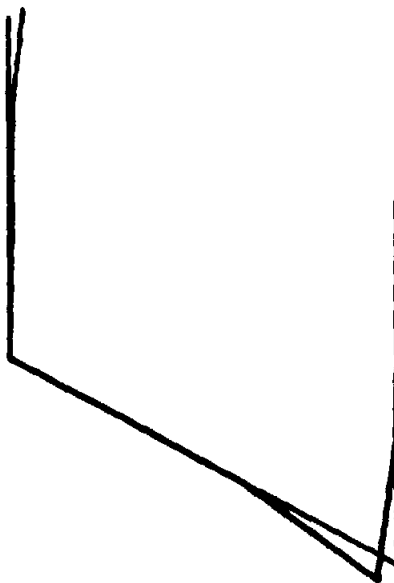
Figure A-3

3RD MODE —

13.6HZ

HELIO. YOKE
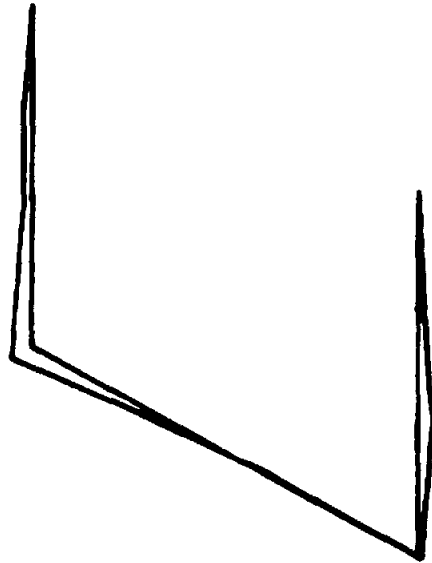
Figure A-4

4TH MODE —

18.29HZ

HELIO. YOKE
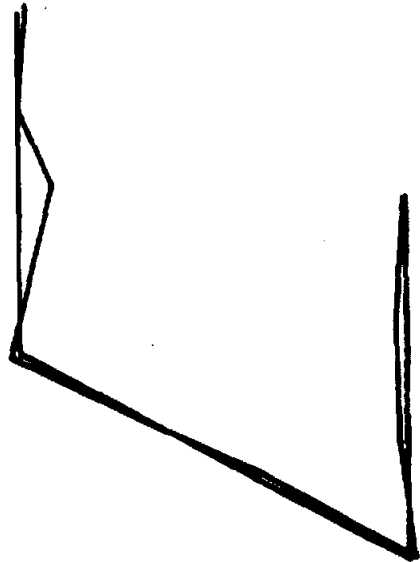
Figure A-5

AMPLITUDE UNITS: IN/LB

MEAS   *   *   *   *   *   MODES   *   *   *   *   *

	1		2		3		4	
	AMPL	PHS	AMPL	PHS	AMPL	PHS	AMPL	PHS
1	.1014E-01	208.9	.3576E-05	26.5	.1404E-03	168.5	.2393E-04	153.7
2	.3127E-02	215.9	.7378E-05	177.6	.5137E-04	185.0	.7554E-05	159.2
3	.2679E-02	48.6	.7898E-06	42.8	.2535E-04	337.8	.2975E-04	329.7
4	.1769E-01	61.7	.1251E-03	32.0	.2323E-04	8.0	.1161E-04	335.4
5	.9120E-02	337.8	.2432E-04	68.1	.9180E-04	354.6	.2831E-04	298.1
6	.1258E-01	340.5	.1335E-04	76.3	.4092E-04	343.7	.4292E-04	298.0
7	.1143E-01	8.8	.3521E-05	5.0	.1473E-04	219.0	.1218E-04	147.6
8	.1372E-01	181.9	.2379E-04	234.9	.6443E-04	190.6	.3787E-04	68.4
9	.1460E-01	185.0	.1834E-04	233.5	.5771E-04	157.3	.5434E-06	234.8
10	.6900E-02	193.3	.2218E-03	273.6	.3138E-03	91.2	.9187E-05	39.3

Figure A-6
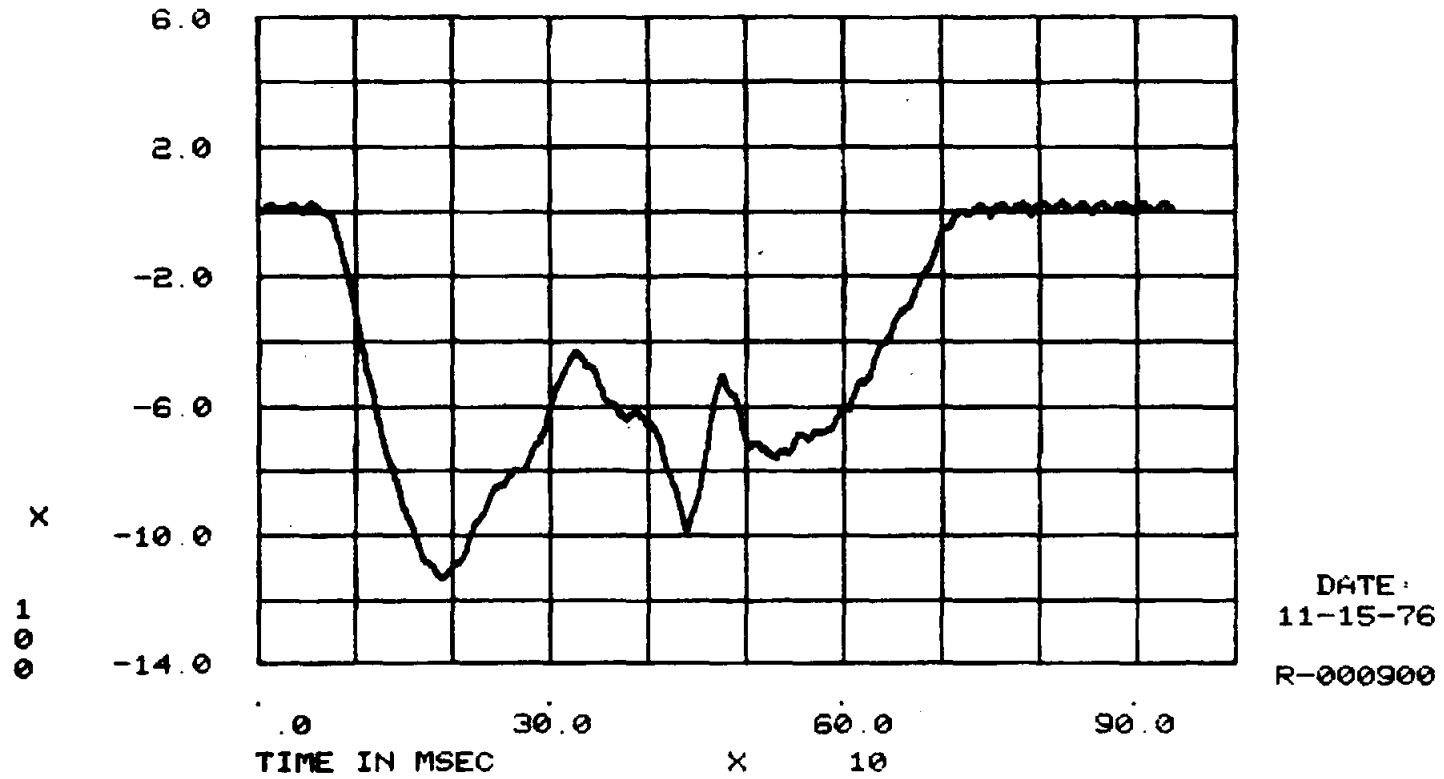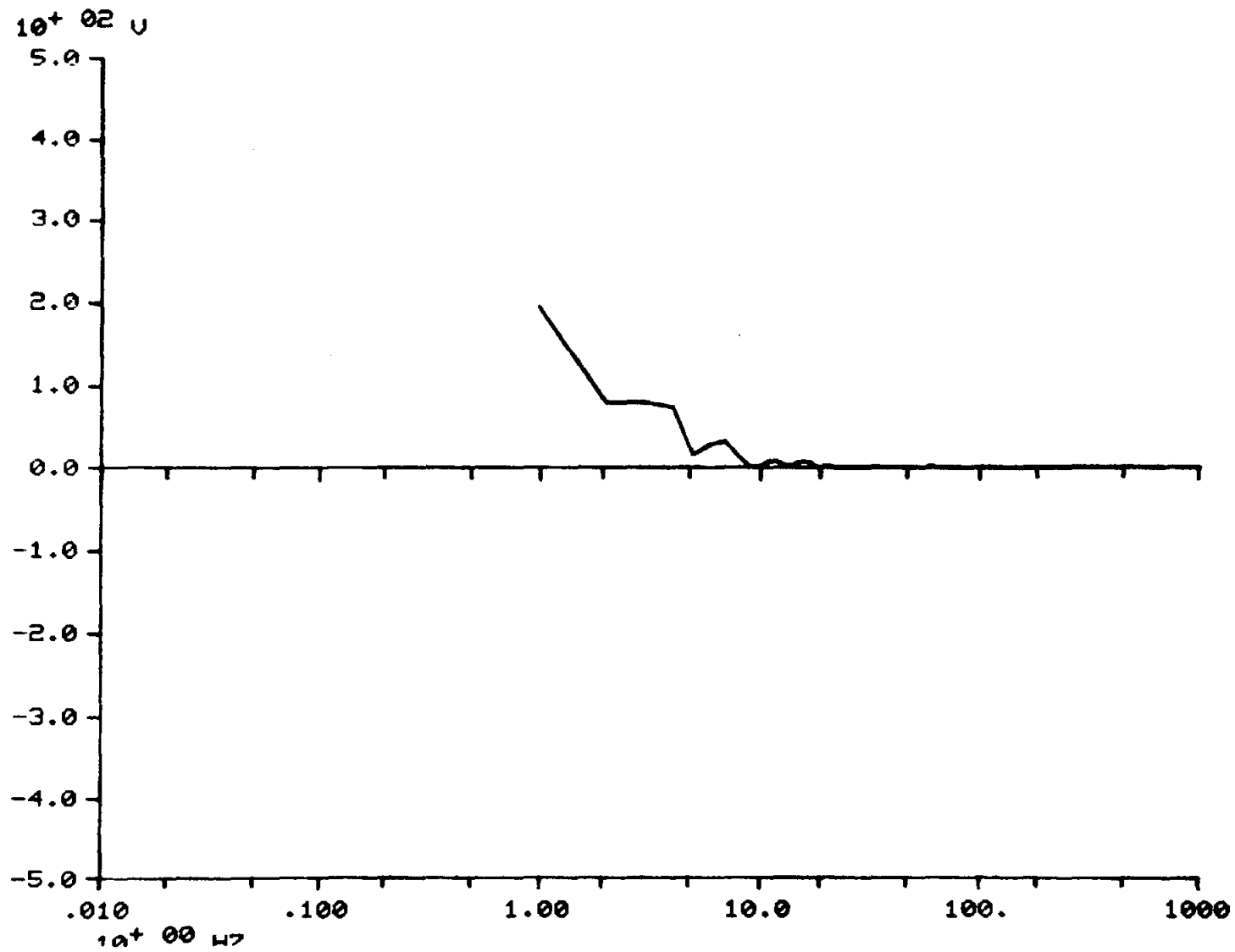
Figure A-7

Figure A-8

Figure A-9

69
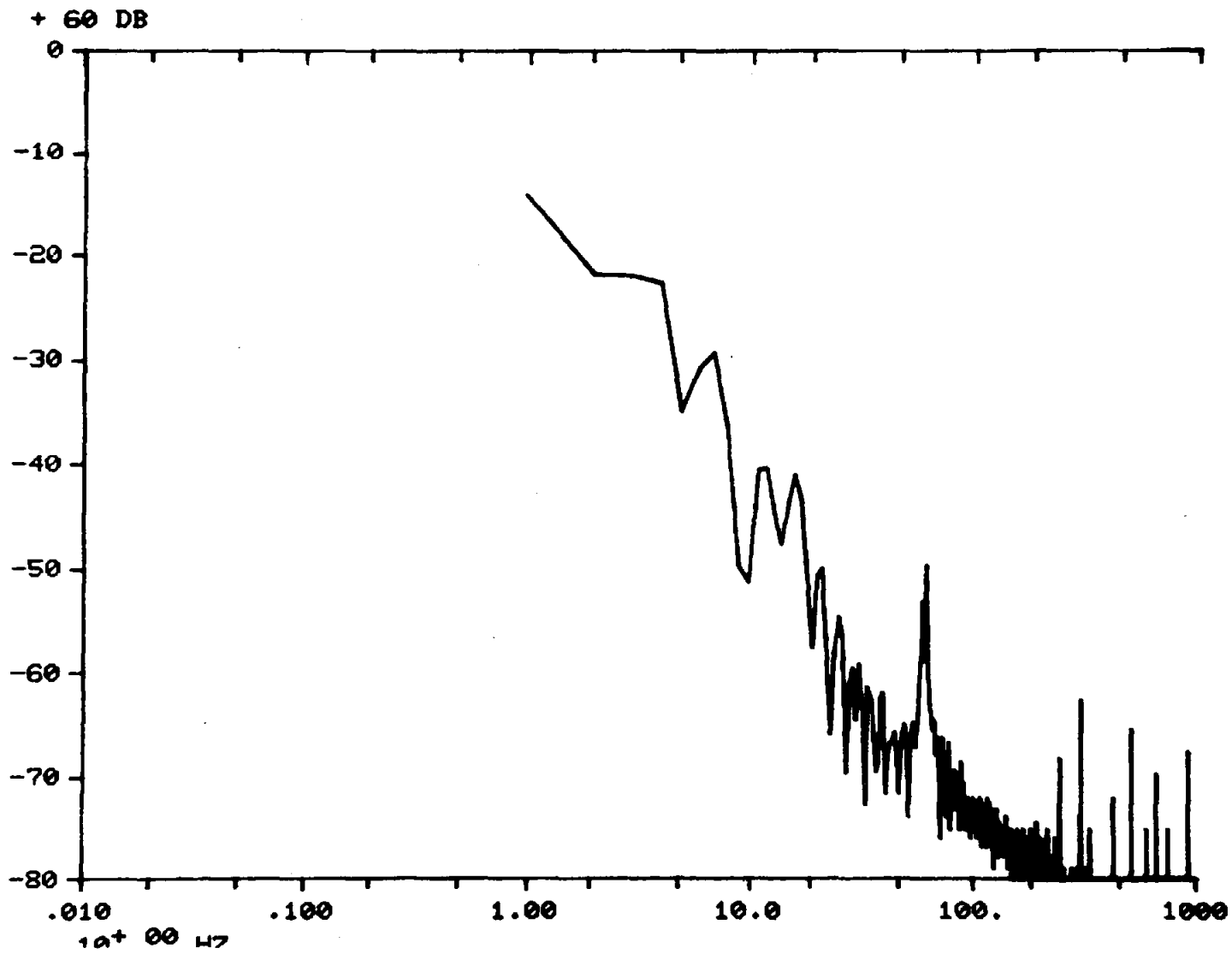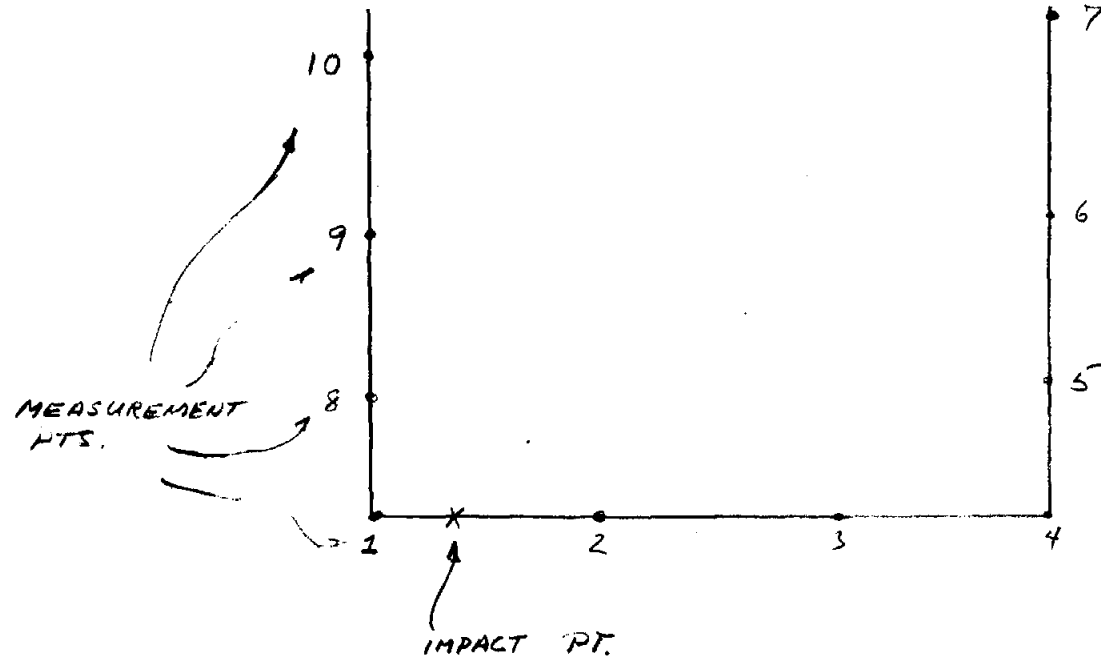
Figure shows measurement points and impact point (points are approximately 4 ft apart).

Figure A-10
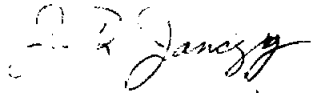
APPENDIX B

Sandia Laboratories

Albuquerque, New Mexico
Livermore, California

date: May 4, 1977

to: Distribution

from: J. R. Janczy - 9342

subject: Heliostat Transportation Study (R670463)

The Heliostat Transportation Study requested by Division 5713 was completed this month. This memo is a compilation of the pertinent data and conclusions.

The study was necessitated by mirror damage experienced during heliostat transport to and from Kirtland West and Area Y. The objective was to determine an improved way of moving the heliostats from site to site. The test consisted of instrumenting a heliostat mounted on the transit trailer. The system would then be subjected to road environments as certain parameters were varied, with the intent of optimization. These parameters were: truck speed, added ballast, tire pressure and facet-arm restraint techniques. The truck traveled at speeds of 5, 15, 20 and 30 miles per hour on asphalt road surfaces, and 5 mph on the gravel road at the Solar Thermal Test Facility. The addition of ballast amounted to 6000 lb of lead distributed over the bottom of the trailer. There were two restraint systems: one consisted of horizontal snubbers with cross-diagonal cabling, and the other just deleted the cables. The effects of the restraint system and ballast were studied at 5 mph (over gravel) and 15 mph (over asphalt). The tire pressure of the rear cab and all trailer tires was reduced to 45 psi from nominal. The reduced pressure was maintained while the heliostat/transport system traversed the route back to Kirtland West from Area Y. Twelve piezoresistive accelerometers (Endevco Model #2262-25) were mounted on the heliostat and support assembly (see Figure 1 for placement diagram). The accelerometer signals were conditioned and recorded by a self-contained unit developed and operated by F. R. Gustke (Division 9344). Mr. Gustke acquired all test data for this study.

Baseline data was obtained while the truck-trailer combination traversed its normal route from Kirtland AFB-West to Area Y. Data used for analysis in this report was acquired at or very near the Solar Thermal Test Facility (STTF) site. Some of the road conditions over which data was taken included asphalt and rough gravel. Rough gravel was the most extensively used test surface, as it provided the highest input acceleration (G) levels.

The original intent of the data analysis phase was to perform a modal analysis of the heliostat and support assembly as it would appear in the actual transportation environment. The recorded signal from the accelerometer mounted on the lower front support (see Figure 1) would be considered

as characterizing the input to the test structure. Transfer functions could then be formed between the input point and all remaining locations of interest. These transfer functions would be analyzed using the Division 9342 Hewlett-Packard Model 5451B Fourier Analyzer System to obtain the mode shapes of the structure shown in Figure 1. The motion of the vertical facet-arms is of prime interest, as excessive out-of-phase motion could result in mirror breakage. This movement is what would have been viewed on either mode shape plots or an animated mode shape display. Unfortunately, the input signal was not uniformly strong over the bandwidth of interest (2 thru 50 Hz). This behavior indicated that other techniques might better display the desired information.

A method that was successfully employed was that of viewing the Power Spectral Density at two of the accelerometer locations for the various test conditions (see Figures 2 thru 16). This technique allows one to study the energy levels over the frequency range of interest and the overall RMS-G level, thereby identifying possible trouble spots.

Signals from the accelerometers mounted, in the X-direction, on the lower front support (LFT) and the tip of the second forward vertical arm (#2-VERT) were analyzed. Accelerometer #2-VERT was viewed as "worst-case" due to amplification by the facet-arm and support assembly. Accelerometer LFT was analyzed to be able to view what could be considered as input road conditions. All of the gravel road data analyzed was taken on the road into the STTF since it had been judged to be "worst-case."

Figure 17 gives a summary of the data analyzed. Figures 2 thru 5 are data on asphalt with the only varied parameter being truck speed. Figures 6 thru 12 show data taken on the gravel road at the STTF with ballast, restraint system, and rear truck and trailer tire pressure varied. Figures 13 thru 16 show data obtained on asphalt with low tire pressure while truck speed was varied.

The conclusions which can be reached from analysis of the test data are:

1. By comparing Figures 7 and 10 it is seen that adding the 6000 lb of ballast lowered the overall RMS-G level (by approximately .1 RMS-G). The predominant resonance, at 4 Hz, had about the same level of energy for both plots, but all other peaks were reduced in amplitude. The effects of this attempted fix were beneficial.

2. No conclusion can confidently be drawn about positive or negative effects of lowering tire pressure (down to 45 psi) on the rear cab tires and trailer tires. The graphs of Figure 18 show essentially no difference for accelerometer locations LFT and #2-VERT upon lowering the tire pressure as indicated. Any difference is certainly inside the error bounds.

74

3. Speed variations can be viewed by examining Figures 2 thru 5, 13 thru 16 and 18. Increasing speed does seem to increase the value of the overall RMS-G, but it does so by increasing energy most at the higher frequencies (above 20 Hz). As there was no significant reduction of resonant magnitudes below 20 Hz, there does not seem to be any great benefit in increasing the speed of truck transit.

4. The best single system for reducing the overall RMS-G level and energy over the bandwidth of interest (2 thru 20 Hz) is the snubber. Use of cross-cables with the snubber appears to reduce levels slightly, but the difference is too small to allow hard conclusions to be drawn.

Examination of Figures 7, 8 and 10 suggests it may prove useful to combine a snubbing system and increased ballast. Since the heliostat/trailer combination can be approximated as a spring-mass system, we know that increasing the mass (ballast) should decrease resonance problems at high frequencies (probably above 5 Hz) and increasing stiffness should reduce resonance at lower frequencies (in particular the predominant peak at 4 Hz). The snubber would increase the stiffness, while the ballast increases the mass, thereby optimizing the operating range of the heliostat transport system (compare Figures 7, 8 and 10).

JRJ:brs

Distribution:
5713 J. V. Otts
5713 D. J. Kuehl
5713 G. A. Anderson
5715 R. C. Reuter
9342 D. R. Schafer
9344 F. R. Gustke
3144 Central Tech File
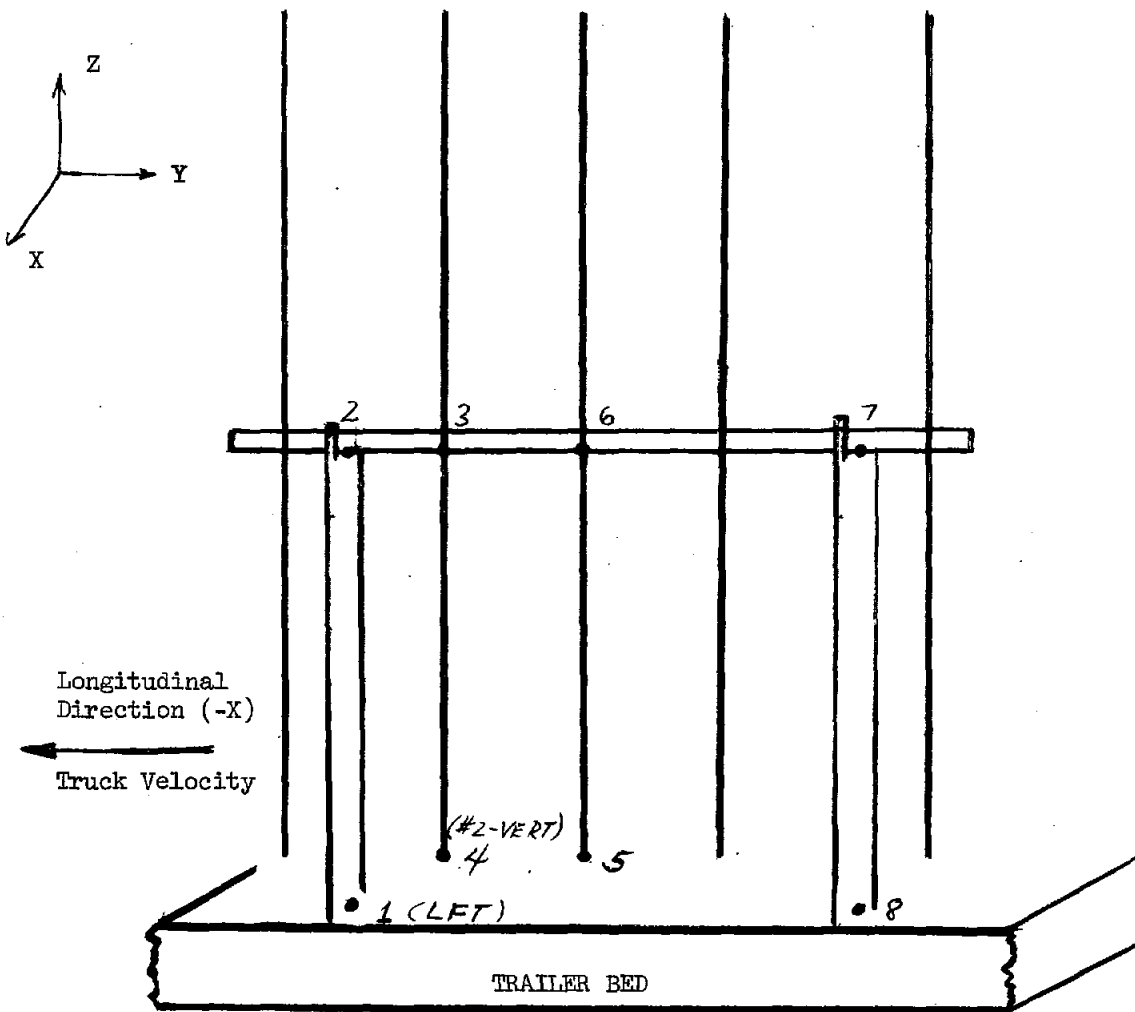
Location	No. of Accels.	Sensitive Axis
1	2	-X, Z
2	2	-X, Z
3	1	-X
4	1	-X
5	1	-X
6	1	-X
7	2	-X, Z
8	2	-X, Z

Figure B-1.   Schematic of Heliostat Trailer Bed Assembly
Showing Accelerometer Locations

PLOT 2

LFT SMOOTH BLKTOP GMPH TEST1
POWER SPECTRAL DENSITY 11 AVG.
RMS LEVEL = .0177

10^N **G**2/HZ**

LFT SMOOTH BLACKTOP 6 MPH TEST 1

Figure B-2

. PLOT 2

POWER SPECTRAL DENSITY   9 AVGS.
RMS LEVEL = .0823

10^N **G✱✱2/HZ**

10.0   **5000**

10^{-1} **HZ LOG**   **#2-VERT SMOOTH** BLACKTOP   **TEST1**
                                                            6 MPH

Figure B-3

PLOT 4

POWER SPECTRAL DENSITY   11 AVGS.

RMS LEVEL = .0385

10^N GX*2/HZ

LFT SMOOTH BLACKTOP 20MPH TEST3
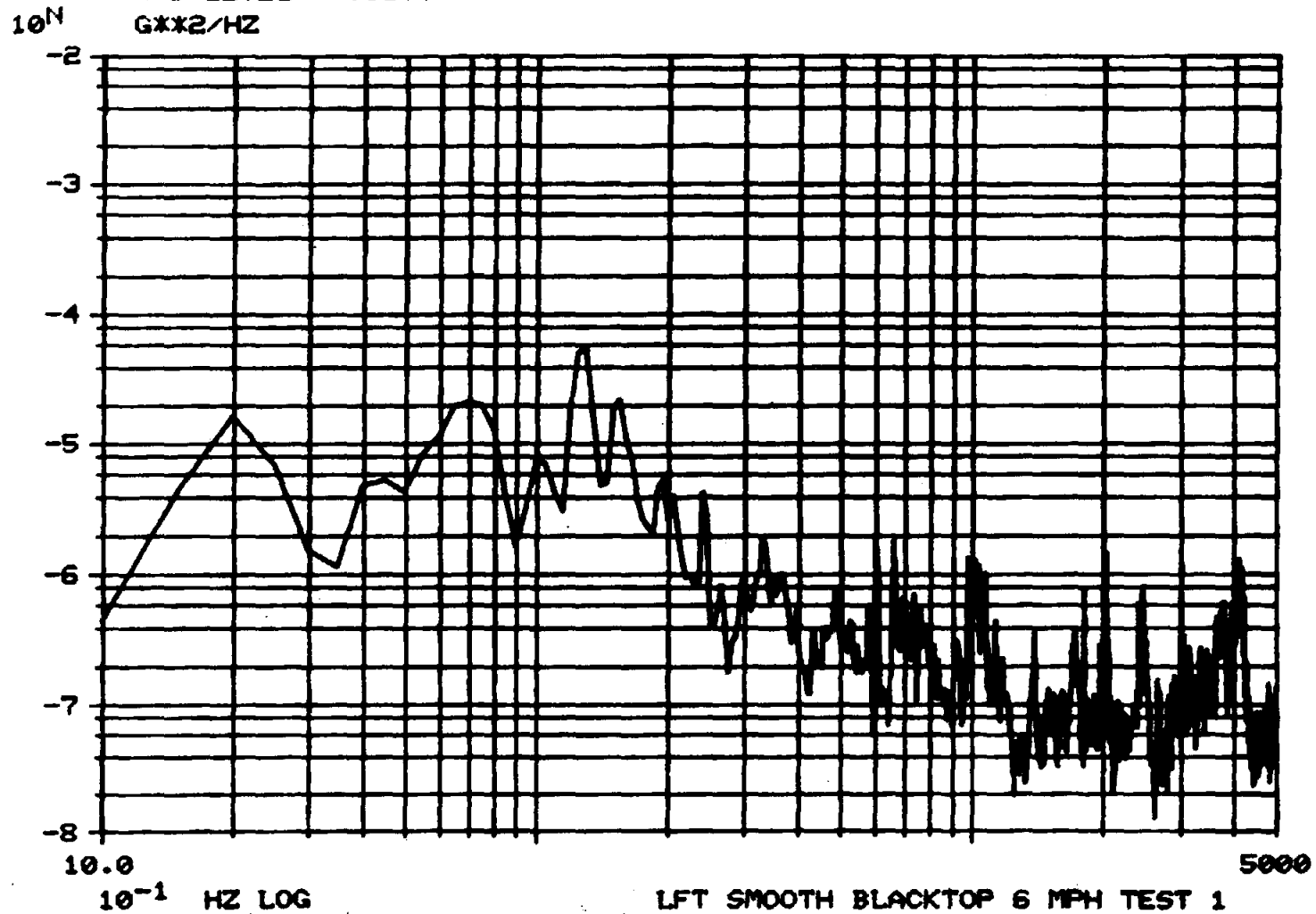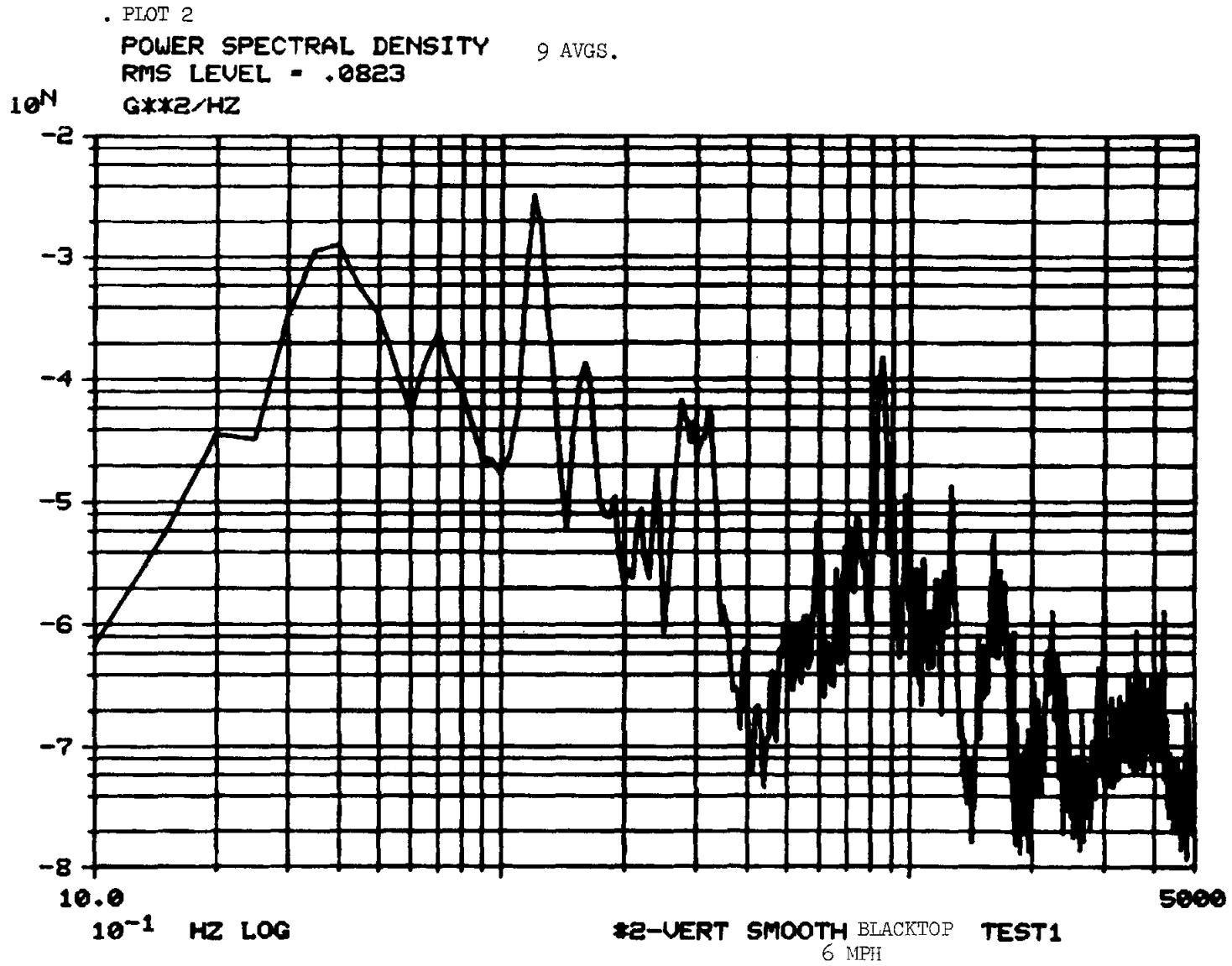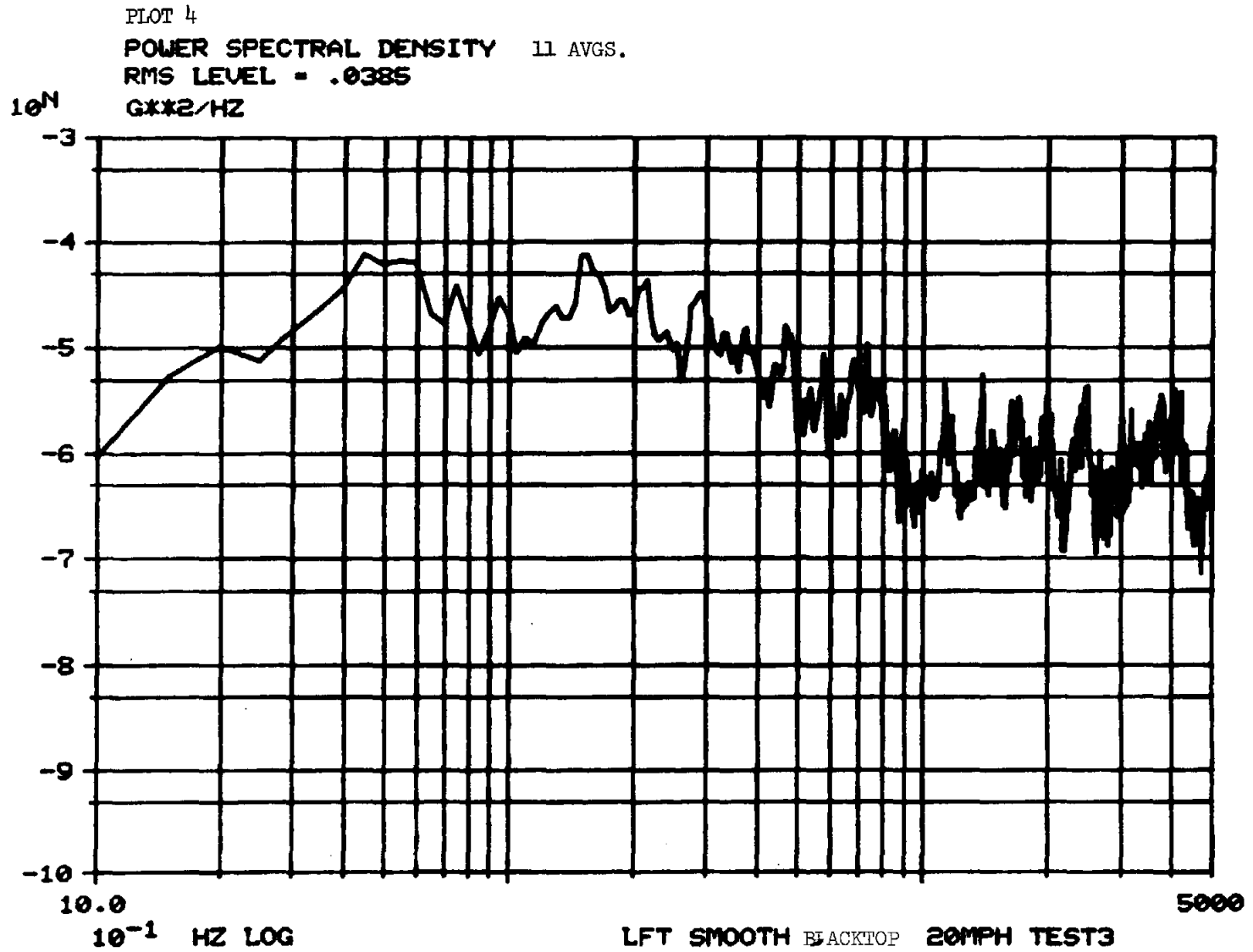
Figure B-4

PLOT 4

2-VERT BLKTOP 20MPH

POWER SPECTRAL DENSITY 11 AVGS

RMS LEVEL = .1968

10^N **G✻✻2/HZ**

-8-

10.0   **5000**

10^{-1} **HZ LOG**   **#2-VERT** BLACKTOP **20MPH TEST3**
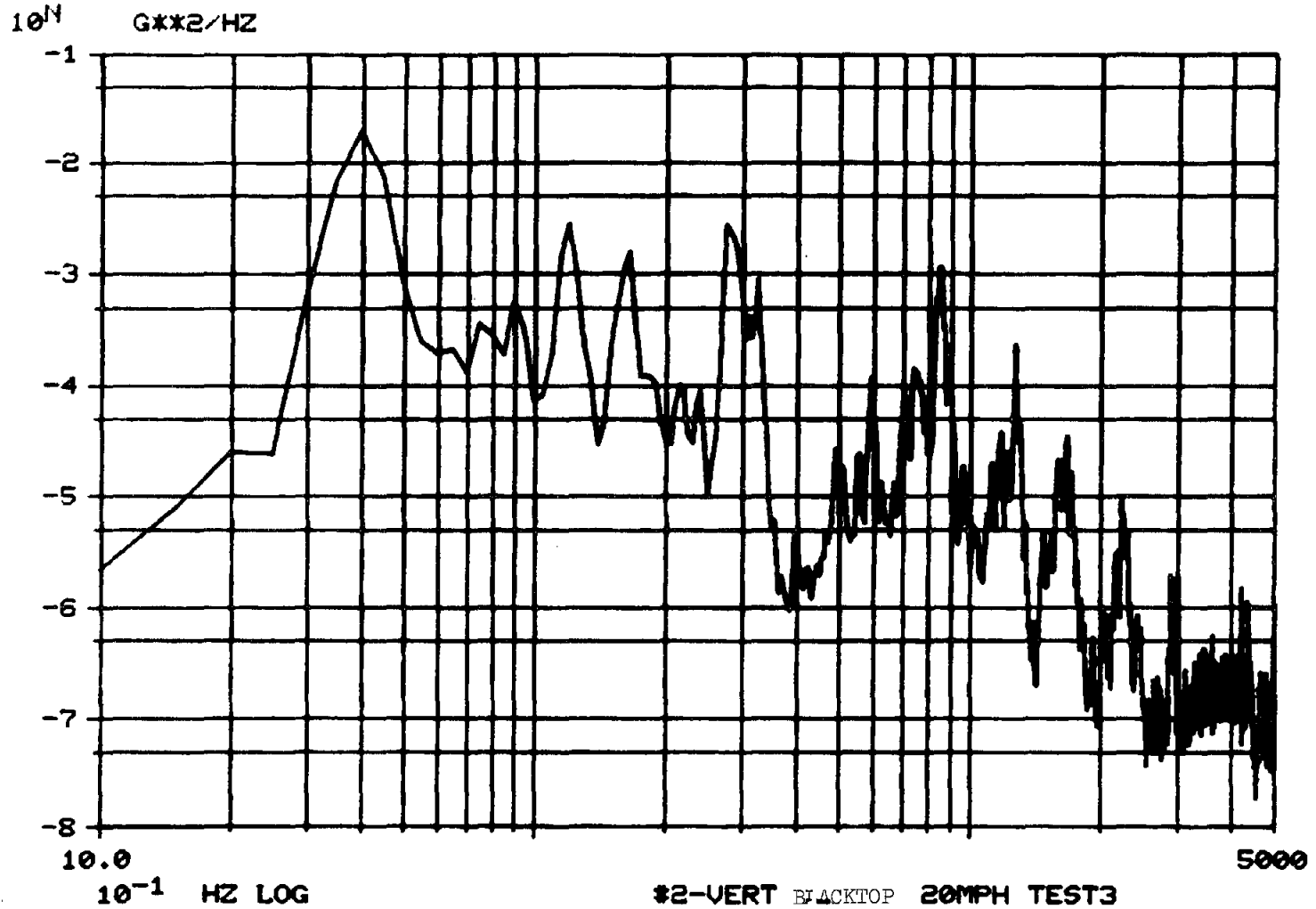
Figure B-5

PLOT 5
LFT   AT-SITE 5MPH
POWER SPECTRAL DENSITY   11 AVGS.
RMS LEVEL = .0793
10^N   G**2/HZ

10.0   5000
10^-1   HZ LOG   LFT GRAVEL AT-SITE 5MPH TEST6
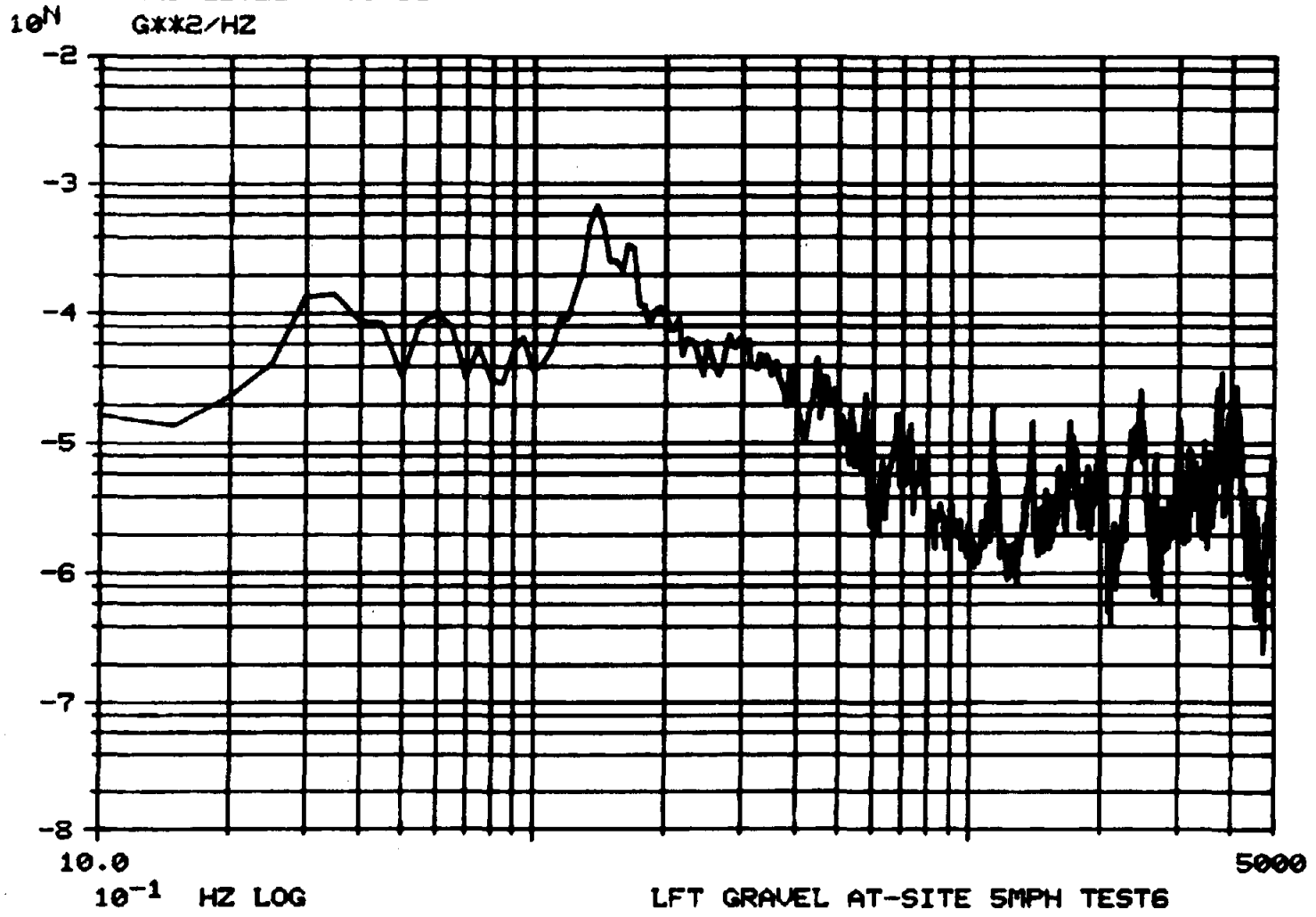
Figure B-6

PLOT 6

#2-VERT AT-SITE 5MPH
POWER SPECTRAL DENSITY 11 AVGS.
RMS LEVEL = .3507

10^N **G**2/HZ**

10.0   5000
10^{-1} **HZ LOG**   **#2-VERT GRAVEL RD AT-SITE 5MPH TEST6**
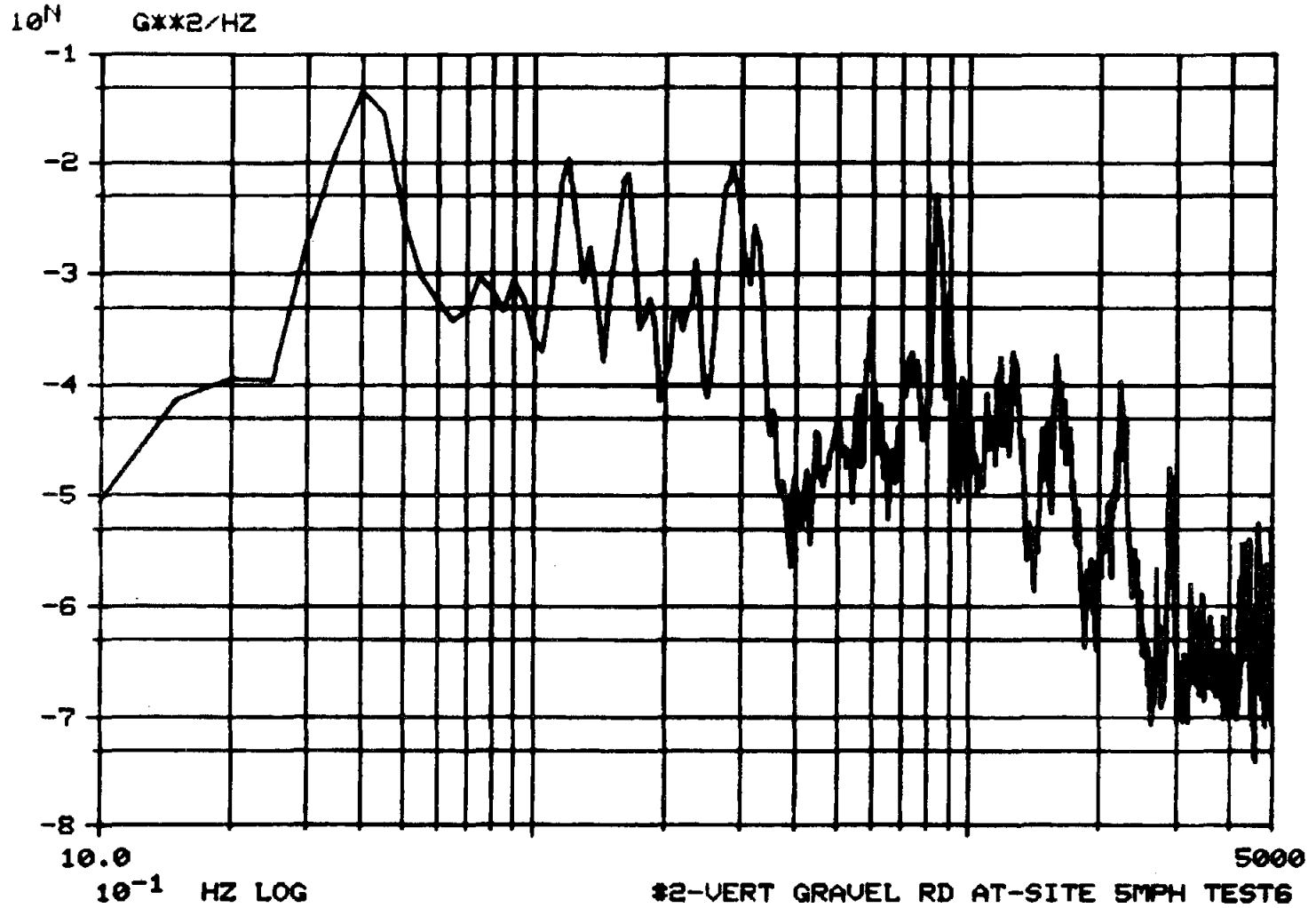
Figure B-7

PLOT7 13AVES
POWER SPECTRAL DENSITY
RMS LEVEL = .2220

10^N G**2/HZ

#2-VERT GRAV AT-SITE w/SNUBBER
AND CROSS-DIAGONAL CABLES @ 5 MPH
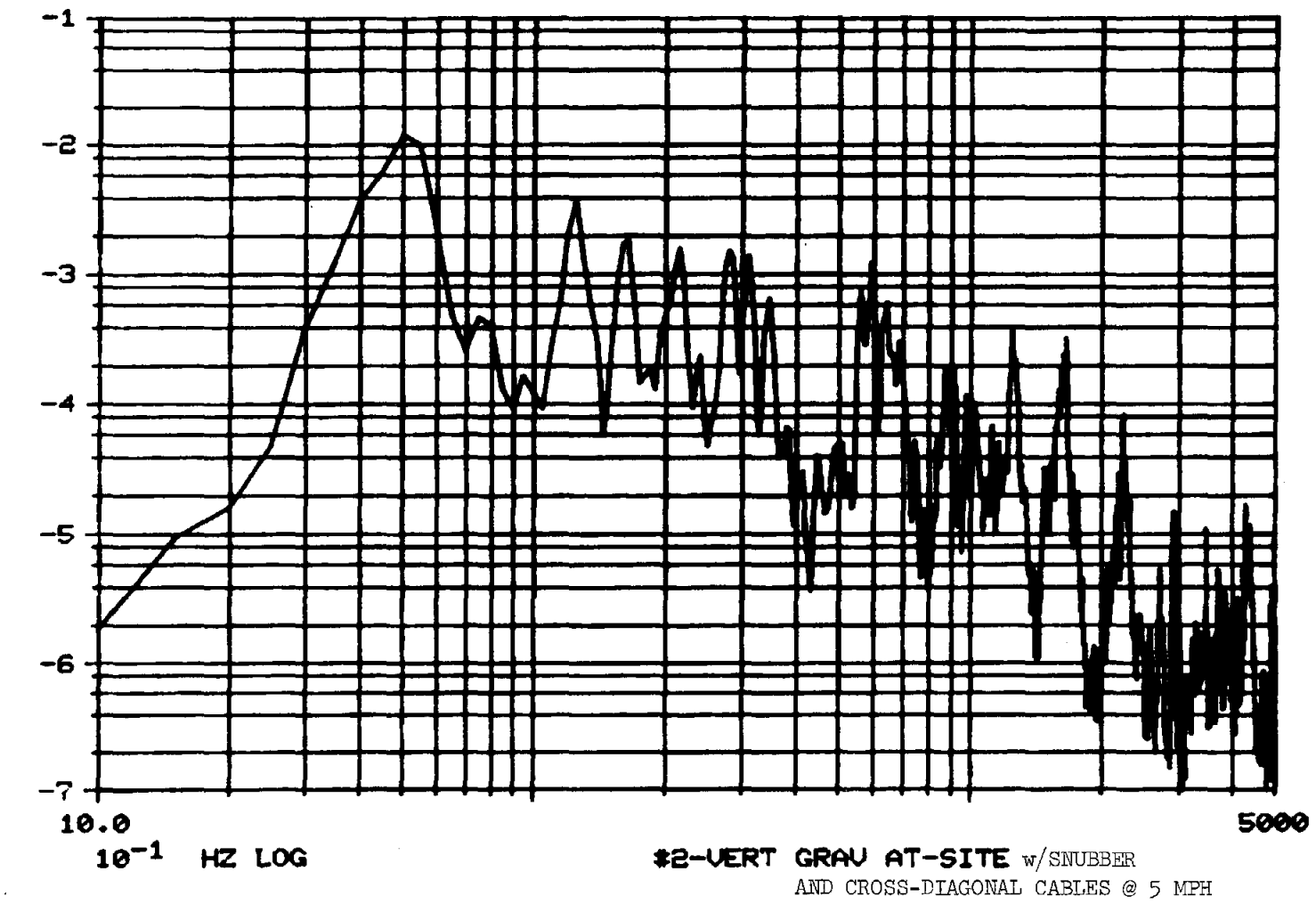
Figure B-8

PLOT 8 11 AVES.
POWER SPECTRAL DENSITY
RMS LEVEL = .2291
10^N G**2/HZ

#2-VERT GRAVEL RD AT-SITE 5MPH w/SNUBBERS ONLY
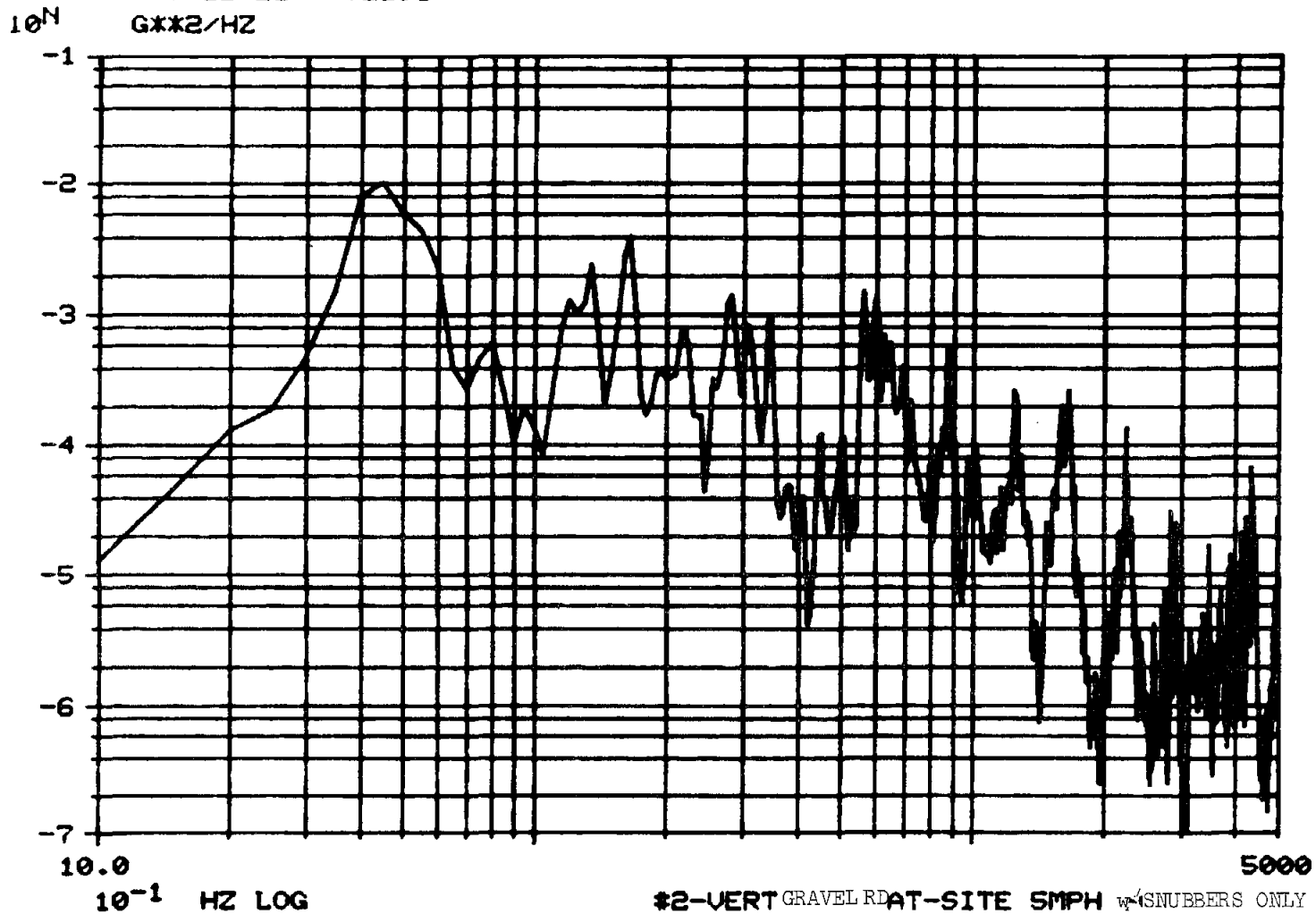
-12-

Figure B-9

PLOT 9 12AVES
POWER SPECTRAL DENSITY
.2537 RMS-G

10^N G**2/HZ

10.0
10^{-1} HZ LOG

#2-VERT NO SNUBERS w/6 KIP LEAD
@ 5 MPH

5000

-13-

Figure B-10

PLOT 10
POWER SPECTRAL DENSITY
RMS LEVEL = .0698

10^N **G**2/HZ**

LFT GRAVEL ROAD w/LOW TIRE PRESSURE   @ 5 mph
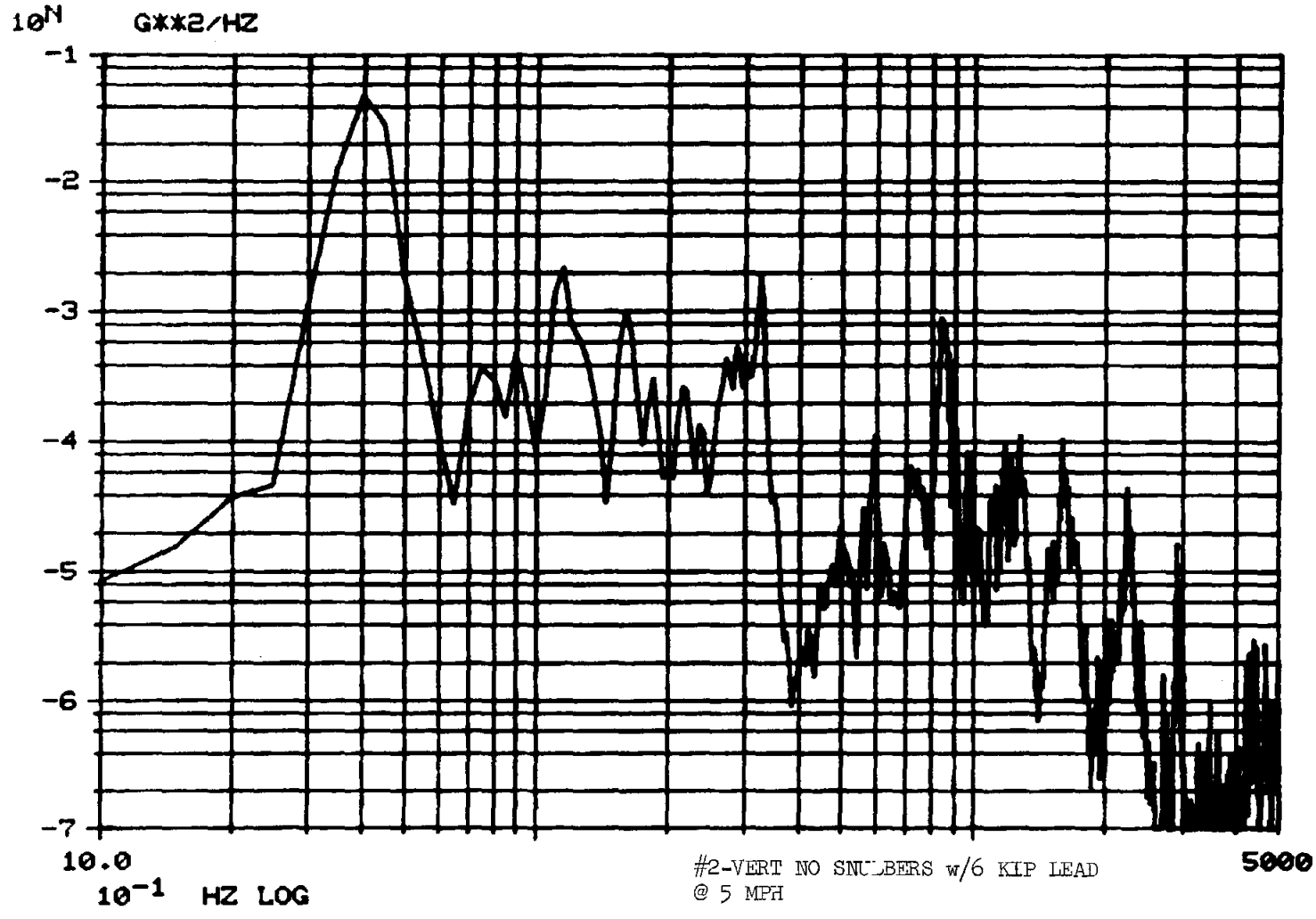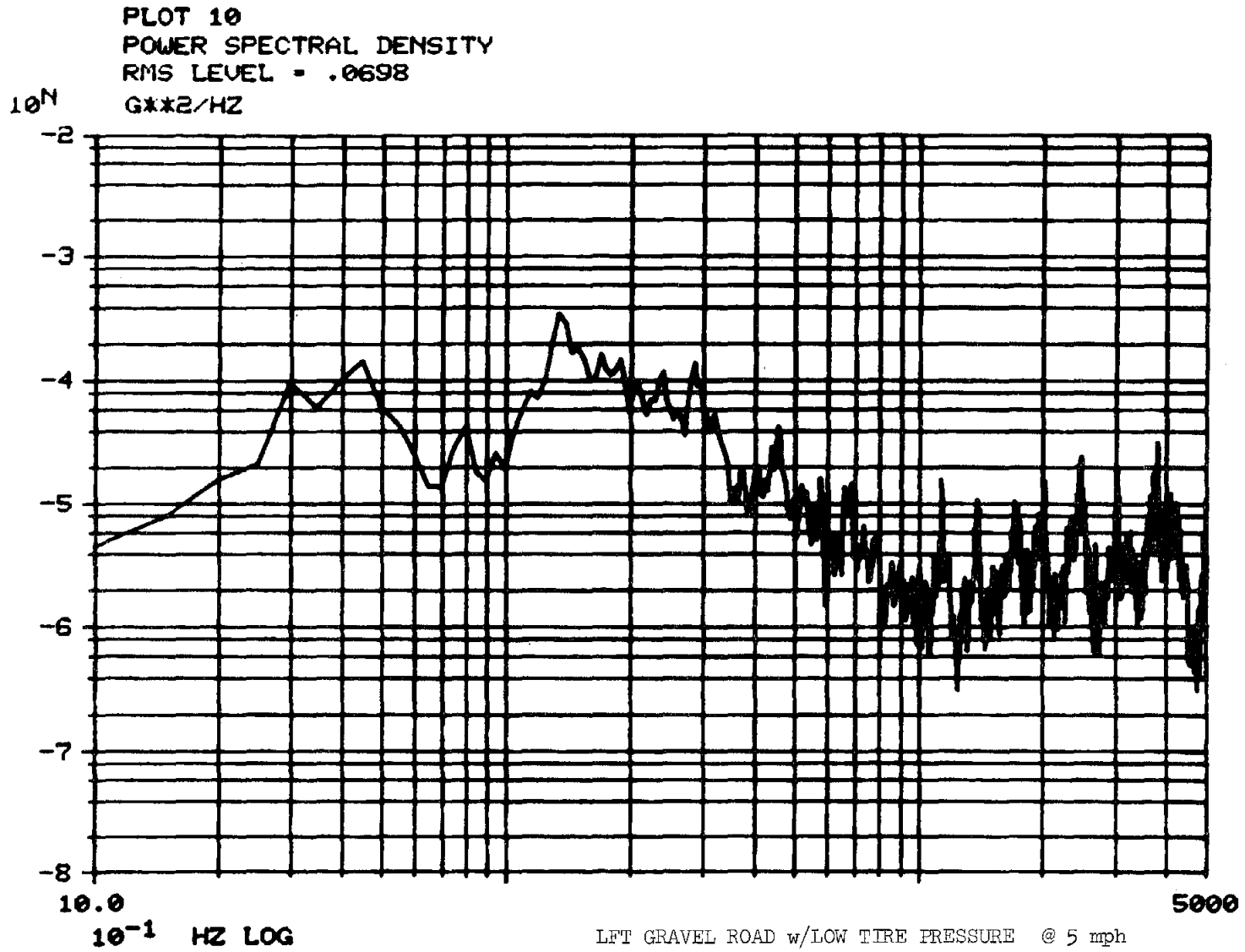
Figure B-11

PLOT11 10AVES
POWER SPECTRAL DENSITY
RMS LEVEL = .3571

10^N G**2/HZ

#2-VERT GRAVEL ROAD w/LOW **TIRE PRES** @ 5 MPH

Figure B-12

PLOT12 14AVES
POWER SPECTRAL DENSITY
RMS LEVEL = .0335

10^N G**2/HZ

LFT w/LOW **TIRE PRES 15MPH BLACKTOP**
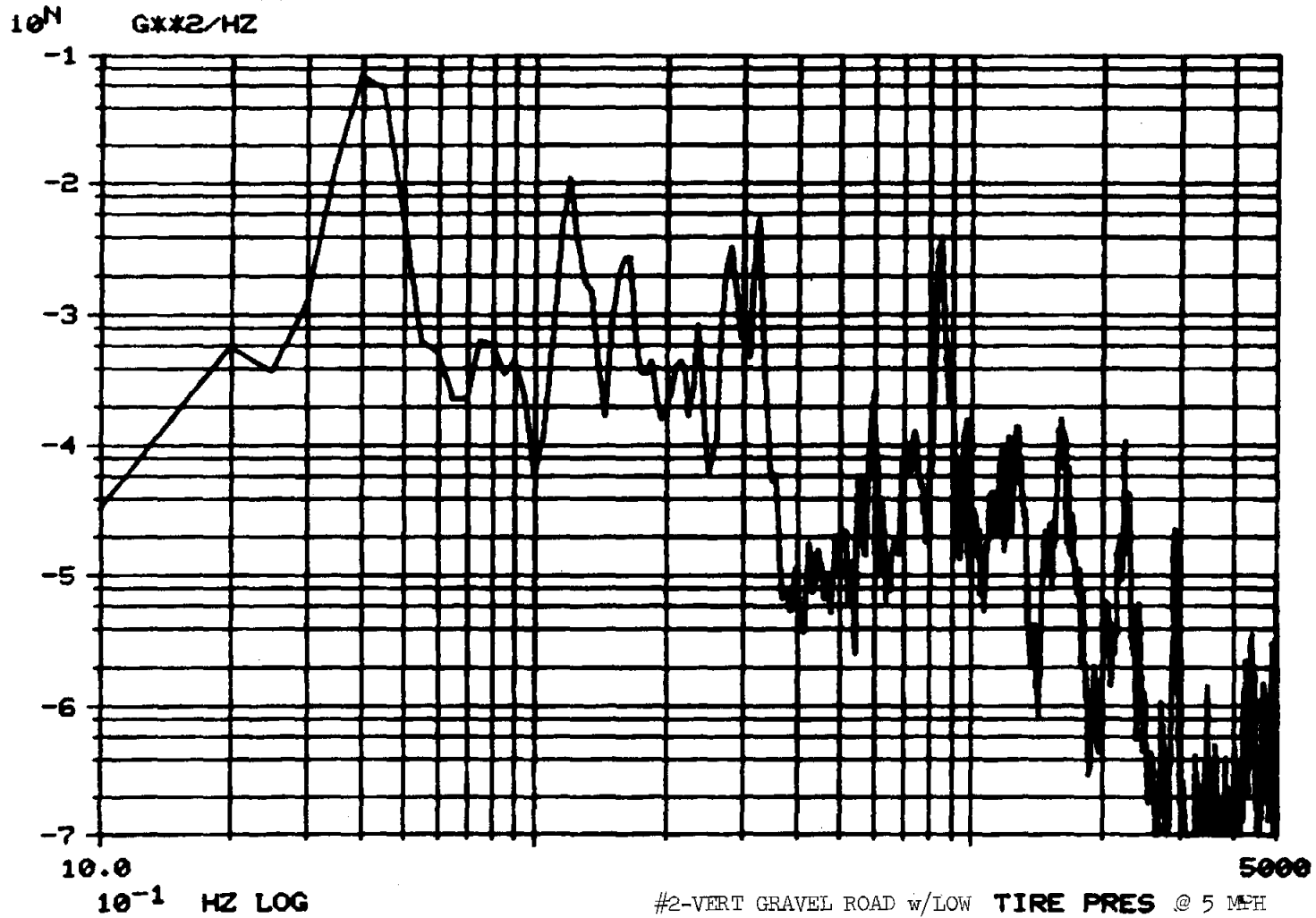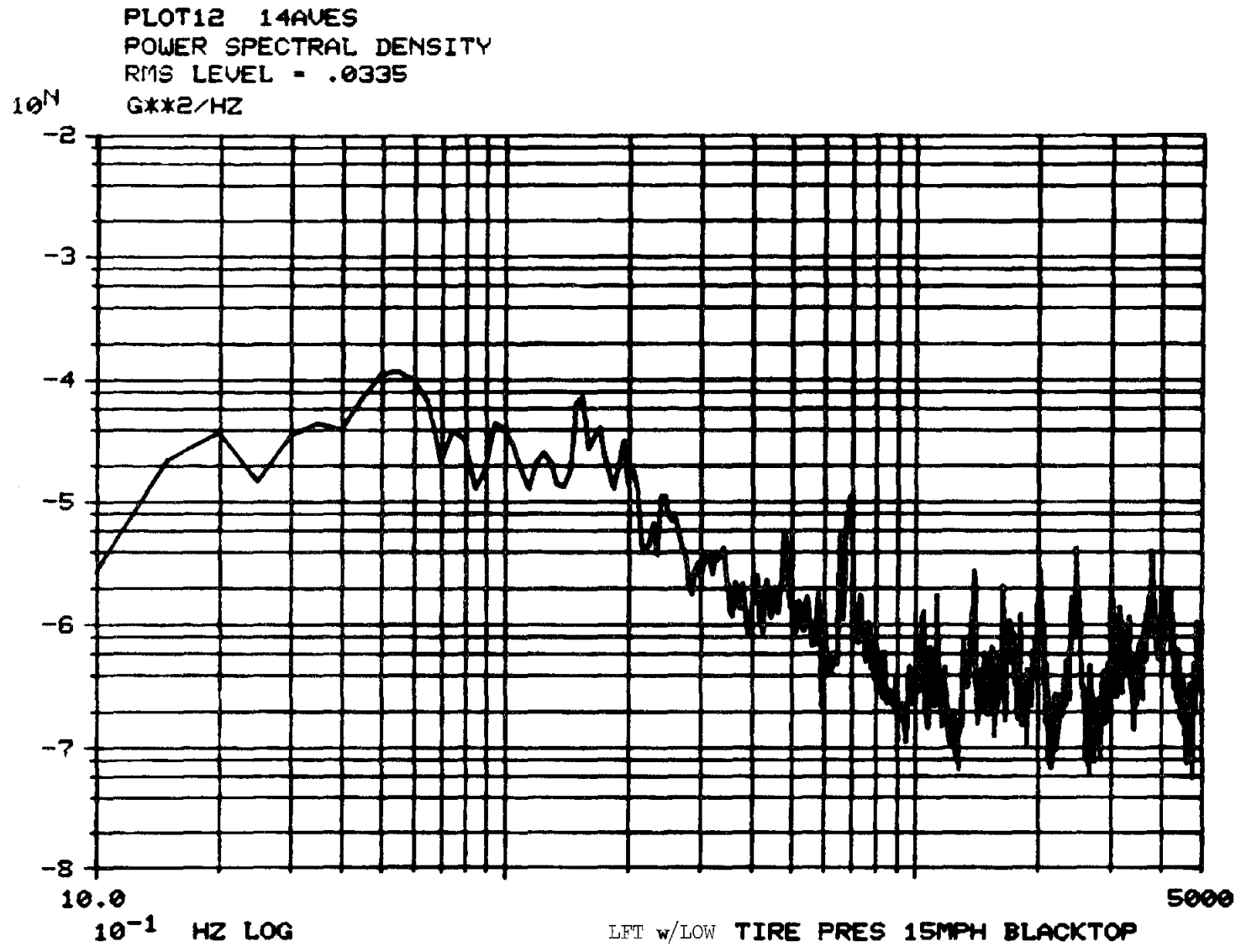
Figure B-13

PLOT13 11AVES
POWER SPECTRAL DENSITY
RMS LEVEL = .1468

10^N G**2/HZ
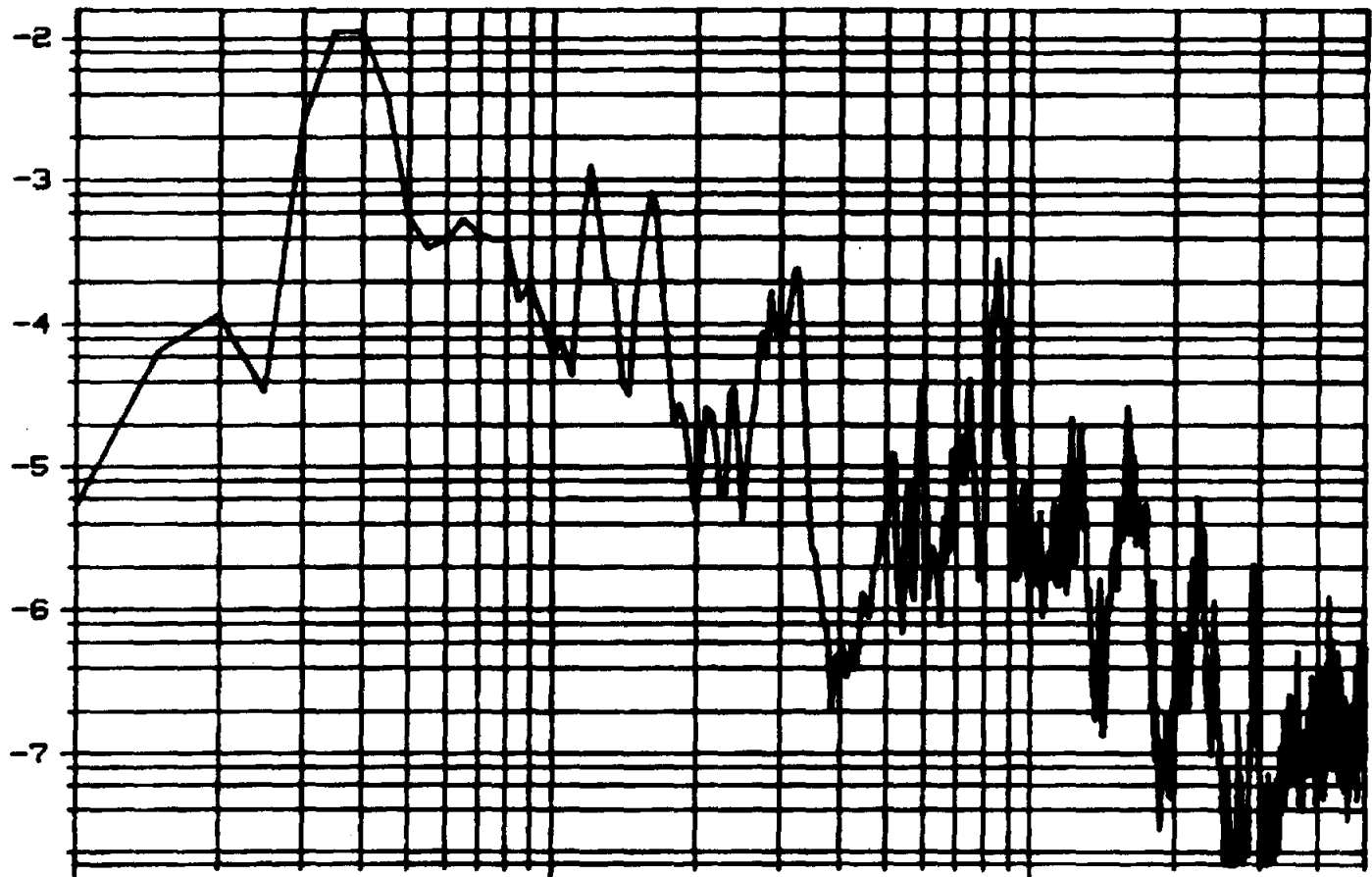
10.0   5000
10^{-1} HZ LOG   #2-VERT w/LOW TIRE PRESSURE @ 15MPH BLACKTOP

-17-

Figure B-14
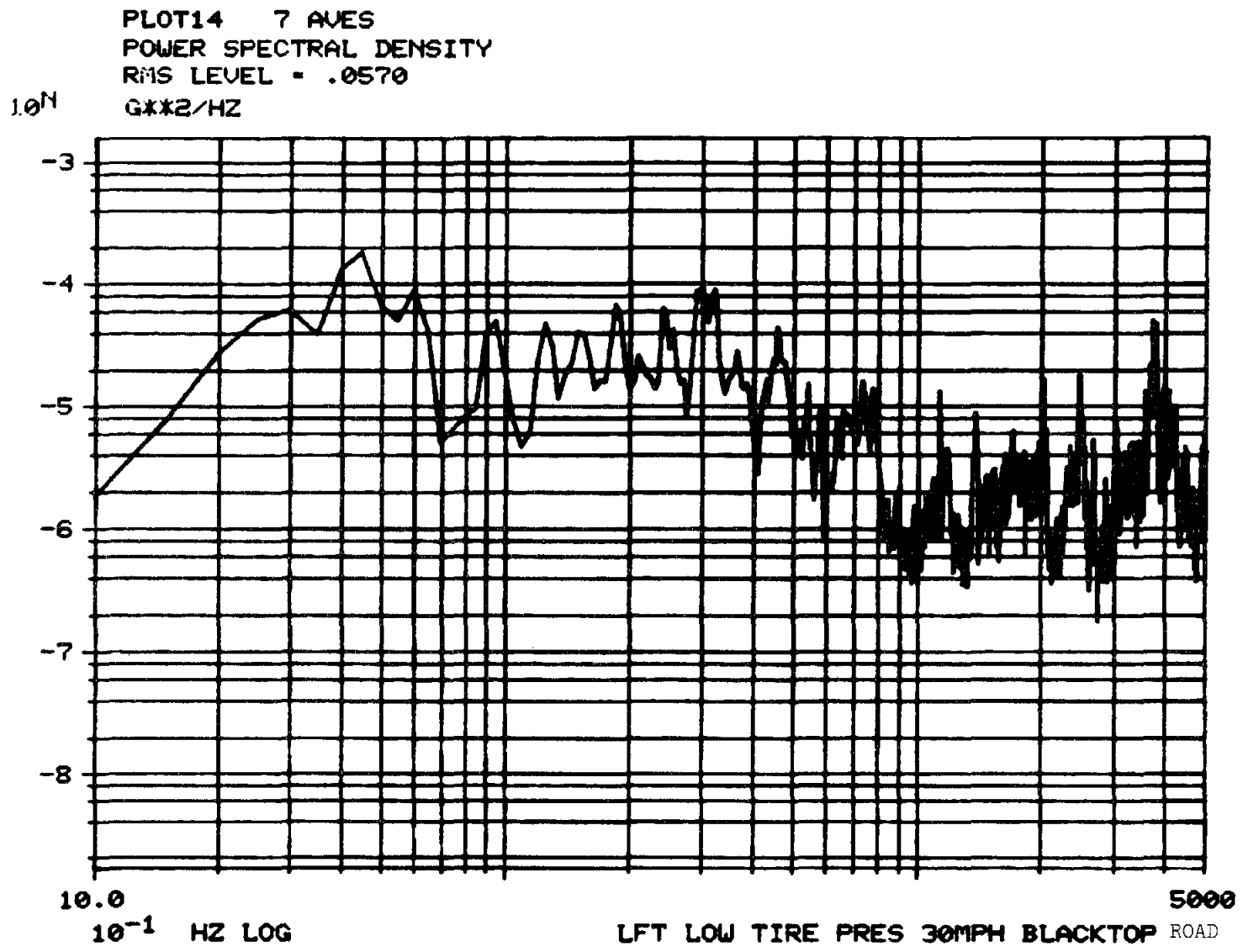
PLOT14   7 AVES
POWER SPECTRAL DENSITY
RMS LEVEL = .0570

1.0^N G**2/HZ
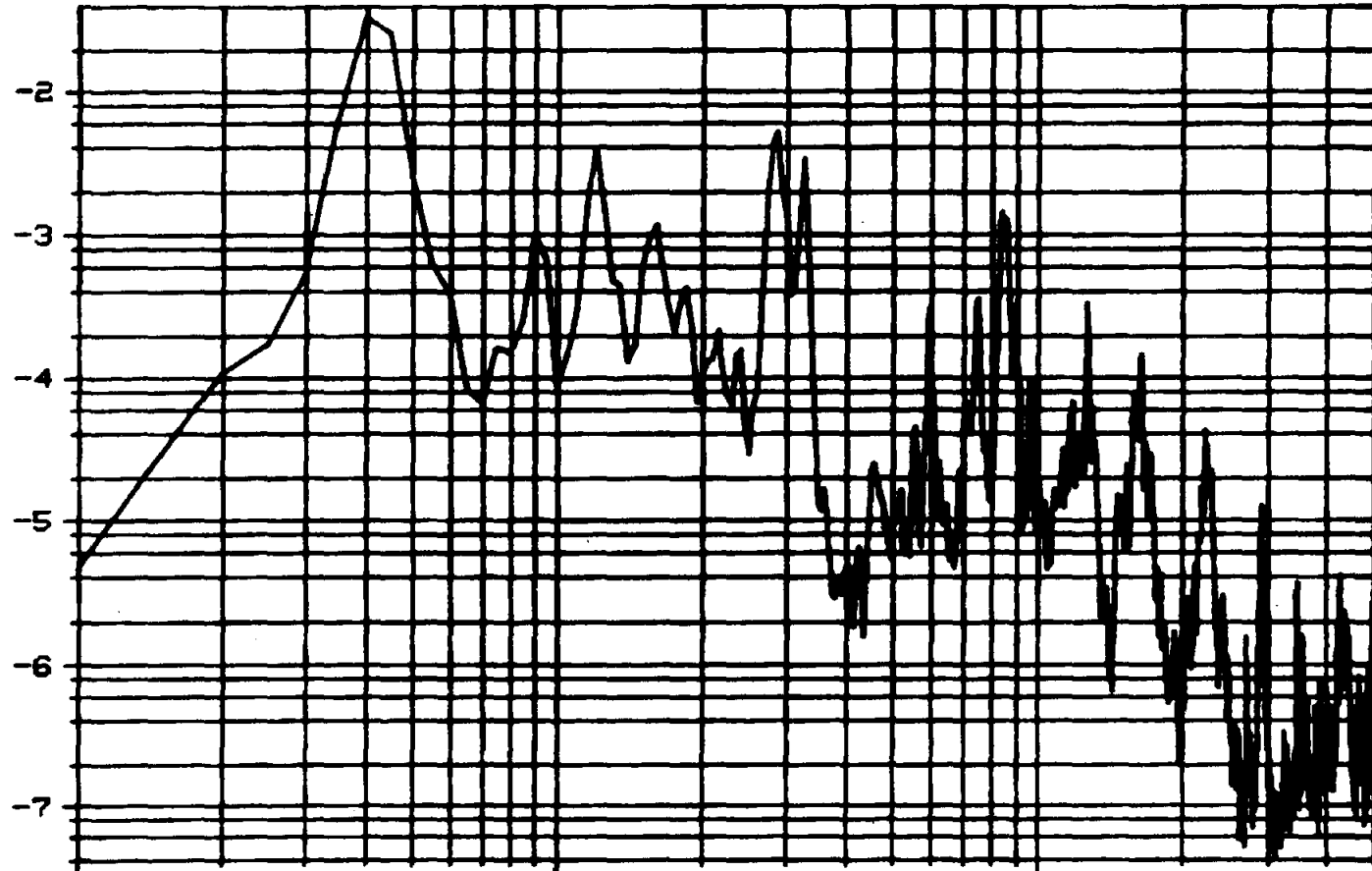
10.0   5000
10^{-1} HZ LOG   LFT LOW TIRE PRES 30MPH BLACKTOP ROAD

-18-

Figure B-15

Figure B-16

-20-

Figure 17. Summary

Accelerometer Location	Plot No.	RMS-G	Test Description	Comments *
Lower Front Support (LFT)	1	.018	Asphalt Road @ 6 mph	Major resonances at 2 Hz, 4.5 Hz, 7 Hz, and 14 Hz
Tip of 2nd Heliostat Arm (#2-VERT)	2	.082	Asphalt Road @ 6 mph	Highest amplitude peaks at 4 Hz and 14 Hz
LFT	3	.039	Asphalt @ 20 mph	Energy more evely distributed from 2 to 30 Hz
#2-VERT	4	.197	Asphalt @ 20 mph	Increased energy at higher frequencies
LFT	5	.079	Gravel Road at STTF @ 5 mph	Excitation at approx. 3.5, 6, 14 Hz
#2-VERT	6	.351	Gravel Road at STTF @ 5mph	Major peak at 4 Hz w/amplitude $= 10^{-1.4}g^2/Hz$
#2-VERT	7	.222	Gravel Road at STTF w/snubber & cable @ 5 mph	Major peak at 4 Hz w/amplitude of $10^{-2}g^2/Hz$
#2-VERT	8	.229	Gravel Road at STTF w/snubber only-5 mph	Major resonance at 4 Hz w/amplitude of $10^{-2}g^2/Hz$
#2-VERT	9	.254	Gravel Road, no snubber w/6 KIP of lead on trailer-5 mph	Major resonance at 4 Hz with amplitude of $10^{-1.5}g^2/Hz$
LFT	10	.070	Gravel Road, low tire pres. for trailer and rear truck tires (45 psi)	Most energy between 2 to 5 Hz and 10 to 30 Hz
#2-VERT	11	.357	Gravel Road at STTF w/rear tire pres. of truck and trailer tires to 45 psi	Major resonance at 4 Hz with an amplitude of approx. $10^{-1.3}g^2/Hz$. Amplitude of 2 Hz peak increased

*All accelerometers sense longitudinal motion.

92

Accelerometer Location	Plot No.	RMS-G	Test Description	Comments
LFT	12	.034	Asphalt Road @ 15 mph Low tire pressure	Peak at 2 Hz is higher than that of Plot #3
#2-VERT	13	.147	Asphalt Roat @ 15 mph w/low tire pressure	
LFT	14	.057	Asphalt Road @ 30 mph w/low tire pressure	Only 7 averages were used for this sample vs between 11 and 14 for others
#2-VERT	15	.262	Asphalt Road @ 30 mph w/low tire pressure	All peaks increased in amplitude as compared to Plot #13
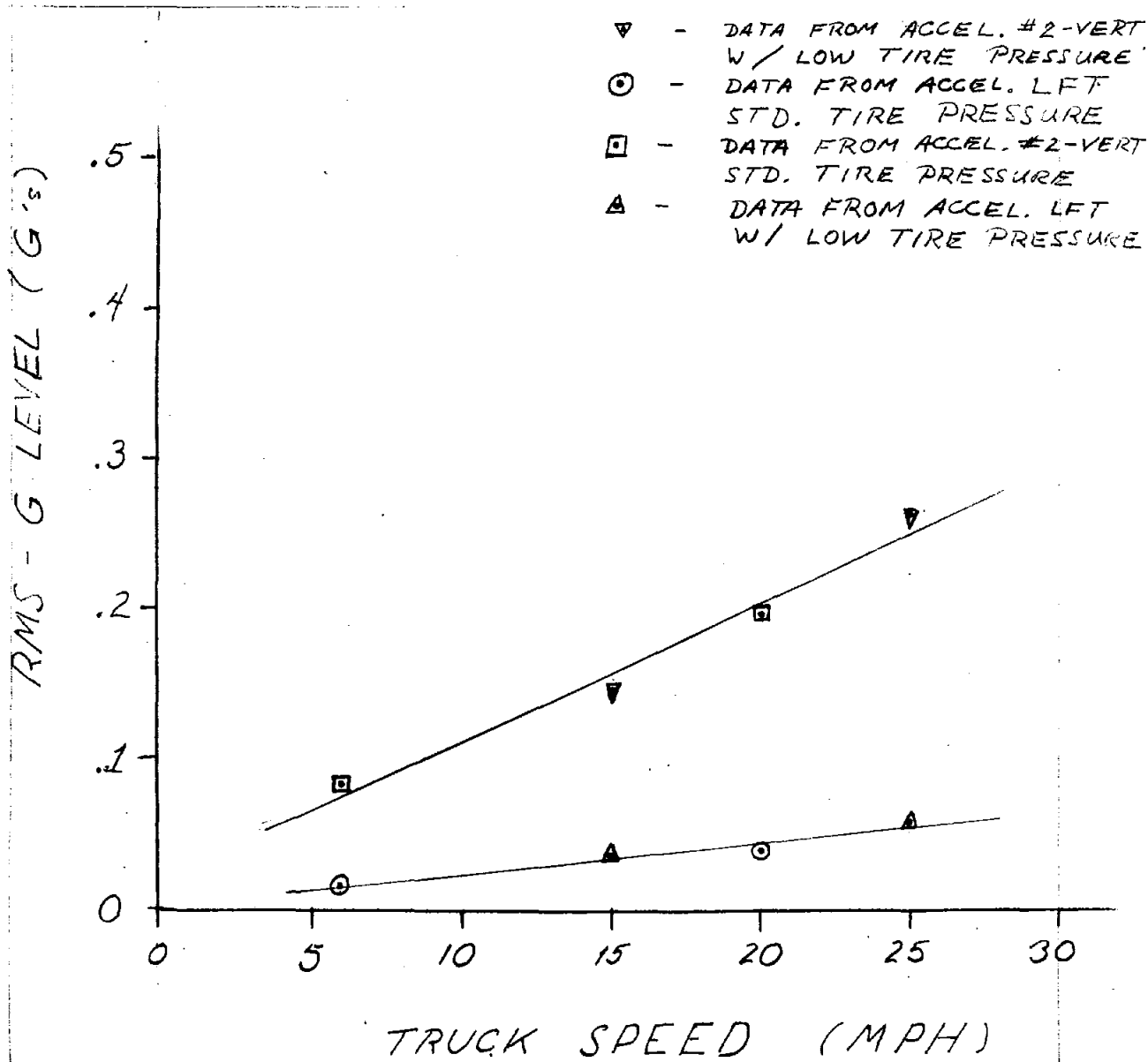
Figure B-18. Plots of RMS-G Level vs Speed for
Accelerometers #2-VERT and LFT with
and without Lowered Tire Pressure
(Down 45 psi)

APPENDIX C

AMPLITUDE UNITS: G'S/ LB-SEC

MEAS. 1
MODE   FREQ(HZ)   DAMP(%)   AMPL   PHS
  1   1.7369   22.7142   .0018   9.3

  2   2.8065   2.2385   .0004   196.4
  3   3.4496   .4448   .0003   32.9
  4   3.9983   .1971   .0004   283.1
  5   4.4186   4.8007   .0009   205.9
RES.FUNCT. 1   -.1860E-06   .5319E-07
           1   -.6735E-06   -.3091E-05

MEAS. 2
MODE   FREQ(HZ)   DAMP(%)   AMPL   PHS
  1   1.8065   21.1801   .0030   352.8

  2   2.7899   2.1383   .0005   206.4
  3   3.4548   .2113   .0005   32.7
  4   4.0017   .0508   .0006   274.3
  5   4.2585   4.3742   .0011   245.6
RES.FUNCT. 1   -.3096E-06   .1338E-06
           1   .2386E-05   -.6459E-06

MEAS. 3
MODE   FREQ(HZ)   DAMP(%)   AMPL   PHS
  1   1.6016   23.6682   .0017   340.0

  2   2.7045   .5564   .0000   311.1
  3   3.4612   1.1352   .0003   13.2
  4   3.9325   1.1954   .0003   322.6
  5   4.5703   .0030   .0001   257.9
RES.FUNCT. 1   -.4456E-06   .8239E-07
           1   .8874E-05   .1221E-06

Figure C-1. Modal Fit Data for Heliostat Yoke Assembly

```
MEAS.    4
MODE    FREQ(HZ)    DAMP( % )        AMPL      PHS
   1       1.4629    10.0682         .0002    321.8

   2       2.6948      .0943         .0000    342.4
   3       3.4360      .7994         .0003     20.9
   4       3.9046      .2793         .0000      3.2
   5       4.5703      .0018         .0001    115.6
RES.FUNCT. 1  -.3650E-06     .4484E-07
           1   .6824E-05  -.5173E-06


MEAS.    5
MODE    FREQ(HZ)    DAMP( % )        AMPL      PHS
   1       1.1671    21.4740         .0001    102.1

   2       2.6919      .0577         .0000    295.4
   3       3.4326      .7042         .0001     17.1
   4       3.9415      .6696         .0001    298.6
   5       4.5703      .0017         .0001    255.3
RES.FUNCT. 1  -.1123E-06     .2232E-07
           1   .2372E-05  -.8673E-06


MEAS.    6
MODE    FREQ(HZ)    DAMP( % )        AMPL      PHS
   1       1.2198    26.0192         .0002    275.7

   2       2.7050      .4017         .0000    222.3
   3       3.4224      .4781         .0001    202.7
   4       3.9301      .2110         .0000    103.4
   5       4.5988      .0270         .0000    142.8
RES.FUNCT. 1   .8862E-07  -.1397E-07
           1  -.1411E-05   .6585E-06


MEAS.    7
MODE    FREQ(HZ)    DAMP( % )        AMPL      PHS
   1       1.2314    30.8806         .0007    281.6

   2       2.6873      .1538         .0000    257.5
   3       3.4158      .4305         .0002    195.6
   4       3.9331      .1324         .0001     93.4
   5       4.5981      .0147         .0001    134.5
RES.FUNCT. 1   .2074E-06  -.5080E-07
           1  -.4469E-05   .2571E-06
```

```
MEAS.   8
MODE    FREQ(HZ)    DAMP( % )        AMPL    PHS
  1        1.2960     27.7222          .0016   870.2

  2        2.8371      2.1698          .0003   175.5
  3        3.4097       .3867          .0004   198.4
  4        3.9356       .0688          .0001    90.6
  5        4.5977       .0086          .0001   148.2
RES.FUNCT. 1    .4021E-06   -.1019E-06
           1   -.7271E-05    .4522E-05


MEAS.   9
MODE    FREQ(HZ)    DAMP( % )        AMPL    PHS
  1        1.2607     46.7727          .0020   328.0

  2        2.8540      3.7524          .0003   167.0
  3        3.4083       .3567          .0002   197.5
  4        3.9373       .0325          .0001    85.5
  5        4.5973       .0043          .0000   152.1
RES.FUNCT. 1    .2080E-06   -.2273E-07
           1   -.1414E-05    .1222E-05


MEAS.  10 *
MODE    FREQ(HZ)    DAMP( % )        AMPL    PHS
  1        1.4580     27.7221          .0015   191.8

  2        2.8250      2.6457          .0003   172.8
  3        3.4689       .6850          .0003   217.1
  4        3.9902       .5995          .0003   143.2
  5        4.5408      2.1679          .0001   237.4
RES.FUNCT. 1    .4050E-06   -.4706E-07
           1   -.4004E-05   -.9749E-06
```

AMPLITUDE UNITS: G'S/ LB-SEC

MEAS. 1 X
MODE   FREQ(HZ)   DAMP(%)   AMPL   PHS
  1   1.7272   12.8528   .0025   319.0
  2   2.0187   5.9145   .0030   28.6
  3   2.9773   2.3820   .0007   1.5
  4   4.8130   2.8594   .0053   160.2
  5   5.7071   .4526   .0006   353.9
  6   6.2522   1.4704   .0004   98.8
RES.FUNCT. 0   -.2477E-03   -.9580E-04
           2   -.3815E-06   .7978E-07

MEAS. 2
MODE   FREQ(HZ)   DAMP(%)   AMPL   PHS
  1   1.7342   26.5469   .0063   31.9
  2   2.3363   4.3038   .0016   14.8
  3   3.2834   2.5770   .0004   143.3
  4   5.5274   4.3856   .0095   168.5

  5   5.7207   1.4070   .0016   358.6
  6   6.6101   .4629   .0004   340.8
RES.FUNCT. 0   -.4042E-03   -.5977E-04
           2   -.2332E-06   .6272E-07

MEAS. 3
MODE   FREQ(HZ)   DAMP(%)   AMPL   PHS
  1   1.6732   19.9660   .0024   347.7
  2   2.1730   28.3591   .0055   13.9
  3   3.1057   15.1208   .0025   99.3
  4   4.4807   5.5729   .0026   173.5
  5   5.9438   4.8315   .0008   294.3
  6   6.7812   11.0914   .0033   40.0
RES.FUNCT. 0   -.5129E-03   .5686E-04
           2   .1158E-06   .1894E-06

MEAS. 4
MODE   FREQ(HZ)   DAMP(%)   AMPL   PHS
  1   1.7787   27.5791   .0079   38.9
  2   2.3446   8.4835   .0014   176.5
  3   3.2899   2.9082   .0014   195.7
  4   5.0985   2.9097   .0015   98.7
  5   5.4335   1.5987   .0019   220.2
  6   6.3505   .3182   .0004   166.2
RES.FUNCT. 0   -.4321E-03   -.3924E-04
           2   -.1027E-06   .1473E-06

Figure C-2. Modal Fit Data for Heliostat Facet Assembly

```
MEAS.    5
MODE    FREQ(HZ)    DAMP( % )        AMPL    PHS
  1      1.9007      20.8363         .0086   16.5
  2      2.3343       5.3079         .0021  163.5
  3      3.2993       2.5480         .0022  191.4

  4      5.0656       3.8430         .0028   90.0
  5      5.3914       1.0212         .0041  272.7
  6      6.3203        .6387         .0009  190.2
RES.FUNCT.  0   -.3932E-03    .5058E-05
            2   -.1737E-06   -.6409E-07


MEAS.    6
MODE    FREQ(HZ)    DAMP( % )        AMPL    PHS
  1      1.9775      39.8156         .0049   18.5
  2      2.3117       3.2789         .0016   38.9
  3      3.1897       6.2132         .0008  120.1
  4      5.4196       4.9856         .0033  189.9
  5      5.7480       4.4212         .0012   46.0
  6      6.5480        .8497         .0012  181.8
RES.FUNCT.  0   -.3008E-03    .2294E-04
            2    .7252E-07    .1761E-06


MEAS.    7
MODE    FREQ(HZ)    DAMP( % )        AMPL    PHS
  1      1.7691      18.8340         .0012    2.5
  2      2.3410       4.4495         .0015   13.1
  3      3.1352       4.1191         .0003  235.4
  4      5.1242      10.2391         .0027  243.5
  5      5.6011       2.8299         .0013  121.8
  6      6.5382        .8880         .0006  189.7
RES.FUNCT.  0   -.6861E-04    .3923E-07
            2   -.3952E-07   -.2538E-07


MEAS.    8
MODE    FREQ(HZ)    DAMP( % )        AMPL    PHS
  1      1.7297      32.7430         .0026   45.1
  2      2.2491       1.8297         .0003   32.3
  3      3.2795       2.8997         .0003  199.7
  4      5.3352       5.9824         .0043  152.5
  5      5.6571       5.1689         .0022  257.1
  6      6.0923      11.6514         .0028  311.0
RES.FUNCT.  0   -.9396E-04    .7362E-05
            2    .4177E-07   -.6797E-07
```

101

```
MEAS.  9
MODE   FREQ(HZ)    DAMP( % )        AMPL      PHS
  1      1.7450     33.0477         .0041     53.8
  2      2.2764      5.9121         .0008    209.3
  3      3.2926      2.7712         .0015    196.6
  4      5.2063     13.3655         .0047    212.7
  5      5.4195      1.0575         .0003     79.8
  6      6.5435      9.9095         .0031    330.2
RES.FUNCT. 0  -.1118E-03    .3479E-05
           2   .4533E-07   -.2262E-08


MEAS.  10
MODE   FREQ(HZ)    DAMP( % )        AMPL      PHS
  1      1.7295     30.9902         .0023     60.4
  2      2.2576      3.0592         .0009    212.4
  3      3.2947      2.3587         .0014    194.6
  4      5.3491      1.7213         .0020    127.1
  5      5.6447      5.2888         .0016    229.2
  6      6.3624       .8795         .0004    346.2
RES.FUNCT. 0   .4395E-05   -.2621E-04
           2  -.7680E-07   -.4907E-07


MEAS.  11
MODE   FREQ(HZ)    DAMP( % )        AMPL      PHS
  1      1.8720     19.5904         .0010    354.1
  2      2.3036      3.9572         .0011     44.4
  3      3.4418      5.1975         .0006    146.1
  4      5.5966      3.2303         .0007     32.0
  5      5.7510      3.4111         .0012    152.2
  6      6.5336      1.5078         .0006    183.5
RES.FUNCT. 0  -.6004E-04   -.2558E-04
           2  -.6698E-07    .7421E-07


MEAS.  12
MODE   FREQ(HZ)    DAMP( % )        AMPL      PHS
  1      1.6423     13.9854         .0006     13.3
  2      2.2394      7.6215         .0009     37.3
  3      3.2838      3.6582         .0011    180.6
  4      5.2902      2.3015         .0007    137.3
  5      5.8174       .1138         .0002    177.2
  6      6.5589       .1290         .0001     95.4
RES.FUNCT. 0  -.5335E-04   -.3486E-04
           2  -.5546E-07    .4333E-07
```

```
MEAS.  13
MODE    FREQ(HZ)    DAMP( % )       AMPL    PHS
  1       1.7443     27.2345        .0019    41.7
  2       2.4469     10.7288        .0007   136.9
  3       3.2961      2.7322        .0011   191.6
  4       5.3184      2.1834        .0014   146.7
  5       5.6268      2.3177        .0004   251.6
  6       6.5436       .3032        .0001   251.1
RES.FUNCT.  0  -.5034E-04  -.2232E-04
            2  -.4114E-07   .7027E-08


MEAS.  14
MODE    FREQ(HZ)    DAMP( % )       AMPL    PHS

  1       1.9334     11.9626        .0015    11.0
  2       2.2954      2.8930        .0008   192.3
  3       3.2869      2.3215        .0015   201.7
  4       5.4198      2.8306        .0007   113.7
  5       5.8347      5.1716        .0012   168.6
  6       6.3444       .4690        .0006   357.8
RES.FUNCT.  0   .4447E-04  -.1312E-03
            2  -.2512E-06  -.1045E-09


MEAS.  15
MODE    FREQ(HZ)    DAMP( % )       AMPL    PHS
  1       1.8572     30.7939        .0028   217.3
  2       2.3378      3.4890        .0017    24.6
  3       3.2766      5.5562        .0004   218.0
  4       5.3722      3.9880        .0024    44.7
  5       5.6539       .8830        .0013   267.7
  6       6.5646      1.0536        .0021   181.4
RES.FUNCT.  0   .1762E-03  -.8344E-04
            2  -.2605E-06  -.4337E-07


MEAS.  16
MODE    FREQ(HZ)    DAMP( % )       AMPL    PHS
  1       1.7667     23.6078        .0009   241.9
  2       2.3814      3.1605        .0011    43.1
  3       3.4700      2.9533        .0006   197.1
  4       5.4192      4.2392        .0007    84.5
  5       5.7595      1.3719        .0010   237.8
  6       6.6914       .9264        .0009   184.2
RES.FUNCT.  0   .4954E-04  -.6372E-05
            2  -.2733E-07  -.5971E-07
```

MEAS. 17
```
MODE   FREQ(HZ)    DAMP( % )        AMPL      PHS
  1     2.0204      4.1994          .0002     86.6
  2     2.1950      2.5186          .0002     98.8
  3     3.2812      3.6132          .0014    182.6
  4     5.3531      1.5694          .0005    100.1
  5     5.8222       .1595          .0002    187.8
  6     6.2238      2.3013          .0003    218.4
RES.FUNCT.  0    .7462E-04   -.3750E-04
            2   -.8122E-07    .1667E-07
```

MEAS. 18
```
MODE   FREQ(HZ)    DAMP( % )        AMPL      PHS
  1     1.7058     49.8291          .0029     95.0
  2     2.1618     25.5852          .0014    212.8
  3     3.2754      3.3625          .0015    187.9
  4     5.3387      1.7522          .0019    103.5
  5     5.8364       .0243          .0002    219.9
  6     6.2041       .7327          .0003    179.3
RES.FUNCT.  0    .4876E-04   -.7111E-04
            2   -.1286E-06    .7846E-07
```

MEAS. 19
```
MODE   FREQ(HZ)    DAMP( % )        AMPL      PHS
  1     1.7373     29.4475          .0026     88.0
  2     2.3361     12.2142          .0018    185.0
  3     3.2794      3.8200          .0023    184.4
  4     5.3278      1.8781          .0039    108.9
  5     5.8359       .0266          .0002    253.0
  6     6.2330       .5444          .0005    147.7
RES.FUNCT.  0    .1040E-03   -.1798E-03
            2   -.2592E-06    .1638E-06
```

MEAS. 20
```
MODE   FREQ(HZ)    DAMP( % )        AMPL      PHS
  1     1.7976     14.1432          .0015    211.0
  2     2.2936      1.3055          .0011    118.2
  3     3.2462     13.1790          .0026    236.5
  4     5.6518      1.8388          .0047    349.8
  5     5.8352       .0088          .0006    313.3
  6     6.6927       .8989          .0011    186.7
RES.FUNCT.  0    .1276E-03    .1547E-03
            2    .2561E-06   -.4427E-06
```

```
MEAS. 21
MODE   FREQ(HZ)   DAMP( % )        AMPL     PHS
  1       1.8046     26.9250         .0028   231.8
  2       2.3757      2.2771         .0007    43.2
  3       3.4967      2.0881         .0006   188.8
  4       5.4076      5.9992         .0014    80.1
  5       5.7468      1.4796         .0017   299.7
  6       6.6826      1.0272         .0005   192.6
RES.FUNCT. 0    .2014E-03  -.1054E-04
           2    .7665E-08  -.1323E-06


MEAS. 22
MODE   FREQ(HZ)   DAMP( % )        AMPL     PHS
  1       1.9286     26.6789         .0023   185.1
  2       2.0987      1.5100         .0001   180.0
  3       3.2687      3.4906         .0012   196.2
  4       5.4195       .5204         .0002    55.7
  5       5.7950       .1396         .0003   214.8
  6       5.9652      1.9264         .0005   313.0
RES.FUNCT. 0    .2206E-03  -.3542E-04
           2   -.9134E-07  -.3307E-07


MEAS. 23
MODE   FREQ(HZ)   DAMP( % )        AMPL     PHS
  1       2.1261     21.2251         .0030    75.2
  2       2.2263     19.8638         .0039   207.6
  3       3.3901      3.7436         .0012   171.3
  4       5.4514      1.7817         .0032   132.4
  5       5.3292      2.5985         .0013   218.1
  6       6.5395      3.3883         .0008   268.3
RES.FUNCT. 0    .2685E-03  -.9596E-04
           2   -.1100E-06   .8986E-07


MEAS. 24
MODE   FREQ(HZ)   DAMP( % )        AMPL     PHS
  1       1.8019      9.3882         .0010   113.5
  2       2.2848     18.2237         .0065   174.0
  3       3.2432      4.4009         .0013   211.3
  4       5.2809      2.5216         .0089   133.7
  5       5.6293      3.7592         .0048   282.0
  6       6.3201      1.9721         .0038   227.6
RES.FUNCT. 0    .6633E-03  -.9868E-04
           2   -.3442E-08  -.1011E-06
```

```
MEAS. 25
MODE    FREQ(HZ)    DAMP( % )        AMPL     PHS
  1       1.7672     23.6923         .0063   227.9
  2       2.3218      2.2819         .0009    96.2
  3       3.5146      2.7067         .0014   181.9
  4       5.5114      3.0979         .0057     9.2
  5       5.7089      1.1340         .0041   330.6
  6       6.7056      1.1824         .0037     3.7
RES.FUNCT.  0    .2624E-03    .7391E-04
            2    .9707E-07   -.6755E-07


MEAS. 26
MODE    FREQ(HZ)    DAMP( % )        AMPL     PHS
  1       1.7418     27.8805         .0046   212.9
  2       2.1197      6.1833         .0006   184.2
  3       3.3968      3.5683         .0009   165.7
  4       5.3404      3.7950         .0019   239.2
  5       5.5614      6.2731         .0042     5.3
  6       5.9953      1.1436         .0005   115.6
RES.FUNCT.  0    .3912E-03   -.2624E-04
            2    .1031E-06    .3287E-07


MEAS. 27
MODE    FREQ(HZ)    DAMP( % )        AMPL     PHS
  1       2.0431     18.0458         .0050   144.2
  2       2.2158     15.2416         .0031   248.5
  3       3.3742      4.8373         .0010   171.1
  4       5.3162      3.4869         .0028   214.1
  5       5.5433      1.1455         .0020    52.1
  6       6.4125       .9368         .0010   204.3
RES.FUNCT.  0    .4124E-03   -.6301E-04
            2    .1063E-06    .6848E-07


MEAS. 28
MODE    FREQ(HZ)    DAMP( % )        AMPL     PHS
  1       2.0117     15.5283         .0054    82.2
  2       2.1317     15.6594         .0080   215.8
  3       3.5269     10.2919         .0027   124.7
  4       5.4600      2.0377         .0092   127.6
  5       5.7496      4.0446         .0054   243.8
  6       6.3940      1.1443         .0032   209.4
RES.FUNCT.  0    .6541E-03   -.1622E-03

            2   -.2399E-07    .1835E-06
```

```
MEAS. 29
MODE    FREQ(HZ)    DAMP( % )        AMPL      PHS
  1      1.8867     19.2583         .0059     198.2
  2      2.3551      1.4521         .0004      69.7
  3      3.5502      2.0438         .0010     165.7
  4      5.6579      5.1099         .0129       2.7
  5      5.8722      1.3430         .0019     195.4
  6      6.4572      5.5412         .0042      75.9
RES.FUNCT. 0    .9973E-04   -.1046E-04
           2    .2910E-06    .2909E-06


MEAS. 30
MODE    FREQ(HZ)    DAMP( % )        AMPL      PHS
  1      1.8713     18.6577         .0066     202.5
  2      2.3459      1.2207         .0003      88.9
  3      3.5655      1.7564         .0012     151.8
  4      5.4669      9.3660         .0094      47.0
  5      5.7741      1.7598         .0028     286.8
  6      6.7451      1.0878         .0007       6.5
RES.FUNCT. 0    .3559E-03    .4377E-04
           2    .2437E-06    .1179E-06


MEAS. 31
MODE    FREQ(HZ)    DAMP( % )        AMPL      PHS
  1      1.7747     32.2072         .0073     221.0
  2      2.2430      4.5138         .0005     120.6
  3      3.4085      2.9583         .0008     160.7
  4      5.5512      9.9752         .0076     329.5
  5      5.7486      7.8323         .0034     127.1
  6      6.6823       .0641         .0000      16.0

RES.FUNCT. 0    .5093E-03   -.2993E-04
           2    .1191E-06   -.7828E-09


MEAS. 32
MODE    FREQ(HZ)    DAMP( % )        AMPL      PHS
  1      1.9135     12.1125         .0028     104.7
  2      2.1188     17.4730         .0097     197.8
  3      3.3809      8.5356         .0030     164.4
  4      5.4179      1.5086         .0026     162.1
  5      5.6704      1.6157         .0013     322.1
  6      6.3814      1.1809         .0013     218.3
RES.FUNCT. 0    .8283E-03   -.1384E-03
           2    .2511E-07    .1137E-06
```

MEAS. 33
MODE	FREQ(HZ)	DAMP(%)	AMPL	PHS
1	1.9337	17.3105	.0025	155.8
2	2.2641	14.1589	.0036	177.6
3	3.4786	14.3220	.0045	131.9
4	5.4682	1.6140	.0042	120.2
5	5.8686	3.4108	.0022	206.5
6	6.3880	1.3376	.0018	213.7

RES.FUNCT. 0   .5394E-03   -.1453E-03
          2 -.1078E-06   .1836E-06

AMPLITUDE UNITS: G/S/ LB-SEC

MEAS. 1 Y
MODE	FREQ(HZ)	DAMP(R/S)	AMPL	PHS
1	1.7272	1.4065	.0025	319.0
2	2.0137	.7515	.0030	28.6
3	2.9773	.4457	.0007	1.5
4	4.8130	.8651	.0053	160.2
5	5.7071	.1623	.0006	353.9
6	6.2522	.5777	.0004	98.8

RES.FUNCT. 0 -.2477E-03   -.9580E-04
          2 -.3815E-06   .7978E-07

MEAS. 2
MODE	FREQ(HZ)	DAMP(R/S)	AMPL	PHS
1	1.7342	3.0004	.0063	31.9
2	2.3363	.6331	.0016	14.2
3	3.2234	.5318	.0004	143.3
4	5.5274	1.5246	.0095	168.5
5	5.7207	.5058	.0016	358.6
6	6.6101	.1923	.0004	340.8

RES.FUNCT. 0 -.4042E-03   -.5977E-04
          2 -.2332E-06   .6272E-07

MEAS. 3
MODE	FREQ(HZ)	DAMP(R/S)	AMPL	PHS
1	1.6732	2.1422	.0024	347.7
2	2.1730	4.0378	.0055	13.9
3	3.1057	2.9850	.0025	99.3
4	4.4807	1.5714	.0026	173.5
5	5.9438	1.8065	.0008	294.3
6	6.7812	4.7551	.0033	40.0

RES.FUNCT. 0 -.5129E-03   .5686E-04
          2   .1158E-06   .1894E-06

```
MEAS.   4
MODE   FREQ(HZ)    DAMP(R/S)        AMPL      PHS
  1      1.7787     3.2065          .0079     38.9
  2      2.3446     1.2543          .0014    176.5
  3      3.2899      .6014          .0014    195.7
  4      5.0985      .9325          .0015     98.7
  5      5.4335      .5459          .0019    220.2
  6      6.3505      .1270          .0004    166.2
RES.FUNCT.  0  -.4321E-03  -.3924E-04
            2  -.1027E-06   .1473E-06


MEAS.   5
MODE   FREQ(HZ)    DAMP(R/S)        AMPL      PHS
  1      1.9007     2.5443          .0086     16.5
  2      2.3343      .7796          .0021    163.5
  3      3.2993      .5284          .0022    191.4
  4      5.0656     1.2241          .0028     90.0
  5      5.3914      .3459          .0041    272.7
  6      6.3203      .2536          .0009    190.2
RES.FUNCT.  0  -.3932E-03   .8058E-05
            2  -.1737E-06  -.6409E-07


MEAS.   6
MODE   FREQ(HZ)    DAMP(R/S)        AMPL      PHS
  1      1.9775     5.3929          .0049     18.5
  2      2.3117      .4765          .0016     38.9
  3      3.1397     1.2476          .0008    120.1
  4      5.4196     1.6998          .0033    189.9
  5      5.7480     1.5983          .0012     46.0
  6      6.5480      .3496          .0012    181.8
RES.FUNCT.  0  -.3008E-03   .2294E-04
            2   .7252E-07   .1761E-06


MEAS.   7
MODE   FREQ(HZ)    DAMP(R/S)        AMPL      PHS
  1      1.7691     2.1316          .0012      2.5
  2      2.3410      .6551          .0015     13.1
  3      3.1352      .8121          .0003    235.4
  4      5.1242     3.3141          .0027    243.5
  5      5.6011      .9963          .0013    121.8
  6      6.5382      .3648          .0006    189.7
RES.FUNCT.  0  -.6861E-04   .3923E-07
            2  -.3952E-07  -.2538E-07
```

```
MEAS.   8
MODE    FREQ(HZ)     DAMP(R/S)      AMPL     PHS
  1      1.7297       3.7662        .0026    45.1
  2      2.2491        .2586        .0003    32.3
  3      3.2795        .5978        .0008   199.7
  4      5.3352       2.0090        .0043   152.5
  5      5.6571       1.8397        .0022   257.1
  6      6.0923       4.4906        .0028   311.0
RES.FUNCT.  0   -.9396E-04     .7862E-05
            2    .4177E-07    -.6797E-07


MEAS.   9
MODE    FREQ(HZ)     DAMP(R/S)      AMPL     PHS
  1      1.7450       3.8390        .0041    53.8
  2      2.2764        .8471        .0008   209.3
  3      3.2926        .5735        .0015   196.6
  4      5.2063       4.4118        .0047   212.7
  5      5.4195        .3601        .0003    79.8
  6      6.5435       4.0943        .0031   330.2
RES.FUNCT.  0   -.1118E-03     .3479E-05
            2    .4533E-07    -.2262E-08


MEAS.  10
MODE    FREQ(HZ)     DAMP(R/S)      AMPL     PHS
  1      1.7295       3.5419        .0023    60.4
  2      2.2576        .4342        .0009   212.4
  3      3.2947        .4884        .0014   194.6
  4      5.3491        .5786        .0020   127.1
  5      5.6447       1.8784        .0016   229.2
  6      6.3624        .3516        .0004   346.2
RES.FUNCT.  0    .4395E-05    -.2621E-04
            2   -.7680E-07    -.4907E-07


MEAS.  11
MODE    FREQ(HZ)     DAMP(R/S)      AMPL     PHS
  1      1.2720       2.3497        .0010   354.1
  2      2.3036        .5732        .0011    44.4
  3      3.4413       1.1255        .0006   146.1
  4      5.5966       1.1365        .0007    32.0
  5      5.7510       1.2333        .0012   152.2
  6      6.5336        .6190        .0006   183.5
RES.FUNCT.  0   -.6004E-04    -.2558E-04
            2   -.6698E-07     .7421E-07
```

```
MEAS. 12
MODE    FREG(HZ)    DAMP(R/S)         AMPL      PHS
  1      1.6423      1.4574          .0006     13.3
  2      2.2394      1.0755          .0009     37.3
  3      3.2838       .7553          .0011    180.6
  4      5.2902       .7652          .0007    137.3
  5      5.3174       .0416          .0002    177.2
  6      6.5589       .0532          .0001     95.4
RES.FUNCT.  0  -.5335E-04  -.3486E-04
            2  -.5546E-07   .4333E-07


MEAS. 13
MODE    FREG(HZ)    DAMP(R/S)         AMPL      PHS
  1      1.7443      3.1021          .0019     41.7
  2      2.4469      1.6590          .0007    136.9
  3      3.2961       .5661          .0011    191.6
  4      5.3184       .7298          .0014    146.7
  5      5.6268       .8196          .0004    251.6
  6      6.5436       .1246          .0001    251.1
RES.FUNCT.  0  -.5034E-04  -.2232E-04
            2  -.4114E-07   .7027E-08


MEAS. 14
MODE    FREG(HZ)    DAMP(R/S)         AMPL      PHS
  1      1.9334      1.4637          .0015     11.0
  2      2.2954       .4174          .0008    192.3
  3      3.2369       .4796          .0015    201.7
  4      5.4193       .9643          .0007    113.7
  5      5.8347      1.8924          .0012    168.6
  6      6.3444       .1870          .0006    357.8
RES.FUNCT.  0   .4447E-04  -.1312E-03
            2  -.2512E-06  -.1045E-09


MEAS. 15
MODE    FREG(HZ)    DAMP(R/S)         AMPL      PHS
  1      1.8572      3.7769          .0028    217.3
  2      2.3378       .5128          .0017     24.6
  3      3.2766      1.1457          .0004    218.0
  4      5.3722      1.3472          .0024     44.7
  5      5.6539       .3137          .0013    267.7
  6      6.5646       .4346          .0021    181.4
RES.FUNCT.  0   .1762E-03  -.8344E-04
            2  -.2605E-06  -.4337E-07
```

```
MEAS. 16
MODE    FREQ(HZ)    DAMP(R/S)         AMPL      PHS
  1      1.7667      2.6968           .0009    241.9
  2      2.3814       .4731           .0011     43.1
  3      3.4700       .6442           .0006    197.1
  4      5.4192      1.4447           .0007     84.5
  5      5.7595       .4965           .0010    287.8
  6      6.6914       .3895           .0009    184.2
RES.FUNCT. 0    .4954E-04   -.6372E-05
           2   -.2733E-07   -.5971E-07


MEAS. 17
MODE    FREQ(HZ)    DAMP(R/S)         AMPL      PHS
  1      2.0804       .5494           .0002     86.6
  2      2.1950       .3475           .0002     98.8
  3      3.2812       .7454           .0014    182.6
  4      5.3531       .5279           .0005    100.1
  5      5.3222       .0584           .0002    187.3
  6      6.2238       .9002           .0003    218.4
RES.FUNCT. 0    .7462E-04   -.3750E-04
           2   -.8122E-07    .1667E-07


MEAS. 18
MODE    FREQ(HZ)    DAMP(R/S)         AMPL      PHS
  1      1.7058      6.1599           .0029     95.0
  2      2.1618      3.5949           .0014    212.8
  3      3.2754       .6924           .0015    187.9
  4      5.3387       .5878           .0019    103.5
  5      5.3364       .0089           .0002    219.9
  6      6.2041       .2856           .0003    179.3
RES.FUNCT. 0    .4876E-04   -.7111E-04
           2   -.1286E-06    .7846E-07


MEAS. 19
MODE    FREQ(HZ)    DAMP(R/S)         AMPL      PHS
  1      1.7373      3.3636           .0026     88.0
  2      2.3361      1.8063           .0018    185.0
  3      3.2794       .7877           .0023    184.4
  4      5.3278       .6288           .0039    108.9
  5      5.8359       .0097           .0002    253.0
  6      6.2330       .2132           .0005    147.7
RES.FUNCT. 0    .1040E-03   -.1798E-03
           2   -.2592E-06    .1638E-06
```

MEAS. 20
MODE	FREQ(HZ)	DAMP(R/S)	AMPL	PHS
1	1.7976	1.6137	.0015	211.0
2	2.2986	.1886	.0011	118.2
3	3.2462	2.7117	.0026	236.5
4	5.6518	.6708	.0047	349.8
5	5.8352	.0032	.0006	313.3
6	6.6927	.3780	.0011	186.7

RES.FUNCT. 0   .1276E-03   .1547E-03
            2   .2561E-06   -.4427E-06

MEAS. 21
MODE	FREQ(HZ)	DAMP(R/S)	AMPL	PHS
1	1.8046	3.1700	.0028	231.8
2	2.3757	.3400	.0007	43.2
3	3.4967	.4589	.0006	188.8
4	5.4076	2.0420	.0014	80.1
5	5.7468	.5343	.0017	299.7
6	6.6826	.4313	.0005	192.6

RES.FUNCT. 0   .2014E-03   -.1054E-04
            2   .7665E-08   -.1323E-06

MEAS. 22
MODE	FREQ(HZ)	DAMP(R/S)	AMPL	PHS
1	1.9286	3.3545	.0023	185.1
2	2.0987	.1991	.0001	180.0
3	3.2687	.7173	.0012	196.2
4	5.4195	.1772	.0002	55.7
5	5.7950	.0690	.0003	214.8
6	5.9652	.7222	.0005	313.0

RES.FUNCT. 0   .2206E-03   -.3542E-04
            2   -.9134E-07   -.3307E-07

MEAS. 23
MODE	FREQ(HZ)	DAMP(R/S)	AMPL	PHS
1	2.1261	2.9015	.0030	75.2
2	2.2263	2.8351	.0039	207.5
3	3.3901	.7980	.0012	171.3
4	5.4514	.6104	.0032	132.4
5	5.8292	.9521	.0013	218.1
6	6.5395	1.3930	.0008	268.3

RES.FUNCT. 0   .2685E-03   -.9596E-04
            2   -.1100E-06   .8986E-07

113

MEAS. 24
```
MODE    FREQ(HZ)    DAMP(R/S)        AMPL      PHS
  1       1.8019      1.0676          .0010    113.5
  2       2.2848      2.6607          .0065    174.0
  3       3.2432       .8977          .0013    211.3
  4       5.2809       .8370          .0089    133.7
  5       5.6293      1.3306          .0048    282.0
  6       6.3201       .7833          .0038    227.6
RES.FUNCT. 0    .6633E-03   -.9868E-04
           2   -.3442E-08   -.1011E-06
```

MEAS. 25
```
MODE    FREQ(HZ)    DAMP(R/S)        AMPL      PHS
  1       1.7672      2.7078          .0063    227.9
  2       2.3218       .3330          .0009     96.2
  3       3.5146       .5979          .0014    181.9
  4       5.5114      1.0733          .0057      9.2
  5       5.7089       .4068          .0041    330.6
  6       6.7056       .4982          .0037      3.7
RES.FUNCT. 0    .2624E-03    .7391E-04
           2    .9707E-07   -.6755E-07
```

MEAS. 26
```
MODE    FREQ(HZ)    DAMP(R/S)        AMPL      PHS
  1       1.7418      3.1773          .0046    212.9
  2       2.1197       .8251          .0006    184.2
  3       3.3968       .7621          .0009    165.7
  4       5.3404      1.2743          .0019    239.2
  5       5.5614      2.1964          .0042      5.3
  6       5.9953       .4308          .0005    115.6
RES.FUNCT. 0    .3912E-03   -.2624E-04
           2    .1031E-06    .3287E-07
```

MEAS. 27
```
MODE    FREQ(HZ)    DAMP(R/S)        AMPL      PHS
  1       2.0431      2.3553          .0050    144.2
  2       2.2158      2.1471          .0031    248.5
  3       3.3742      1.0267          .0010    171.1
  4       5.3162      1.1654          .0028    214.1
  5       5.5433       .3990          .0020     52.1
  6       6.4125       .3775          .0010    204.3
RES.FUNCT. 0    .4124E-03   -.6301E-04
           2    .1063E-06    .6848E-07
```

```
MEAS. 28
MODE    FREQ(HZ)    DAMP(R/S)        AMPL      PHS
  1       2.0117      1.9869         .0054     82.2
  2       2.1317      2.1236         .0080    215.8
  3       3.5269      2.2929         .0027    124.7
  4       5.4600       .6992         .0092    127.6
  5       5.7496      1.4624         .0054    243.8
  6       6.3940       .4597         .0032    209.4
RES.FUNCT.  0    .6541E-03   -.1622E-03
            2   -.2399E-07    .1835E-06


MEAS. 29
MODE    FREQ(HZ)    DAMP(R/S)        AMPL      PHS
  1       1.8367      2.3266         .0059    198.2
  2       2.3551       .2149         .0004     69.7
  3       3.5502       .4560         .0010    165.7
  4       5.6579      1.8189         .0129      2.7
  5       5.8722       .4956         .0019    195.4
  6       6.4572      2.2516         .0042     75.9
RES.FUNCT.  0    .9973E-04   -.1046E-04
            2    .2910E-06    .2909E-06


MEAS. 30
MODE    FREQ(HZ)    DAMP(R/S)        AMPL      PHS
  1       1.8713      2.2329         .0066    202.5
  2       2.3459       .1799         .0003     88.9
  3       3.5655       .3935         .0012    151.8
  4       5.4669      3.2314         .0094     47.0
  5       5.7741       .6386         .0028    286.8
  6       6.7451       .4611         .0007      6.5
RES.FUNCT.  0    .3559E-03    .4377E-04
            2    .2437E-06    .1179E-06


MEAS. 31
MODE    FREQ(HZ)    DAMP(R/S)        AMPL      PHS
  1       1.7747      3.7934         .0073    221.0
  2       2.2430       .6368         .0005    120.6
  3       3.4085       .6338         .0008    160.7
  4       5.5518      3.4971         .0076    329.5
  5       5.7486      2.8377         .0034    127.1
  6       6.6823       .0269         .0000     16.0
RES.FUNCT.  0    .5093E-03   -.2998E-04
            2    .1191E-06   -.7828E-09
```

MEAS. 32
MODE	FREQ(HZ)	DAMP(R/S)	AMPL	PHS
1	1.9135	1.4671	.0028	104.7
2	2.1188	2.3625	.0097	197.8
3	3.3809	1.8199	.0030	164.4
4	5.4179	.5136	.0026	162.1
5	5.6704	.5757	.0013	322.1
6	6.3814	.4735	.0013	218.3

RES.FUNCT. 0   .8283E-03   -.1384E-03
           2   .2511E-07   .1137E-06

MEAS. 33
MODE	FREQ(HZ)	DAMP(R/S)	AMPL	PHS
1	1.9337	2.1355	.0025	155.8
2	2.2641	2.0347	.0036	177.6
3	3.4786	3.1629	.0045	131.9
4	5.4682	.5546	.0042	120.2
5	5.8686	1.2584	.0022	206.5
6	6.3880	.5369	.0018	213.7

RES.FUNCT. 0   .5394E-03   -.1453E-03
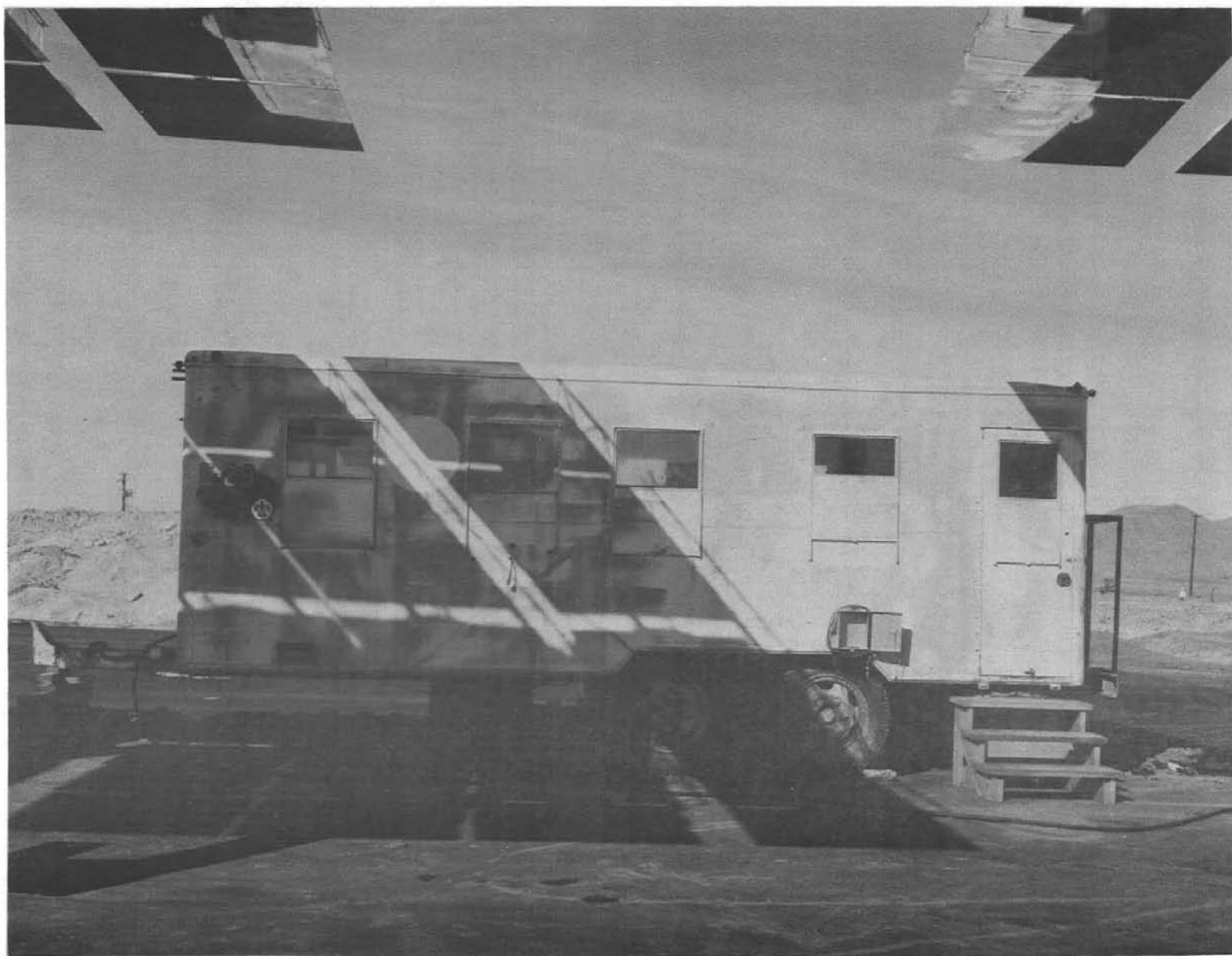   2 -.1078E-06   .1836E-06

116

APPENDIX D
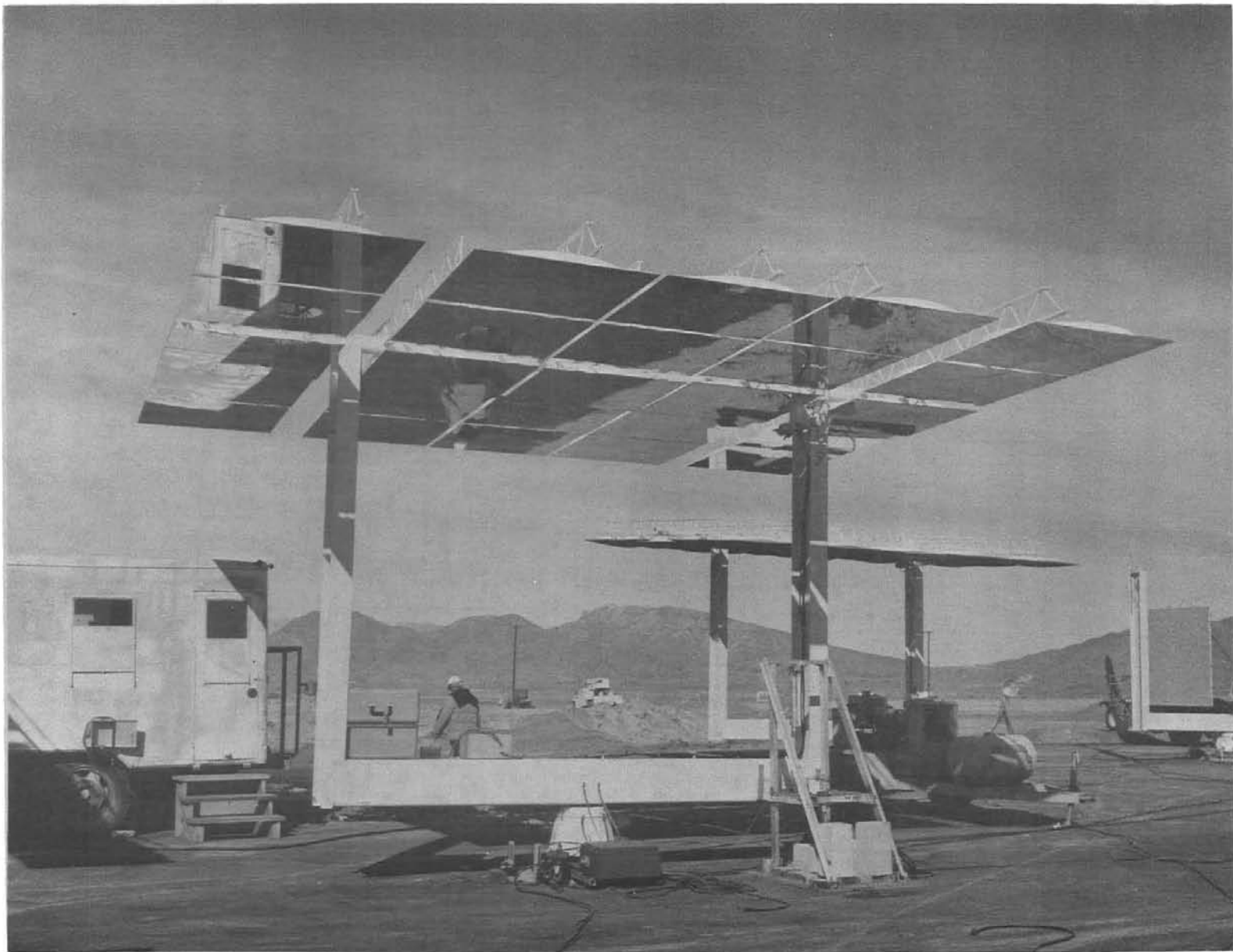
Photograph D-1.   Heliostat (in stowed position) and Relation of Exciter
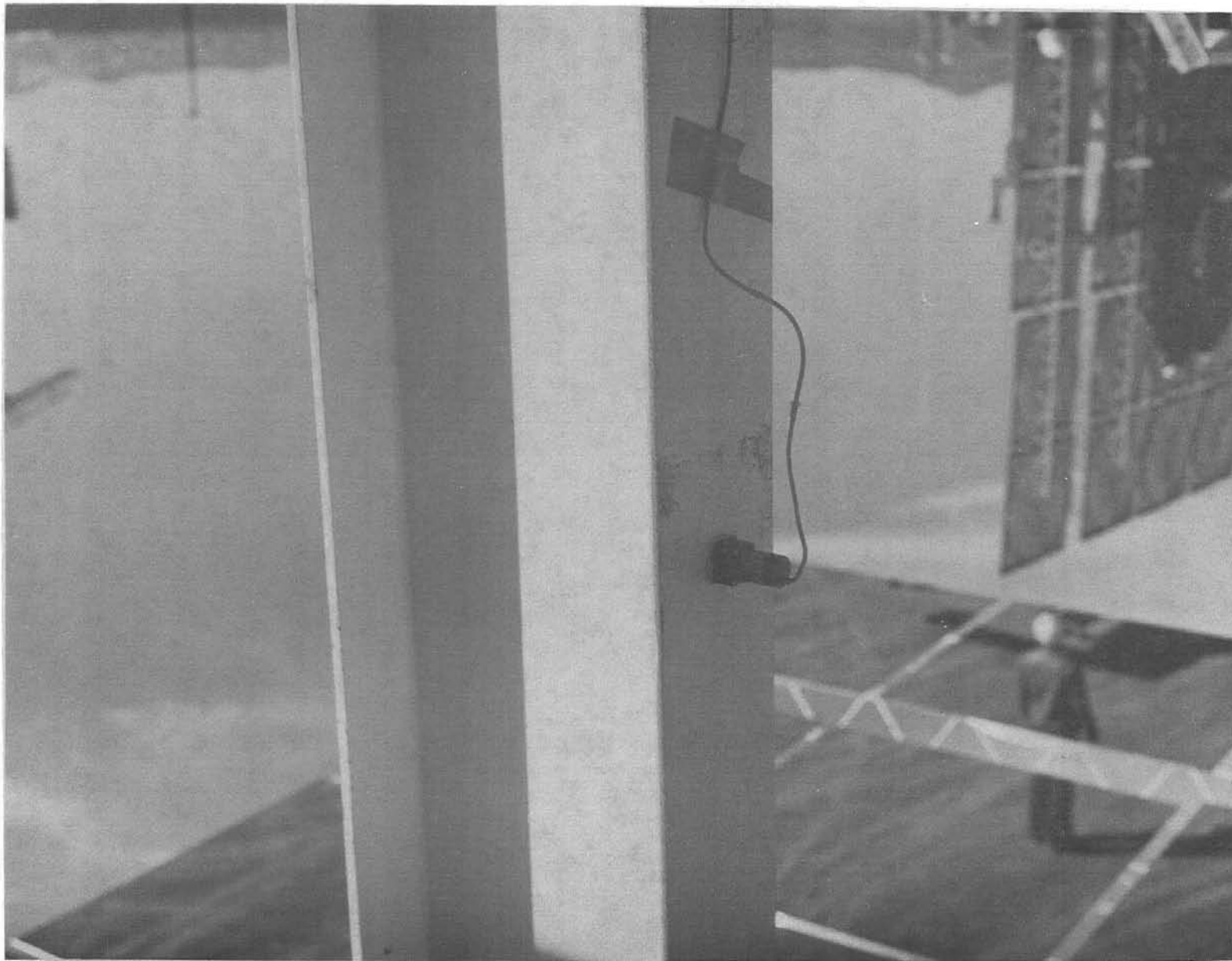
Photograph D-2. Typical Placement of the Kistler 303T Servo-Accelerometer

Photograph D-3. Instrumentation Trailer

DISTRIBUTION:
1284   P. P. Stirbis
5710   G. E. Brandvold
5713   J. V. Otts (3)
5713   D. J. Kuehl
5715   R. C. Reuter
8132   A. C. Skinrud
9300   W. A. Gardner
9330   A. J. Clark, Jr.
9340   W. E. Caldes
9341   M. L. Shannon
9342   D. R. Schafer
9342   J. R. Janczy (10)
9343   E. H. Copeland
9344   J. L. Mortley
9350   F. W. Neilson
8266   E. A. Aas (2)
3141   C. A. Pepmueller (Actg) (5)
3151   W. L. Garner (3)
        (For ERDA/TIC Unlimited Release)
ERDA/TIC (25)
        (R. P. Campbell, 3172-3)